

**RADIOLOGICAL, TRACE ELEMENTAL AND
PETROGRAPHIC CHARACTERIZATION OF MAIGANGA
COAL DEPOSIT OF NORTHERN BENUE TROUGH,
NORTH-EASTERN NIGERIA**

KOLO MATTHEW TIKPANGI

**FACULTY OF SCIENCE
UNIVERSITY OF MALAYA
KUALA LUMPUR**

2016

**RADIOLOGICAL, TRACE ELEMENTAL AND
PETROGRAPHIC CHARACTERIZATION OF
MAIGANGA COAL DEPOSIT OF NORTHERN BENUE
TROUGH, NORTH-EASTERN NIGERIA**

KOLO MATTHEW TIKPANGI

**THESIS SUBMITTED IN FULFILMENT OF THE
REQUIREMENTS FOR THE DEGREE OF DOCTOR OF
PHILOSOPHY**

**FACULTY OF SCIENCE
UNIVERSITY OF MALAYA
KUALA LUMPUR**

2016

UNIVERSITY OF MALAYA
ORIGINAL LITERARY WORK DECLARATION

Name of Candidate: **Kolo Matthew Tikpangi**

Matric No: **SHC 130004**

Name of Degree: **PhD**

Title of Project Paper/Research Report/Dissertation/Thesis (“this Work”):

RADIOLOGICAL, TRACE ELEMENTAL AND PETROGRAPHIC CHARACTERIZATION OF MAIGANGA COAL DEPOSIT OF NORTHERN BENUE TROUGH, NORTH-EASTERN NIGERIA

Field of Study: **RADIATION PHYSICS**

I do solemnly and sincerely declare that:

- (1) I am the sole author/writer of this Work;
- (2) This Work is original;
- (3) Any use of any work in which copyright exists was done by way of fair dealing and for permitted purposes and any excerpt or extract from, or reference to or reproduction of any copyright work has been disclosed expressly and sufficiently and the title of the Work and its authorship have been acknowledged in this Work;
- (4) I do not have any actual knowledge nor do I ought reasonably to know that the making of this work constitutes an infringement of any copyright work;
- (5) I hereby assign all and every rights in the copyright to this Work to the University of Malaya (“UM”), who henceforth shall be owner of the copyright in this Work and that any reproduction or use in any form or by any means whatsoever is prohibited without the written consent of UM having been first had and obtained;
- (6) I am fully aware that if in the course of making this Work I have infringed any copyright whether intentionally or otherwise, I may be subject to legal action or any other action as may be determined by UM.

Candidate’s Signature

Date:

Subscribed and solemnly declared before,

Witness’s Signature

Date:

Name: **MAYEEN UDDIN KHANDAKER**

Designation: **ASSOCIATE PROFESSOR**

ABSTRACT

To meet the increasing demand for power generation due to the rapid growing urbanization and industrialization, Nigeria-the most populated country of Africa, is reactivating her coal industry as supplementary energy source. Maiganga coal-field is one of the recently discovered coal deposits in northeast Nigeria that is receiving great attention from the investors and entrepreneurs of coal energy. The deposit is also a prime target for power generation by Nigerian government, yet little is known about the basic properties of the deposit. In this study, radiological, trace elemental and petrographic analyses were performed in coal samples from Maiganga coal-field in order to determine the intrinsic characteristics of the coal deposit, and to understand the environmental and human health challenges that may be associated with its exploitation and utilization. Radiological characterization of coal samples from Maiganga coal-field was done using a P-type coaxial HPGe gamma-ray detector, while the trace elemental concentrations was determined by using inductively coupled plasma-mass spectrometry (ICP-MS). Organic petrographic analysis was performed on polished coal blocks using a LEICA CTR 6000 Orthoplan microscope under monochromatic and ultraviolet light illumination. Proximate analysis was carried out on pulverized coal samples using Perkin Elmer Diamond Thermogravimetric-Differential Thermal Analyser (TG-DTA). The obtained results showed that mean activity concentrations of ^{226}Ra , ^{232}Th , and ^{40}K in the analyzed coal samples were 8.0 ± 3.5 , 7.0 ± 2.4 and 27.4 ± 11.4 Bq kg^{-1} respectively. These values were found to be very low relative to the world average values of 20, 20, and 50 Bq kg^{-1} respectively, provided by the United Nations Scientific Committee on the Effects of Atomic Radiation. Calculated radiological hazard parameters were all below safety limits provided for environmental and human protection. Concentrations of trace elements were found to be low relative to the world average values for low rank coals. Estimated enrichment/depletion factor was found to be less than one, indicating that coals from

Maiganga coal-field are depleted in trace elements including those that are potentially hazardous. The results of petrographic analyses revealed that among the three available maceral groups, vitrinite macerals dominated the studied coal samples with average percentage composition of 41.50%. Mean random vitrinite reflectance varies from 0.25 to 0.52%. This suggested thermally immature lignite to subbituminous coal rank. The studied coal samples were characterized by low ash yield (3.9 to 9.9 %), which justifies government's expectations of good quality coal for power generation, and for industrial and domestic consumption. This study revealed that exploitation and utilization of coals from Maiganga coal-field for whatever purpose is therefore safe from the perspective of human health and environmental protection.

ABSTRAK

Bagi memenuhi permintaan yang semakin meningkat bagi penjanaan kuasa kerana perkembangan pesat urbanisasi dan perindustrian yang pesat Nigeria negara yang paling ramai penduduk di Afrika, telah mengaktifkan semula industri arang batu sebagai sumber tenaga tambahan. Medan arang batu Maiganga adalah salah satu daripada deposit arang batu yang baru-baru ini ditemui di timur laut Nigeria telah menerima perhatian yang besar daripada pelabur dan usahawan tenaga arang batu. Deposit ini juga merupakan sasaran utama untuk penjanaan kuasa oleh kerajaan Nigeria, namun hanya sedikit yang diketahui mengenai sifat-sifat asas deposit ini. Dalam kajian ini, radiologi, analisa unsur-unsur dan analisis petrografi telah dijalankan ke atas sampel arang batu dari medan arang batu Maiganga untuk menentukan ciri-ciri intrinsik deposit arang batu tersebut dan untuk memahami cabaran alam sekitar dan kesihatan manusia yang boleh dikaitkan dengan eksploitasi dan penggunaannya. Pencirian Radiologi sampel arang batu dari lombong arang batu Maiganga telah dilakukan dengan menggunakan HPGe gamma spektrometer, manakala sampel telah dianalisis untuk mengesan kepekatan unsur menggunakan induktif ditambah spektrometri jisim plasma (ICP-MS). Analisis petrografi organik telah dilakukan ke atas blok arang batu yang digilap menggunakan LEICA CTR 6000 Orthoplan mikroskop di bawah pencahayaan cahaya monokromatik dan ultraungu. Analisis proksimat telah dijalankan ke atas sampel arang batu hancur menggunakan PerkinElmer Diamond Termogravimetri-Berbeza Analyser Thermal (TG-DTA). Hasil kajian menunjukkan bahawa kepekatan aktiviti min ^{226}Ra , ^{232}Th dan ^{40}K dalam sampel arang batu adalah masing-masing 8.18 ± 3.5 , 6.97 ± 2.4 dan 27.38 ± 11.4 Bq kg⁻¹. Nilai-nilai ini didapati relatif sangat rendah dibanding dengan nilai purata dunia sebanyak 20, 20 dan 50 Bq kg⁻¹ masing-masing mengikut yang disediakan secara turutan oleh Jawatankuasa Sainifik Pertubuhan Bangsa-Bangsa Bersatu mengenai Kesan Radiasi Atom. Didapati semua parameter bahaya radiologi adalah di bawah had keselamatan yang diperuntukkan

bagi perlindungan alam sekitar dan manusia. Kepekatan unsur surih didapati rendah berbanding nilai purata dunia untuk arang pangkat rendah. Anggaran faktor pengkayaan / pengurangan telah didapati kurang daripada satu, yang menunjukkan bahawa arang dari lombong arang batu Maiganga berkuranga dalam unsur-unsur surih yang berpotensi merbahaya. Keputusan juga menunjukkan bahawa antara ketiga-tiga kumpulan maceral yang diwakili secara petrografik, macerals vitrinite menguasai sampel arang batu yang dikaji dengan purata komposisi peratusan 41.50%. Min pantulan vitrinite rawak berbeza 0.25-0.52%, menunjukkan arang batu subbituminous tidak matang haba ber darjat dari lignit ke arang batu subbitumin. Sampel arang batu dikaji telah menghasilkan rendah abu yang (3.9 hingga 9.9%), yang mewajarkan jangkaan kerajaan bahawa arang batu ini berkualiti untuk penjanaan kuasa untuk kegunaan industri dan domestik. Kajian ini mendedahkan bahawa eksploitasi dan penggunaan arang dari Maiganga medan arang batu untuk apa sahaja tujuan adalah selamat dari perspektif kesihatan manusia dan perlindungan alam sekitar

ACKNOWLEDGEMENTS

“I had fainted, unless I had believed to see the goodness of the LORD in the land of the living (Psalms 27:13)”

The successful completion of this research work is one of the numerous goodness of the LORD I have seen in my life. I give all the glory, honour, and adoration to HIM who liveth forevermore, and never fails. I owe it all to HIM.

My supervisors, Prof. Dr. Yusoff Mohd Amin, Prof. Dr. Wan Hasiah Binti Abdullah, and Assoc. Prof. Dr. Mayeen Uddin Khandaker, contributed in no small measure to see to the successful completion of this research. Their dedication, devotion, availability, advice, and critical scrutiny of this work brought out the substance thereof. I will forever remain grateful to them.

University of Malaya provided enabling environment for this research. Their financial contribution through the research grants: **FP042-2013A**, and **RP006D-13AFR**, are highly acknowledged.

I am highly indebted to the Federal Government of Nigeria, and the management of Federal University of Technology, Minna, for the sponsorship of this research through the provision of Tertiary Education Fund (TetFund).

The cooperation, and assistance of the management, and members of staff of Maiganga coal mine, and Ashaka Cement Factory, Gombe, during my sample collection exercise is highly appreciated.

My dear friend, sister, and colleague, Mrs. Irene Crown of blessed memory; we began this race together but it pleased the LORD to call you home so early. My colleagues in the department of Physics, FUT, Minna, especially my head of department, Prof. Uno Uno, Dr. Kasim Uthman Isah and Prof. A. N. Baba-kutigi who stood through with me, I say thank you. The efforts of my good friend in Geology department, Dr. U. S. Onoduku who assisted all through the period of the research never go unnoticed.

My friends, and colleagues in Radiation Laboratory: Mr. Azman Mat Nor, Asaduzzaman Khandoker, Farhad, Ahmed Rufai, Michael Olakunle, Hauwaukulu Shuaibu, and Mrs. Becky. We worked together, played together, and laughed together until this work is completed. I appreciate your friendship. The cooperation and contributions of Mr Zamri and other members of staff of Organic Petrology Laboratory, ICP-MS and XRF laboratories are highly appreciated.

Pantai Baptist Church has been a very wonderful and exciting home away from home for me. Members of my care group (CG) led by brother Prathab have been so supportive in prayers, care and fellowship all through the period of this research. Members of The Life Chapel played very significant role in making sure I was comfortable throughout my research period. Your labours of love will never go unrewarded.

My Chaplain, Pastor Dr. Michael Onimole, and the entire members of Chapel of Grace, FUT Minna who stood with me in prayers, and thoughts throughout the period of this research, I say thank you. Late Mrs. Biola Onimole (Mama Chaplain) who labored in prayers and thoughts to see that I finish this work. It pleased the LORD to call you home before the completion but the proof of your labour still stands as a testimony. I love you dearly mama and will always remember you.

My family, the KOLOS and the OSSOMS...I really appreciate you all. My friends too numerous to mention who contributed in cash, kind, prayers, and thoughts to the success of this research. I am forever thankful.

Finally, the wife of my youth, Mary. Your understanding, support, and sacrifice throughout the time of my being away from home and from you can never go unnoticed. You were there all the way, and prayed through with me. I love you, and appreciate you.

University of Malaysia

TABLE OF CONTENTS

Abstract	iii
Abstrak	v
Acknowledgements	vii
Table of Contents	ix
List of Figures	xiii
List of Tables.....	xv
List of Symbols and Abbreviations.....	xvii
List of Appendices	xix
CHAPTER 1: INTRODUCTION.....	1
1.1 General Background	1
1.2 Objectives of this research.....	5
1.3 Scope of the study.....	6
CHAPTER 2: LITERATURE REVIEW.....	10
2.1 Introduction.....	10
2.2 Natural Radioactivity.....	10
2.2.1 Cosmogenic radioactivity	12
2.2.2 Primordial radioactivity.....	13
2.2.2.1 Non-series radionuclides	15
2.2.2.2 Decay series radionuclides	16
2.2.3 Anthropogenic radioactivity.....	23
2.3 Secular Radioactive Equilibrium.....	25
2.4 Radioactive Disequilibrium	27
2.5 Environmental and Health Impacts of Coal Use	27

2.6	Natural Radioactivity in Coal	30
2.7	Potentially Hazardous Trace Elements in Coal	37
2.8	Gamma-ray Spectrometry	46
2.8.1	Detector characterization	48
2.8.1.1	Energy resolution	49
2.8.1.2	Energy calibration	49
2.8.1.3	Efficiency calibration	49
2.8.2	Minimum detectable activity (MDA)	50
2.9	Elemental Analysis of Coal using the ICP-MS Technique	51
2.10	Geology of Coal	55
2.10.1	Lignite	56
2.10.2	Bituminous coal	57
2.10.3	Anthracite	57
2.11	Coal Petrography	57
2.11.1	The Vitrinite (Huminite) Group	58
2.11.2	The Liptinite (Exinite) Group	58
2.11.3	The inertinite Group	58
2.11.4	The vitrinite reflectance (R_0 %)	59
CHAPTER 3: MATERIALS AND METHODS		64
3.1	Sample Site	64
3.2	Sample Collection and Processing	64
3.3	Sample Preparation and Analysis	67
3.3.1	Radiological Analysis	67
3.3.1.1	Gamma spectrometric measurement	67
3.3.1.2	Radiation hazard indices	73
3.3.2	Trace Elements Analysis	77

3.3.3	Proximate Analysis.....	79
3.3.4	Petrographic Analysis.....	79
CHAPTER 4: RESULTS.....		82
4.1	Detector Efficiency Curve	82
4.2	Minimum Detectable Activity (MDA)	83
4.3	Natural Radioactivity in Coal from Maiganga Coalfield	83
4.4	Natural Radioactivity in Coal Mine Tailings from Maiganga Coalfield.....	88
4.5	Natural Radioactivity in Soil Samples around Ashaka Cement Factory	91
4.6	Trace Elements Concentrations in Coal Samples from Maiganga Coalfield	95
4.7	Proximate and Petrographic Analysis of Coal from Maiganga Coalfield	97
4.7.1	Maceral Composition	100
4.7.2	Vitrinite Reflectance.....	101
CHAPTER 5: DISCUSSIONS		102
5.1	Natural Radioactivity Contents of Coal Samples from Maiganga Coalfield	102
5.1.1	Correlation Coefficients of Radiological Parameters of Coal Samples from Maiganga Coalfield	107
5.2	Trace Elements Contents of Coal Samples from Maiganga Coalfield.....	108
CHAPTER 6: CONCLUSION.....		112
	References	115
	List of Publications and Papers Presented	132
	Appendix A	135
	Appendix B	152
	Appendix C	153
	Appendix D.....	155

Appendix E	158
Appendix F.....	162
Appendix G.....	164
Appendix H.....	167

University of Malaya

LIST OF FIGURES

Figure 1.1: Geographical location of the Benue Trough in Nigeria (after Obaje & Ligouis, 1996)	6
Figure 1.2: Coal/Lignite occurrences in Nigeria (Modified from Adedosu et al., 2007) .	7
Figure 2.1: Secular equilibrium between the parent and daughter radionuclides (after Martin, 2006)	26
Figure 2.2: Block diagram of a gamma-ray spectrometer	47
Figure 2.3: Block diagram of ICP-MS	54
Figure 2.4: Schematic presentation of coalification process and coal classification (www.uky.edu/KGS/coal/coalkinds.htm)	56
Figure 3.1: Map of Nigeria showing the sample site	65
Figure 3.2: Maiganga coal mine tailings: (a) panoramic view (b) close up view	66
Figure 3.3: Coal and tailings samples preparation and packaging for the current study	68
Figure 3.4: High purity germanium detector system used in the present study	70
Figure 3.5: Standard gamma-ray calibration source	71
Figure 3.6: (a) Digested coal samples (b) Agilent Technologies 7500 series	78
Figure 3.7: Perkin Elmer Diamond Thermogravimetric-Differential Thermal Analyzer (TG-DTA) used in this study	79
Figure 3.8: Polished coal blocks	80
Figure 3.9: LEICA CTR DM6000 Orthoplan Microscope used in this study	81
Figure 4.1: Efficiency calibration curve of the HPGe gamma-ray detector used in this study	82
Figure 4.2: Proximate analysis of Maiganga coal using TGA	98
Figure 5.1: Frequency distribution histograms of (a) ^{226}Ra , (b) ^{232}Th , (c) ^{40}K in coal samples from Maiganga coalfield	104
Figure 5.2: Comparison of activity concentrations (Bq kg^{-1}) of ^{226}Ra , ^{232}Th and ^{40}K in coal samples from Maiganga coalfield with the World average values and those of other published works	105

Figure 5.3: Elemental concentration of ^{226}Ra , ^{232}Th (ppm) and total ^{40}K (%) in coal samples from Maiganga coalfield 106

University of Malaya

LIST OF TABLES

Table 2.1: The Global Average Annual Effective Dose from Natural Radiation Sources (UNSCEAR, 1988)	11
Table 2.2: Most precisely studied cosmogenic nuclides in the earth's atmosphere (modified from Froehlich, 2010).....	12
Table 2.3: Primordial natural radionuclides, half-lives, typical range of concentrations in the earth, and the type of decay (α , β^- , γ , electron capture EC), (Froehlich, 2010). ...	14
Table 2.4: Non-series radionuclides (Froehlich, 2010).....	16
Table 2.5: ^{238}U decay series (Adopted from IAEA, 2004)	18
Table 2.6: ^{235}U decay series (Adopted from IAEA, 2004)	19
Table 2.7: ^{232}Th decay series (Adopted from IAEA, 2004).....	20
Table 3.1: Nuclides contained in the standard calibration source with their respective energies	71
Table 4.1: Decay data for radionuclides and the respective gamma lines and MDA (Bq kg^{-1}) used for activity determination	83
Table 4.2: Activity concentrations (Bq kg^{-1}) of ^{226}Ra , ^{232}Th , and ^{40}K , in coal samples from Maiganga coalfield.....	85
Table 4.3: Radiation hazard indices of coal samples from Maiganga coalfield	87
Table 4.4: Descriptive statistics of activity concentrations, and concentration ratios of ^{226}Ra , ^{232}Th , ^{40}K , in coal mine tailings from Maiganga coalfield	89
Table 4.5: Radiological hazard indices of coal mine tailings from Maiganga coalfield.	91
Table 4.6: Activity concentrations (Bq kg^{-1}) of ^{226}Ra , ^{232}Th , and ^{40}K , in soil samples around AshakaCem	92
Table 4.7: Radiological hazard indices of soil samples around AshakaCem	94
Table 4.8: Trace elements concentrations (mg kg^{-1}) of coal samples from Maiganga coalfield. PHTEs are bold and underlined	95
Table 4.9: Descriptive statistics including minimum, maximum, mean and standard deviation of trace elements concentrations (mg kg^{-1}) in coal samples from Maiganga coalfield, along with their respective Clarke values and enrichment/depletion factors..	97

Table 4.10: Proximate analysis of coal samples from Maiganga coalfield.....	99
Table 4.11: Mean random vitrinite reflectance (R_{om}) and maceral composition of coal samples from Maiganga coal-field.....	100
Table 5.1: Descriptive statistics of radiological parameters of coal samples from Maiganga coalfield.....	103
Table 5.2: Correlation matrix of radiological variables for coal samples from Maiganga coalfield.....	108
Table 5.3: Correlation matrix of elemental composition and ash yield for coal samples from Maiganga coalfield	110

University of Malaya

LIST OF SYMBOLS AND ABBREVIATIONS

AAS	:	Atomic absorption spectrometry
AEDE	:	Annual effective dose equivalent
ALARA	:	As low as reasonably achievable
AMD	:	Acid mine drainage
ASS	:	Ashaka soil sample
AUI	:	Activity utilization index
bdl	:	Below detection limit
CFTPP	:	Coal fired thermal power plant
D _R	:	Absorbed dose
EDF	:	Enrichment/depletion factor
EDXRF	:	Energy dispersive x-ray fluorescence
ELCR	:	Excess lifetime cancer risk
H _{ex}	:	External hazard index
H _{in}	:	Internal hazard index
HPGe	:	High purity germanium
IAEA	:	International atomic energy agency
ICP-MS	:	Inductively coupled plasma mass spectrometry
ICP-OES	:	Inductively coupled plasma optical emission spectrometry
ICRP	;	International commission for radiological protection
INAA	:	Instrumental neutron activation analysis
MCS	:	Maiganga coal sample
MDA	:	Minimum detectable activity
NEA-OECD	:	Nuclear energy agency-Organization of economic cooperation and development

NORM	:	Naturally occurring radioactive materials
PHTEs	:	Potentially hazardous trace elements
PIXE	:	Particle induced x-ray emission
R _{aeq}	:	Radium equivalent activity
TENORM	:	Technologically enhanced naturally occurring radioactive materials
TG-DTA	:	Thermogravimetric-Differential thermal analyzer
UNSCEAR	:	United nations scientific committee on the effects of atomic radiation
USEPA	:	United states environmental protection agency
WDXRF	:	Wavelength dispersive x-ray fluorescence
XRF	:	X-ray fluorescence

University of Malaya

LIST OF APPENDICES

Appendix A: Physics of radioactive decay.....	135
Appendix B: Certificate of gamma-ray calibration standard source for HPGe.....	152
Appendix C: Certificate of calibration standard source for ICP-MS.....	153
Appendix D: Calculation of activity concentrations for primordial radionuclides	155
Appendix E: Calibration curves of standards for trace elements.....	158
Appendix F: Vitrinite reflectance histograms for coal.....	162
Appendix G: Photomicrographs of maceral composition of coal.....	165
Appendix H: Graphs of proximate analysis of coal.....	167

University of Malaya

CHAPTER 1: INTRODUCTION

1.1 General Background

Increasing attention worldwide, has been focused on effective utilization of fuel resources in an environmentally friendly manner to meet the global energy demand due to population explosion and the challenge of industrial and technological exploits of the 21st century. With coal being a basic natural fossil fuel principally for power generation in most parts of the world, and a major contributor to national economy (Tsikritzis et al., 2008), a detailed understanding of its intrinsic properties is paramount to the development of clean coal technologies to enhance its use effectively. This therefore make coal characterization a principal goal to pursue (Gupta, 2007). Coal is a highly heterogeneous and complex natural fuel, whose characterization pose serious challenge especially in relating its basic structure to its conversion and processing characteristics. Various analytical techniques are therefore required to accurately predict the behavior of this complex material during its combustion, gasification, coking, and liquefaction processes.

The most resourceful, easily accessible, readily available and relatively abundant fossil energy source that powered the industrial revolution of the tenth century was coal. Coal, which ranked second after crude oil in the energy resources chat of the world, still remains an indispensable energy source in Nigeria and many developing nations. Coal offers a readily available substitute for fuel wood in meeting the domestic energy demands of developing nations.

One of Africa's largest deposits of coal is found in Nigeria. Coal was the first energy source exploited in Nigeria (Borishade et al., 1985; Obaje et al., 1996; Ogala et al., 2012), and played a very significant role in her economic development and in powering of the Nigerian railway transport system. The discovery of crude oil, and the appearance of petroleum on the economic scene of Nigeria, along with the commissioning of hydro-

electric dams and complete dieselization of Nigerian railways, led to a complete neglect of the coal industry with all its great economic potentials, and established an economic system that is almost entirely driven by crude oil and its by-products. Researches have however shown that at present exploitation rate, static and dynamic life indices of Nigeria's crude oil and natural gas are declining at a very fast rate (Borishade et al, 1985). Recent power problems in Nigeria also shows that the dependence on oil and hydroelectric dams for power generation which have suffered due to interruptions in oil output/supply and severe dry seasons, has not yet leveraged Nigeria for electricity and power generation. In response to these challenges, therefore, the Nigerian government is aggressively pushing for the resuscitation and reactivation of her coal industry to serve as a supplementary energy source for Nigeria's growing economy. Coal deposits which have long been neglected and abandoned as a result of crude oil discovery are being re-investigated for their power generation potentials and other coal conversion derivatives. The progressive search for coking coals for steel and iron industries, and continuous search for potential raw materials for the production of wide variety of industrial chemicals like dyes, resins, waxes, adhesives, has also stimulated Nigeria's current interest in in-depth assessment of entire coal industry of the country.

Exploration and exploitation of coal deposits in Nigeria have been intensified in recent years with a view to diversify the nation's oil and gas driven economy. Coal from Nigeria is conveniently efficient as boiler fuel, for production of high calorific gas, and manufacturing of coal briquettes as a viable substitute for kerosene, charcoal, gas and firewood. Ogala et al. (2012), reported that in present day Nigeria, coal has become useful domestic fuel in cement production, brick making industries, foundries, laundries and bakeries. It is an indispensable raw material for the manufacturing of tire and batteries, and a proven alternative for wood in domestic cooking and heating. Coal beds also serve

as principal sources of associated and non-associated gases and have therefore become exploration targets for gas accumulations (Obaje et al., 1996).

However, despite these obvious and indispensable benefits of coal, the entire coal cycle, beginning from exploration to energy production, gave rise to high rate of resource consumption and unprecedented impacts on human health and environment. Domestic coal use in several nations have resulted in severe consequences on human health, which can only be minimized through a clear understanding of coal quality parameters. Coal, like most materials found in nature, contains trace quantities of naturally occurring radioactive materials (NORM) and diverse amounts of potentially hazardous trace elements (PHTE) in their overall composition, some of which, if present in high amounts, could preclude coal from being used in environmentally sensitive situations (Ward, 1984). All processes of coal fuel-cycle, beginning from mining and combustion, to the use and disposal of ash residue are potential exposure routes to natural radiation.

NORM contained in the parent coal matrix are assumed to be in circular equilibrium with their decay products, except for radon and thoron which, according to UNSCEAR (1982) and Corbett (1983), can in some cases escape due to their mobility and inertness. Human activities distorts the overlying geological strata, thereby creating an imbalance in the existing radionuclide equilibrium by releasing the parent radionuclides along with their decay daughters from the original coal matrix, and also causing a redistribution of various hazardous metals in the mine wastes. These enriched wastes are often stock piled in free access areas almost without protection, which according to Charro and Pena (2013), can be affected by meteorological conditions resulting in various environmental problems, ranging from impulsive combustion of waste dumps to mobilization of materials and emergence of acid mine drainage (AMD). Radionuclides and hazardous metals in the waste piles could be leached into the surrounding soil and water bodies

thereby causing water contamination, and enhanced potential for human exposure. During coal combustion process, the terrestrial radionuclides (like ^{238}U , ^{232}Th) and toxic elements (like As, Cd, Cr, Ni, Co, Cu and Sb) present in coal are concentrated and enriched in combustion residue and subsequently transferred into the environment through natural environmental processes. Some are released into the atmosphere along with flue gases, and through inhalation, become a potential health threat to man. Furthermore, radiation hazard can come from solid fallouts, which can enhance the natural radioactivity levels of soils around any coal-fired power plants. Direct or indirect release of coal wastes in human environment can thus cause a redistribution of natural radioactivity from deep storage locations, thereby modifying ambient radiation fields and increasing the radiation load on plant workers and the surrounding environment. The general public is also at risk of enhanced exposure when the combustion residues are used as composites of building materials and as materials for insulation in the construction industry, especially that the collective build-up, extreme toxicity and long life of elements contained in it poses health risk to humans, plants and animals. This has therefore, made the entire coal circle a matter of public and scientific concern.

The growing concern about the impact of radioactive elements and potentially hazardous trace elements in coal and coal residues, there is the need to evaluate the human health and environmental impacts of the entire coal fuel cycle. For Nigeria to make quality decision and productive policies for optimum exploitation and utilization of coal in an environmentally friendly conditions, there is the need for a detailed, comprehensive and complimentary information and data on the nature and levels of concentration of the organic and the inorganic components together with potentially hazardous trace elements composition and radionuclide concentrations of Nigerian coals especially for environmental and human protection purposes. Information on the concentrations of these potentially hazardous coal entities and their interrelationships with the inorganic and

organic constituents in which they occur in coals is a necessary tool for anticipating their behaviour in coal cleaning, coal combustion, weathering and leaching processes.

1.2 Objectives of this research

The objectives of this research include:

1. Assessment of activity concentrations of natural radionuclides in coal of the Maiganga coalfield
2. Estimation of radiation hazard parameters from exposure to natural radionuclides in coal from the Maiganga coalfield
3. Measurement of elemental concentrations in coal from the Maiganga coalfield
4. Evaluation of enrichment/depletion levels of potentially hazardous elements in coal from Maiganga coalfield
5. Analysis of petrographic properties of coal from Maiganga coalfield
6. Establishment of baseline data for primordial radionuclides and elemental contents of coal from Maiganga coalfield.

The overall aim of this investigation is to provide sufficient information on radiation exposure of workers and the general public to NORM in the coal industry. This study will also attempt to generate data on PHTE in Nigerian coal. It is hoped that this will assist the Nigerian government to reform her policy for diversifying the economy through the optimal utilization of her coal resources. It is also the intention of this research to assist the regulatory authorities in making quality decisions for the safety of man and his environment from the effects of metal pollution and excessive radiation exposure due to exploitation and utilization of coal.

1.3 Scope of the study

The coal resources of Nigeria are located in the Lower, Middle and the Upper Benue Trough. As seen in Figure 1.1, The Benue Trough of Nigeria is a sedimentary basin that extends in a NE-SW direction, from the Gulf of Guinea in the south to the Chad basin in the north (Ogala et al., 2012).

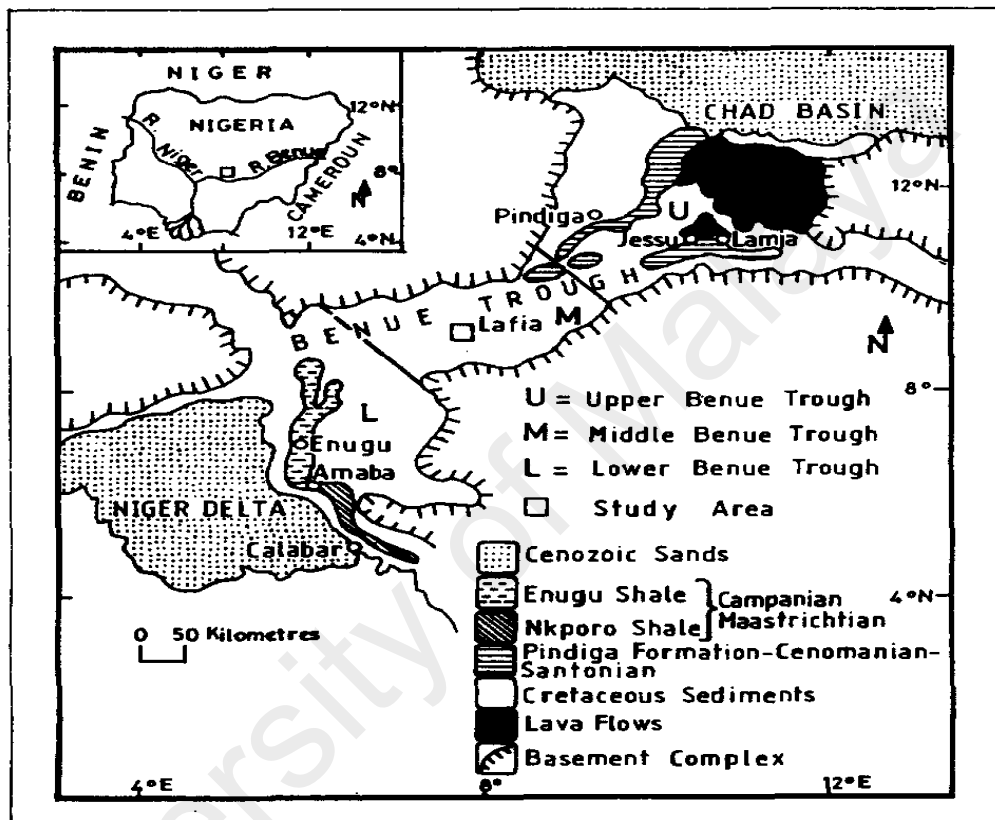


Figure 1.1: Geographical location of the Benue Trough in Nigeria (after Obaje & Ligouis, 1996)

A lot of exploration and exploitation work has been done on majority of Nigerian coal deposits as seen in Figure 1.2, and enough information about their characteristics and petrographic properties have appeared in literatures. Little is however known about the Maiganga coal deposit, being a recently discovered coalfield, which therefore makes it the prime target of this research.

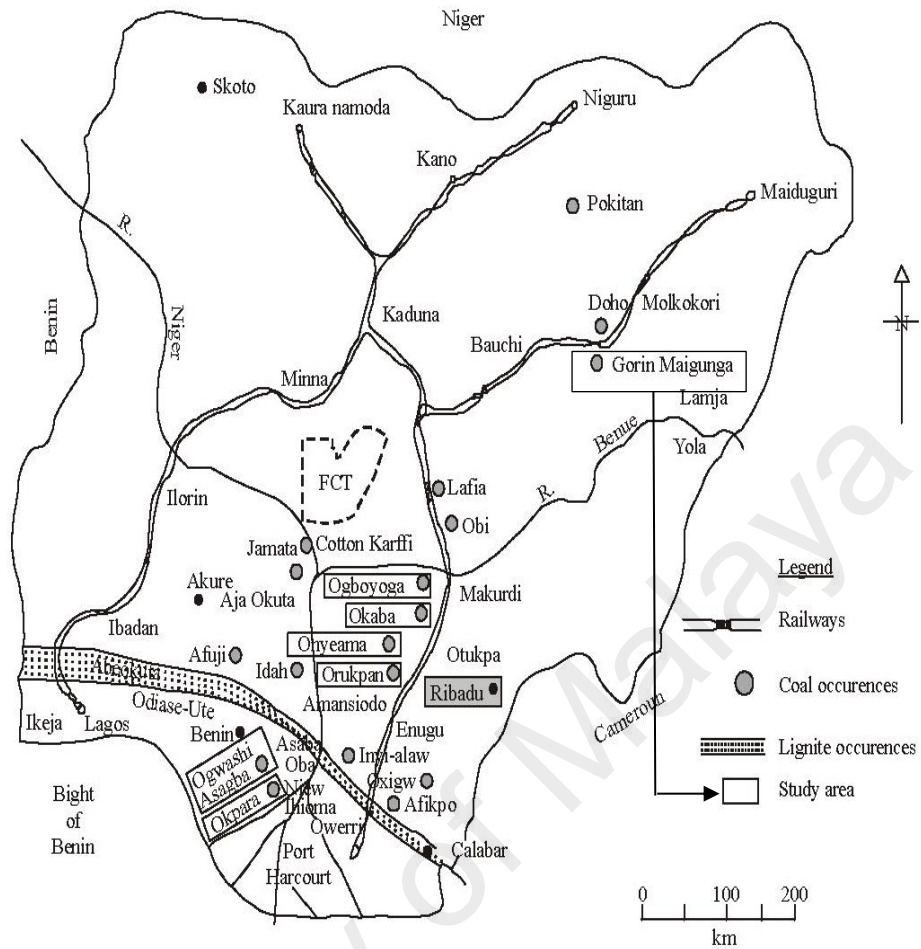


Figure 1.2: Coal/Lignite occurrences in Nigeria (Modified from Adedosu et al., 2007)

Maiganga coal deposit is one of the recently discovered coal fields whose intrinsic characteristics are yet to be understood. This deposited is targeted by the Nigerian government for power generation. Intense exploration is going on presently in this deposit to ascertain the quantity and the quality of the coal. Coal from Maiganga coalfield is mined currently, and used for firing the kilns of the largest cement producing factory in north-eastern Nigeria: the Ashaka Cement Factory, Gombe.

Maiganga is a local community in Akko local government of Gombe state in north-eastern Nigeria. Onoduku et al. (2013) reported that the Maiganga coal mine is underlain by Gombe formation. Gombe Formation which is an integral part of the larger benue

trough of Nigeria, is heterogeneous in nature, composed of a mixture of clays, sands, shales and thin coal seams.

Gamma spectrometric technique using HPGe detector is employed to undertake an in-depth radiological studies of coal samples and coal mine wastes (tailings) collected from the Maiganga coalfield. The coal samples are investigated for their trace element compositions using the inductively coupled plasma mass spectrometry (ICP-MS). Finally, petrographic analysis of coal samples from Maiganga coalfield has been undertaken to gain an idea about the maturity and maceral composition.

It is becoming increasingly important to, as a matter of urgency, resolve the present energy crisis experienced in Nigeria. Current challenges in Nigeria's power supply sector which are consequent upon fluctuations in oil market economy and inconsistent seasonal variations, have proved the futility of relying on oil and hydroelectric dams for power generation. Nigeria must therefore, diversify its power-generation portfolio and consider the effective exploitation of her abundant coal resources for national benefit and development.

Although coal has become a readily available alternative for power generation in Nigeria, the deleterious effects of coal mining and utilization on the health of coal mine workers, general public and the environment cannot be ignored. Mining has been associated generally with accidental deaths and sometimes incurable deadly diseases. It is therefore important that Nigerian government and the regulatory agencies are prepared and well equipped to combat these challenges. This can only be possible if there is clear understanding of the basic properties and characteristics of coal and coal residues. It is the aim of this research therefore to address the critical necessity of acquiring fundamental radiological, elemental and petrographic data of Maiganga coalfield, and to use these

data beyond the traditional boundaries to address local and national environmental issues that may be associated with its exploitation and utilization.

University of Malaya

CHAPTER 2: LITERATURE REVIEW

2.1 Introduction

This chapter comprise a comprehensive literature review on the natural radioactivity in human environment. Natural radioactivity and trace elements contents of coal were discussed from the point of view of human health and environmental protection. The chapter also x-rayed various studies on natural radioactivity and elemental concentrations in different coals around the world and the environmental and human health implications of coal fired thermal power plants. The chapter concluded with a brief discussion on the geology of coal and its petrographic properties.

2.2 Natural Radioactivity

Naturally occurring radioactive materials (NORMs) have been part and parcel of the world since creation. The planet and its atmosphere, the living and the non-living species on earth with the global environment that surrounds them, contains different species of NORM at varying degrees. According to Eisenbud and Gesell (1997), majority of the natural radionuclides that now exist were produced when the matter that formed the universe came into existence several billion years ago; thus life on earth has developed under the ubiquitous presence of environmental radiation. The major constituents of NORMs are uranium (^{238}U), thorium (^{232}Th) and their respective decay daughter radionuclides, together with potassium (^{40}K). These long-lived radionuclides contain some decay daughters with long lives, together with ^{222}Rn in their progeny (IAEA, 2003).

Natural radioactivity is distributed extensively in human environment. It can be found in different geological formations such as water, air, plants, rocks and soils (Ibrahiem et al., 1993; Malanca et al., 1996). Many biochemical processes and actions of some organisms transfers these radionuclides from their respective geologic media into the

biosphere where they get bio-accumulated in the food chain, and so serve as major exposure route to man.

Natural sources of radiation which have accompanied life on earth have traditionally been classified into three main types:

1. Cosmogenic (extra-terrestrial) radioactivity,
2. Primordial (terrestrial) radioactivity, and
3. Anthropogenic (man-made) radioactivity.

Table 2.1, below, give the annual effective dose rates incurred from respective radionuclides.

Table 2.1: The Global Average Annual Effective Dose from Natural Radiation Sources (UNSCEAR, 1988)

Source of irradiation	External (mSv/y)	Internal (mSv/y)	Total (mSv/y)
Cosmic rays	0.410 (17)		0.410 (17)
Cosmogenic radionuclides		0.015 (1)	0.015 (1)
Natural sources:			
⁴⁰ K	0.150 (6)	0.180 (7)	0.330 (13)
²³⁸ U-series	0.100 (4)	1.239 (51)	1.339 (55)
²³² Th-series	0.160 (7)	0.176 (7)	0.336 (14)
Total	0.820 (34)	1.616 (66)	2.436 (100)

Note: relative values are given in brackets (%)

Cosmogenic radionuclides comes from continuous interactions between cosmic rays and the stable nuclides in the atmosphere or the lithosphere. Primordial radionuclides have sufficiently long half-lives relative to earth's existence and through their radioactive decay, have become the parents for the secondary radionuclides on the earth.

Anthropogenic radionuclides on the other hand, are man-made (artificial) radionuclides or some natural radionuclides that have become enhanced through human activities.

2.2.1 Cosmogenic radioactivity

Cosmogenic radionuclides are produced when cosmic particles of very high energy interact with the earth's atmosphere, or from atomic fragmentations in the atmosphere due to constant bombardments and from neutron capture (Kathren, 1998). These primary radiations which consists mainly of protons (87%), alpha (α -) particles (11%), light low atomic number elements ($\approx 1\%$) and electrons of very high energy ($\approx 1\%$), are highly penetrating, and isotropically impinges on the surface of the earth's atmosphere (Eisenbud & Gesell, 1997). Their production has been found to vary considerably with altitude and latitude, while their transport to the earth's surface, according to Kathren (1998), is made possible through precipitation and gravitational procedure. Table 2.2 below shows half-lives of some significant radionuclides that are produced cosmogenically.

Table 2.2: Most precisely studied cosmogenic nuclides in the earth's atmosphere (modified from Froehlich, 2010)

Nuclide	Half-life (years)
^3H	12.3
^7Be	53.6
^{10}Be	1.5×10^6
^{14}C	5730
^{26}Al	7.30×10^5
^{36}Cl	3.08×10^5
^{81}Kr	2.13×10^5

The most biologically important cosmogenic radionuclide as seen in Table 2.2, is the isotopic carbon: ^{14}C with half-life of 5730 years. It is produced in the stratosphere through (n, p) reaction on ^{14}N . The biodynamics of ^{14}C moves from its oxidation to CO_2 which is

photosynthetically taken up by plants and finally get consumed by animals. Excretory processes and death of plants and animals, according to Kathren (1998), transfers this organic ^{14}C to both the aquatic and terrestrial environments where it undergo various natural physical and chemical processes in the active reservoir. It finally becomes transformed into organic carbonates and geologically buried passive reservoirs of coal or oil. Combustion of fossil fuels, volcanism and weathering processes eventually returns the carbon to the atmosphere. The annual equivalent dose to man from ^{14}C is the highest among all the cosmogenic radionuclides, which according to NCRP (1989), accounts for more than 99% of the total. Generally, however, cosmic radiation levels is less on surface of the earth due to the shielding effect of the atmosphere that reduces its intensity.

2.2.2 Primordial radioactivity

These are radionuclides with sufficiently long decay half-lives in comparison with the age of the earth (Eisenbud & Gesell, 1997). Primordial radionuclides with their respective half-lives as listed in Table 2.3, are the most prominent component of natural radionuclides on earth. Considering human exposure scenario, only the three chains of radioactive elements and the long-live ^{40}K accounts for much of the radiation dose to man (Eisenbud & Gesell, 1997), either directly or by incorporation into the body through ingestion or inhalation.

Table 2.3: Primordial natural radionuclides, half-lives, typical range of concentrations in the earth, and the type of decay (α , β^- , γ , electron capture EC), (Froehlich, 2010).

Nuclide	Half-life (y)	Abundance (%)	Decay mode
^{40}K	1.27×10^9	0.012	EC, β^- , γ
^{238}U	4.47×10^9	99.275	α
^{232}Th	1.41×10^{10}	100.000	α
^{235}U	7.04×10^8	0.720	$\alpha\gamma$
^{176}Lu	3.78×10^{10}	2.590	EC, β^- , γ
^{187}Re	4.35×10^{10}	62.600	$(\alpha)\beta^-$
^{87}Rb	4.75×10^{10}	27.835	β^-
^{147}Sm	1.06×10^{11}	15.000	α
^{138}La	1.05×10^{11}	0.090	EC, β^- , γ
^{190}Pt	6.50×10^{11}	0.010	α
^{115}In	4.41×10^{14}	95.710	β^-
^{180}W	1.10×10^{15}	0.135	α
^{144}Nd	2.29×10^{15}	23.800	α
^{50}V	1.40×10^{17}	0.250	EC, β^- , γ
^{142}Ce	$>5.00 \times 10^{16}$	11.080	α
^{152}Gd	1.08×10^{14}	0.200	α
^{152}Gd	$>1.00 \times 10^{14}$	0.146	α
^{209}Bi	$>2.00 \times 10^{18}$	100.000	α

Froehlich (2010), and Eisenbud and Gesell (1997), classified the primordial radionuclides into two groups:

- (a) Those that occur singly and decay directly into a stable nuclide, and
- (b) Those that undergo chain of radioactive decay into a stable isotope of the element lead.

2.2.2.1 Non-series radionuclides

From the bioenvironmental stand point, ^{40}K and ^{87}Rb as seen in Table 2.4, are two significant non-series natural radionuclides that contribute substantially to terrestrial radiation background dose (Froehlich, 2010; Kathren, 1998). ^{40}K , the only radioactive isotope of potassium with isotopic abundance of 0.0118% (Eisenbud & Gesell, 1997), has been judged the single most important NORM of terrestrial origin. Its contribution to total radiation dose incurred by man via ingestion pathway is very significant, judging from its biological uptake and its ubiquity in the natural environment (Kathren, 1998). ^{40}K (with half-life of 1.3×10^9 years) is unstable and thus, undergo beta decay (β , $E_\beta = 1.414$ MeV) to stable ^{40}Ca . It can also decay by electron capture (lower probability) to a meta-stable ^{40}Ar which eventually falls to ^{40}Ar ground state by emitting gamma (γ -) ray. ^{40}K can also decay through positron emission by giving off a characteristic 1.460 MeV photon which, according to Kathren (1998), is extremely suitable for its recognition and measurement by gamma-ray spectroscopy. Potassium is sufficiently widespread in the earth's crust and a paramount radionuclide in normal foods and human tissues. High energetic β emission by ^{40}K makes it a principal source of internal radiation dose after radon and its decay daughters. However, according to UNSCEAR (1982), and Eisenbud and Gesell (1997), potassium in human body is homeostatically controlled and so makes the dose from ^{40}K to be constant within the body.

Table 2.4: Non-series radionuclides (Froehlich, 2010).

Nuclide	Relative abundance (%)	Daughter Nuclide	Half-life (yrs)	Major Radiation
⁴⁰ K	0.0118	⁴⁰ Ar, ⁴⁰ Ca	1.28×10^9	β^- (89%), EC (11%)
⁵⁰ V	0.24	⁵⁰ Ti, ⁵⁰ Cr	6.00×10^{15}	β^- (30%), EC (70%)
⁸⁷ Rb	27.85	⁸⁷ Sr	4.70×10^{10}	β^-
¹¹⁵ In	96.67	¹¹⁵ Sn	5.00×10^{14}	
¹²³ Te	0.87	¹²³ Sb	1.20×10^{13}	
¹³⁸ La	0.089	¹³⁸ Ba, ¹³⁸ Ce	1.10×10^{11}	
¹⁴² Ce	11.7	¹³⁸ Ba	5.00×10^{15}	
¹⁴⁴ Nd	23.8	¹⁴⁰ Ce	2.40×10^{15}	
¹⁴⁷ Sm	15.1	¹⁴³ Nd	1.06×10^{11}	
¹⁴⁸ Sm	11.35	¹⁴⁴ Nd	1.2×10^{13}	
¹⁴⁹ Sm	14	¹⁴⁵ Nd	4.00×10^{14}	
¹⁵² Gd	0.205	¹⁴⁸ Sm	1.10×10^{14}	
¹⁵⁶ Dy	0.057	¹⁵² Gd	2.00×10^{14}	
¹⁷⁴ Hf	0.163	¹⁷⁰ Yb	4.30×10^{15}	
¹⁷⁶ Lu	2.588	¹⁷⁶ Hf	2.20×10^{10}	
¹⁸⁷ Re	62.93	¹⁸⁷ Os	4.00×10^{10}	
¹⁹⁰ Pt	0.0127	¹⁸⁶ Os	7.00×10^{11}	
²⁰⁴ Pb	1.4	²⁰⁰ Hg	1.40×10^{17}	

2.2.2.2 Decay series radionuclides

These are chain decaying natural radionuclides whose individual decay series is determined by the expression

$$A = 4n + m, \quad (2.1)$$

where A is the mass number, n the largest whole integer divisible in A, and m is the remainder. These decay series include:

- (a) Thorium series, headed by ²³²Th (4n-series),
- (b) Neptunium series, headed by ²⁴¹Pu (4n + 1series),

(c) Uranium series, headed by ^{238}U ($4n + 2$ series), and

(d) Actinium series, headed by ^{235}U ($4n + 3$ series).

The parent of neptunium series has comparatively short half-life and is therefore, dead and gone. The remaining three surviving chains whose parents are ^{232}Th with a half-life of 1.39×10^9 years, ^{235}U of half-life 7.13×10^8 years, and ^{238}U whose half-life is 4.46×10^9 years do not attain direct stability. They decay to stable isotope through successive α - and β - disintegration processes. It should be noted also that neither ^{232}Th nor ^{238}U directly emits γ - rays; their concentrations are estimated from the γ -ray emissions of their decay products.

(a) *^{238}U decay series*

Uranium is widely distributed in the environment and is present in soil, rocks and terrestrial and ocean water (Froehlich, 2010). It is found also in coal, coal plant discharges and ash (Kathren, 1998). Three uranium isotopes have been found to exist naturally: ^{238}U which heads the $4n + 2$ decay series, has a natural abundance of 99.28%, and always in equilibrium with ^{234}U whose abundance by weight is 0.0058%. ^{235}U which has natural abundance of 0.71% is the third isotope and heads the $4n + 3$ decay series (Cember & Johnson, 2009; Froehlich, 2010; Kathren, 1998). ^{238}U and ^{235}U undergo a series of 14 decays that terminates in the stable isotope of ^{206}Pb as shown in Tables 2.5 and 2.6 respectively. Some prominent intermediate products of radioactive disintegration naturally exists in circular equilibrium in the ^{238}U decay chain. They include ^{234}U , ^{230}Th , and ^{231}Pa , ^{226}Ra and ^{222}Rn , which is a potential environmental hazard. Since ^{238}U and ^{235}U do not give out gamma rays directly, their concentrations are estimated from the gamma rays emitted by their radioactive daughter products. Radon formed in the ^{238}U decay series is the only radioactive gas in the series. The decay products of radon have relatively short half-lives, and being chemically active, they attach to dust particles, indoor surfaces and human respiratory tracts.

Table 2.5: ^{238}U decay series (Adopted from IAEA, 2004)

Nuclide	Half-life	Major radiation energies (MeV) and intensities*		
		α	β	γ
^{238}U	$4.468 \times 10^9 \text{y}$	4.15 (23%) 4.19 (77%)	–	–
^{234}Th	24.1d	–	~0.103 (19%) 0.191 (81%)	0.063 (3.5%) 0.093 (4%)
^{234}Pa	1.18m	–	2.29 (98%)	0.765 (0.30%) 1.001 (0.60%)
^{234}Pa	6.7h	–	0.53 (66%) 1.13 (13%)	0.10 (50%) 0.70 (24%) 0.90 (70%)
^{234}U	$2.48 \times 10^5 \text{y}$	4.72 (28%) 4.77 (72%)	–	0.053 (0.2%)
^{230}Th	$7.52 \times 10^4 \text{y}$	4.62 (24%) 4.68 (76%)	–	0.068 (0.6%) 0.142 (0.07%)
^{226}Ra	1602y	4.60 (5.5%) 4.78 (94.5%)	–	0.186 (4%)
^{222}Rn	3.825d	5.49 (~100%)	–	0.510 (0.07%)
^{218}Po	3.05m	6.11 (100%)	0.33 (100%)	–
^{214}Pb	26.8m	–	1.03 (6%)	0.295 (19%) 0.352 (36%)
^{218}At	2s	6.65 (6%) 6.70 (94%)	0.67 (94%)	–
^{214}Bi	19.7m	5.61 (100%)	3.26 (100%)	0.609 (47%) 1.120 (17%) 1.764 (17%)
^{214}Po	164 μs	7.83 (100%)	–	0.799 (0.014%)
^{210}Tl	1.32m	–	2.3 (100%)	0.296 (80%) 0.795 (100%) 1.31 (21%)
^{210}Pb	~22y	3.7 ($1.8 \times 10^{-8}\%$)	0.017 (85%) 0.064 (15%)	0.047 (4%)
^{210}Bi	5.02d	4.93 (60%) 4.89 (34%) 4.59 (5%)	1.155 (100%)	–
^{210}Po	138.3d	5.30 (100%)	–	0.803 (0.0011%)
^{206}Tl	4.19m	–	1.520 (100%)	–
^{206}Pb	Stable	–	–	–

* Intensities refer to percentage of disintegrations of the nuclide itself, not to the original parent of the series.

Table 2.6: ^{235}U decay series (Adopted from IAEA, 2004)

Nuclide	Half-life	Major radiation energies (MeV) and intensities*		
		α	β	γ
^{235}U	$7.13 \times 10^8 \text{y}$	4.36 (18%) 4.39 (57%) 4.1-4.6 (8%)	–	0.143 (11%) 0.185 (54%) 0.204 (5%)
^{231}Th	25.64h	–	0.300 (~100%)	0.026 (2%) 0.084 (10%)
^{231}Pa	$3.43 \times 10^4 \text{y}$	5.01 (<20%) 4.99 (25.4%) 4.94 (22.8%)	–	0.027 (6%) 0.29 (6%)
^{227}Ac	22y	4.95 (48.7%) 4.94 (36.1%) 4.87 (6.9%)	0.046 (100%)	0.070 (0.08%)
^{227}Th	18.17d	5.76 (21%) 5.98 (24%) 6.04 (23%)	–	0.050 (8%) 0.237 (15%) 0.31 (8%)
^{223}Fr	21m	5.34 (.005%)	1.15 (100%)	0.050 (40%) 0.080 (13%) 0.234 (4%)
^{223}Ra	11.68d	5.61 (26%) 5.71 (53.7%) 5.75 (9.1%)	–	0.149 (10%) 0.270 (10%) 0.33 (6%)
^{219}Rn	3.92s	6.42 (8%) 6.55 (11%) 6.82 (81%)	–	0.272 (9%) 0.401 (5%)
^{215}Po	1.83ms	7.38 (100%)	–	–
^{211}Pb	36.1m	–	0.95 (1.4%) 0.53 (5.5%) 1.36 (92.4%)	0.405 (3.4%) 0.427 (1.8%) 0.832 (3.4%)
^{211}Bi	2.16m	6.28 (17%) 6.62 (83%)	0.60 (0.28%)	0.351 (14%)
^{211}Po	0.52s	7.43 (99%)	–	0.570 (0.5%) 0.90 (0.5%)
^{207}Tl	4.79m	–	1.44 (100%)	0.897 (0.16%)
^{207}Pb	Stable	–	–	–

* Intensities refer to percentage of disintegrations of the nuclide itself, not to the original parent of the series.

(b) ^{232}Th decay series

Thorium occurs essentially 100% by weight as radioisotope ^{232}Th in nature. It decays continuously until it reaches stability in ^{208}Pb as shown in Table 2.7. It exists in abundance in most crustal rocks but mostly found in acidic materials.

Table 2.7: ^{232}Th decay series (Adopted from IAEA, 2004)

Nuclide	Half-life	Major radiation energies (MeV) and intensities*		
		α	β	γ
^{232}Th	$1.39 \times 10^{10}\text{y}$	3.95 (24%) 4.01 (76%)	–	–
^{228}Ra	5.75y	–	0.055 (100%)	–
^{228}Ac	6.13h	–	2.11 (100%)	0.34 (15%) 0.908 (25%) 0.96 (20%)
^{228}Th	1.913y	5.34 (28%) 5.42 (71%)	–	0.084 (1.6%) 0.214 (0.3%)
^{224}Ra	3.64d	5.45 (5.5%) 5.68 (94.5%)	–	0.241 (3.7%)
^{220}Rn	55.6s	6.30 (~100%)	–	0.55 (0.07%)
^{216}Po	0.145s	6.78 (100%)	–	–
^{212}Pb	10.64h	–	0.580	0.239 (47%) 0.300 (3.2%)
^{212}Bi	60.5m	6.05 (70%) 6.09 (30%)	2.25 (100%)	0.040 (2%) 0.727 (7%) 1.620 (1.8%)
^{212}Po	304ns	8.78 (100%)	–	–
^{208}Tl	3.1m	–	1.80 (100%)	0.511 (23%) 0.583 (86%) 0.860 (12%) 2.614 (100%)
^{208}Pb	Stable	–	–	–

* Intensities refer to percentage of disintegrations of the nuclide itself, not to the original parent of the series.

Thorium, when found in elevated levels in soils, leads to high external natural radiation field. ^{232}Th is divided into three sub-series which include ^{232}Th , $^{228}\text{Ra} \rightarrow ^{224}\text{Ra}$ and $^{220}\text{Rn} \rightarrow ^{208}\text{Pb}$ (Ibeanu, 2002).

All the components of the earth's crust and various geological formations including rocks, soil, water and even plants and air, owe their radioactivity to the three radioactive decay series and the long lived ^{40}K nuclide (Ibrahiem et al., 1993; Malanca et al., 1996). This, according to Eisenbud and Gesell (1997), accounts for substantial amount of background radiation dose to which man is exposed externally. The distribution of the radionuclides in the respective geological medium is assumed to be in dynamic equilibrium and follow a pattern that is dependent on the nature of the parent rock and soil (Khandaker et al., 2012). Majority of uranium is found to be probably associated with the phosphatic sands and clays, while soils that are obtained from acid magmatic rocks and clay contains significant amounts of uranium, thorium and potassium.

Studies on soil bound radioactivity have been carried out all over the world. Quindos et al. (1994) investigated the activity concentrations of natural radionuclides in Spanish soils. Measured activities of ^{226}Ra , ^{232}Th , and ^{40}K in Spanish soils were correlated with external exposure rates. Bonazzola et al. (1993) examined the downward migration of ^{137}Cs and ^{106}Ru , in Italian soils after Chernobyl accident. The topmost layer of grassland soil was found to be polluted with 60–80% of ^{137}Cs and about 60% of ^{106}Ru . Albering et al. (1996) measured ^{222}Rn concentrations in soils and residential houses in the Dutch Belgian border region. Varley and Flowers (1998) conducted similar survey in southwest England. They, however, considered meteorological parameters, variations in depth and local geology, as factors that influenced soil radioactivity and delineated soil as the principal origin of indoor radon. Zarate-Morales and Buenfil (1996) did a radiological survey of Mexico City. Their results showed that gamma dose rates of Mexico City varied

from 83 nGy h⁻¹ to 112 nGy h⁻¹. Volcanic or lacunars soils have outdoor dose rates of about 85 nGy h⁻¹.

Malanca et al. (1993) in their own investigations, recorded average activity values of 29 Bq kg⁻¹, 46.6 Bq kg⁻¹ and 677 Bq kg⁻¹ respectively, for ²²⁶Ra, ²³²Th and ⁴⁰K in soil from Brazilian State of Rio Grande do Norte. Enhanced levels of radioactivity were observed in the bed rock of Santana do Matos. Similar studies were conducted by Ibrahiem et al. (1993), on soils of the Nile Delta and middle Egypt. Clay soils according to their findings, had the highest radioactivity while sandy soils had the lowest. Muddy and dark clay soils recorded the highest ¹³⁷Cs activity.

Terrestrial radiation, cosmic radiation and radon gas along with other radiation sources have made the earth and its environment naturally radioactive. Cement, soil, stones, bricks and other construction materials which are transformed modes of the basic constituents of the earth (Khandaker et al., 2012), also contains some amount of natural radionuclide content in varying degrees that reflect their origin and geological conditions (Ibeanu, 2002). It follows then that building materials can have radiation backgrounds significant enough to have negative consequences, with long duration of exposure, on the health of humans (Arafa, 2004; Khan et al., 2002; Khandaker et al., 2012). Gamma dose rate in residential buildings can also be influenced by cosmic radiation, though according to Malanca et al. (1993), the dose rate in buildings rises in proportion to the specific activity of the soil and rock on which they are built.

Primordial and secondary radionuclides are present also in surface and groundwater, though their bioavailability in the natural environment is limited for this medium since they are chemically bound and chelated in the water by dissolve organic substances.

2.2.3 Anthropogenic radioactivity

Apart from natural radioactivity, technological advancement and the rapid growth in the utilization of nuclear energy as a follow up of the breakthroughs in nuclear physics, has introduced the concept of artificial radioactivity into the environment. This, according to Ibeanu (2002), requires the knowledge of natural radioactivity (as baseline data) for their assessment. Human activities such as ore mining and processing, combustion of fossil fuels, exploitation of natural gas and oil and other industrial activities, can lead to high levels of radionuclide concentration in industrial products, residues and wastes. This is known as technologically enhanced naturally occurring radioactive material (TE-NORM). The concentration or dispersal of radionuclides is governed by their physicochemical properties relative to environmental conditions. Anthropogenic activities alters these ambient conditions which therefore enhances the radioactivity of some products or wastes. This eventually increases the potential for human exposure to radiation. Technological application in processing of mineral raw materials, metallurgical processes and coal burning processes, could be accompanied by concentration of radionuclides.

Naturally occurring radionuclides could exist in circular radioactive equilibrium in normal rocks and soils. However, mineral mining and extraction, coupled with mineral processing, either physically or chemically, redistributes these radionuclides in various materials. This selective mobilization of radionuclides thus, distorts the initial equilibrium. As a result, radioactivity levels of the products from any anthropogenic activity could become greatly enhanced in comparison to that of the initial raw material (IAEA-419, 2003).

Additional exposure of the general public from technologically enhanced natural radiation around mega industrial plants, have attracted great attention (Bem et al., 2002).

Radioactivity of anthropogenic origin involves radionuclides that are produced artificially, those from numerous radiation-emitting equipment and nuclear reactors together with NORM which are redistributed and concentrated by various human processes (IAEA, 2003). Significant radionuclides like ^{210}Pb and ^{210}Po , for example, could be deposited on and inhaled along with dust particles in the vicinity of coal power plants or ore-smelting plants. This can lead to high sickness rate and higher lung cancer mortality rate among the factory workers and the population living around coal operating power plant (Grashchenko, 2005; Knizhnikov et al., 2001)

Environmental radioactivity levels around coal power plants have been greatly enhanced as a result of fossil fuel combustion activities (Adrovic et al., 1997; Tso & Leung, 1996). Fly ashes which are highly enriched in radionuclides normally escape from stacks and get deposited on the surrounding surface soils. This, in addition to inhalation, constitute additional radiation hazard in the vicinity of the power plants (Bem et al., 2002).

Soil radioactivity can be enhanced by application of potassium and phosphate fertilizers (Pfister & Pauly, 1980) in the same way as radioactive sources that are employed in medical diagnosis. These, according to IAEA (2003) report, typically increase annual absorbed dose from natural radiation.

Nuclear bomb tests carried out since 1945 led to the propagation of significant artificially produced radionuclides in human environment. High concentrations of ^{137}Cs , the most long-lived radionuclide from nuclear fallout that accumulates in the top soil layer can be retained in the environment over long period for many decades, with appreciable surficial activity above that of the (Korun et al., 1994). Accidental failures of nuclear power stations and subsequent dispersion of radionuclides in the surrounding

environment are additional sources of nuclear fallout which must be effectively and properly managed to avoid uncontrolled contamination and over exposure of humans.

2.3 Secular Radioactive Equilibrium

The secular radioactive equilibrium is usually put in practice in the indirect measurement of parent radionuclide using gamma spectrometry (Ibeanu, 2002). Secular equilibrium occur between the activity of the parent with infinitely large half-life and that of daughter nuclide. Sometimes a radioactive decay daughter may be unstable and can again undergo series of nuclear transmutations until it attains stability.

Assume a radioactive decay chain comprising radionuclides A, B, C, with respective decay constants λ_A , λ_B and λ_C , such that A decays to nuclide B which itself decays to nuclide C and to a final stable nuclide D i.e.,



If, at $t = 0$ there are N_{A0} atoms of nuclide A, and at later time t , there are N_A , N_B and N_C atoms of nuclides A, B and C respectively, then the activity of individual radionuclides will be:

$$A_A = \lambda_A \cdot N_A, \quad A_B = \lambda_B \cdot N_B, \quad A_C = \lambda_C \cdot N_C \quad (2.2)$$

Such that:

$$\frac{A_B(t)}{A_A(t)} = \frac{\lambda_B}{\lambda_B - \lambda_A} (1 - e^{-(\lambda_B - \lambda_A) \cdot t}) \quad (2.3)$$

If the life span of parent nuclide A is far longer than the daughter B ($\lambda_B \gg \lambda_A$), then,

$$\frac{A_A(t)}{A_B(t)} = 1 - e^{-\lambda_B \cdot t} \quad (2.4)$$

The situation described by Eq. 2.4, where the activity of the daughter nuclide equals that of the parent after a sufficiently long time is called secular equilibrium. This is represented in Figure 2.1.

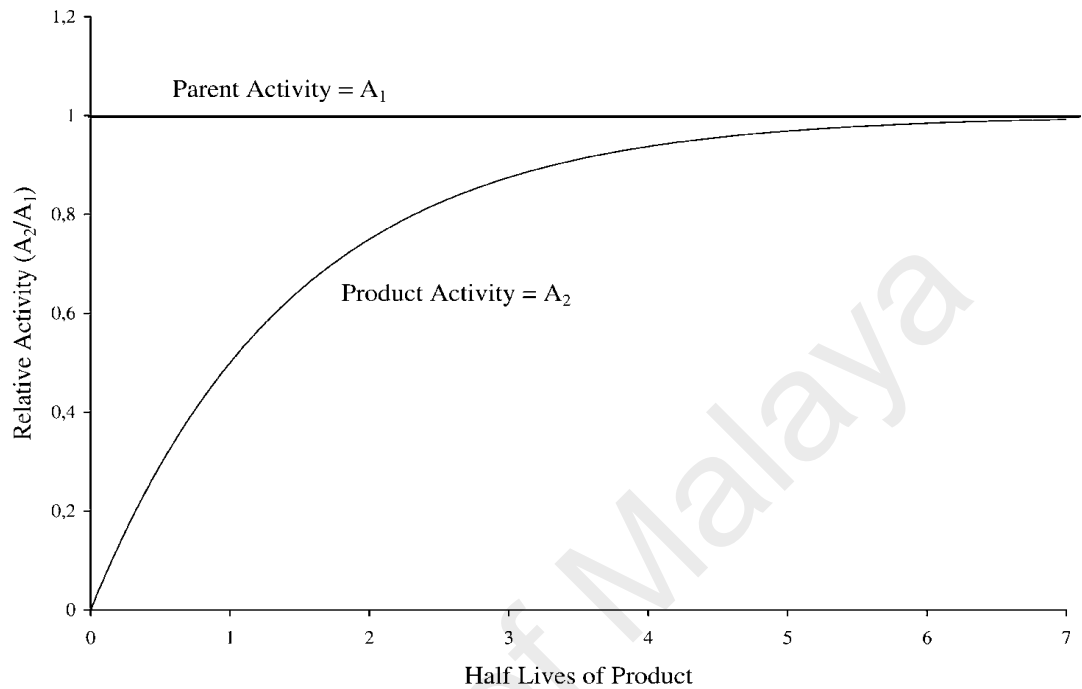


Figure 2.1: Secular equilibrium between the parent and daughter radionuclides
(after Martin, 2006)

At this point, the activity of the daughter is said to be in equilibrium with that of the parent, thus, the decay constants of the parent nuclide and its daughter are in the inverse ratio of the equilibrium concentrations of the parent and daughter (Cember & Johnson, 2009). In any closed system, (without migration losses), production and decay rates are equal, leading to the equilibrium state (Ibeanu, 2002).

The concentration of a radionuclide in a certain compartment of the earth is governed by three terms, namely: the production rate, the decay rate and the migration rate (Ibeanu, 2002). So starting with a specified amount of parent element in a closed system (without migration losses), the number of atoms of the daughter nuclides and their activity grows

until circular equilibrium is attained in the decay chain (IAEA, 2003), in which the activities of both the parent and daughters in the decay chain becomes identical, i.e.

$$\lambda_A N_A = \lambda_B N_B = \lambda_C N_C = \dots = \lambda_i N_i \quad (2.5)$$

Thus, under secular equilibrium, the activity of any of the daughters is a representative activity of the parent. At this point, the activity of the parent radionuclide remain relatively steady across several half-lives of its decay daughters. A uniform distribution of radionuclides is always assumed in gamma spectrometric measurement for the treatment of radioactive equilibrium. So the daughters of ^{234}U and ^{232}Th decay series which include their gaseous ^{222}Rn and ^{220}Rn must be kept at equilibrium with their parents. To achieve this, the samples must be sealed and incubated for a length of time to prevent their escape before analysis.

2.4 Radioactive Disequilibrium

Disequilibrium, according to IAEA (2003), occur when some daughter radionuclides in a decay chain becomes wholly or partially added to or deducted from the system. Disequilibrium problems which are due mainly to some physical processes like erosion and leaching are common in the uranium decay series and takes place at different points within the decay series. Disequilibrium in the uranium decay chain affects the state of the radioactive concentration and thus appear as source of error in the gamma ray spectrum.

2.5 Environmental and Health Impacts of Coal Use

Coal is considered the most polluting energy source which creates very complex environmental problems at various stages of its procurement from mining, transportation, stockpiling, preparation and utilization (Mamurekli, 2010). These complexities according to Ribeiro et al. (2013) are a function of many factors including methods of mining, coal burning technologies, coal composition, geological setting, local hydrology and local

regulations (Dai et al., 2012; Querol et al., 2008; Querol et al., 2011). Lots of information, in-depth reports and research outcomes, have been published in literatures on the environmental impacts of coal mining, processing, combustion and utilization.

Coal mining and exploitation either by open pit underground mining techniques involves phase developments in mines that causes changes in land scape, soil erosion, soil and sediment, surface and groundwater, and air pollution, along with numerous impacts on local biodiversity (Bell et al., 2001; Ribeiro et al., 2013). Bhuiyan et al. (2010) reported that during coal mining, a variety of waste rocks and tailings which may be low in coal content with higher radionuclide concentrations are produced and deposited at the surface sometimes near the mine thereby contaminating the soil, water and plant around the coal mine, thus enhancing human exposure to external radiation (Hu et al., 2005; Hu et al., 2009; Wong, 2003). These waste rock types with different compositions of hazardous metals and radionuclides (TENORM), now exposed to atmospheric conditions, undergo accelerated weathering and/or oxidation processes (Izquierdo et al., 2007; Izquierdo et al., 2011; Izquierdo et al., 2008; Medina et al., 2010), which eventually may lead to spontaneous burning of waste dumps, material mobilization, leaching of elements, formation of acid mine drainage (AMD), acid rain, smog and greenhouse gas emissions (Finkelman et al., 2002; Huggins et al., 2012; Querol et al., 2008; Querol et al., 2011; Ribeiro et al., 2012; Yenilmez et al., 2011).

AMD constitute grave environmental challenge for both the international and local mining industries, which according to Zhao et al. (2007), occurs during the exploitation of coal and coal-bearing measures containing high content of metal sulphides such as pyrite (FeS_2). When these sulphides are exposed to atmospheric oxygen, oxidation process is stimulated that produces acid waters with highly dissolved SO_4^{2-} and Fe, which eventually cause the receiving water bodies and soil to be acidified (Bell et al., 2001;

Yenilmez et al., 2011). The acidification increases the dissolution of heavy and toxic metals from the already exposed mine tailings, waste rock and open pits, and their possible transportation over long distances via surface runoffs. Some of these dissolved metals and radionuclides bioaccumulates along the aquatic food chain, and so disrupts the ecosystem and endanger human health. Dissolution of waste rock and leaching of metals into the water bodies with attendant adverse impacts on the surrounding vegetation and soil can occur as a result of low pH (Bell & Donnelly, 2006; Cherry et al., 2001; Tabaksblat, 2002), which further improve the transportation of contaminants originating from coal mining activities (Yenilmez et al., 2011).

Another environmental and health challenge associated with coal mining and utilization is the coal combustion process. Coal combustion causes a redistribution of radionuclides between the combustion products and also generate emissions of potentially hazardous trace elements. Huge quantities of CO_x, SO_x, NO_x and other environmentally toxic gases are generated (Liu et al., 2004), released and concentrated in human environment (Papp et al., 2002), to the detriment of man's health and safety of his environment. Furthermore, coal dust, depending on their toxicity, chemical composition and concentration in air, can pose a serious inhalation hazard to coal workers and the public (Borm, 1997). These toxic particles, when inhaled, are deposited in the lungs, which after long periods of accumulation beyond the lungs cleaning potential can lead to respiratory illnesses such as black lung disease and chronic bronchitis (Borm, 1997; Finkelman et al., 2002; Jamil et al., 1998).

Entire coal fuel cycle constitutes wide range of environmental challenges and diverse health risks for both coal miners and the general public (Jamil et al., 1998). These health challenges can sometimes be complex, widespread and in some cases, severe, but can however, be minimized by efficiently reducing the emission of potentially hazardous

elements through the use of sophisticated pollution control systems (Finkelman et al., 2002).

2.6 Natural Radioactivity in Coal

Naturally Occurring Radioactive Materials (NORM) has since from creation, been part of our world, the planet, its atmosphere and even the human body. The components of NORMs in the earth crust have been found to be mainly due to the long lived radionuclides, ^{238}U , ^{235}U , and ^{232}Th , which forms the three natural radioactive decay series; and the presence of ^{40}K . Alvarez and Vivero (1998), reported a uniform distribution of these radionuclides in the earth components and that any noticed variation in the natural radionuclides content of any geological formation will be a function of its composition or rock type, and the geological history.

Coal being a sedimentary rock contains trace quantities of naturally occurring radionuclides (Corbett, 1983). UNSCEAR (1998), based on a radiological investigation of coal from fifteen (15) countries, published a report that gave an estimate of the mean specific activities of ^{40}K , ^{238}U , and ^{232}Th in coal to be 50, 20, 20 Bq kg⁻¹ respectively, which according to UNSCEAR (2000), are with the range for common rocks and soils. Eisenbud and Gesell (1997), and Beck et al. (1980), also documented values for activity concentrations of natural radionuclides in US coals.

According to Zielinski and Finkelman (1997), most ^{232}Th are retained in monazite, apatite or other phosphate minerals in coal, while the organic and mineral components of coal contains high percentage of uranium. Coal can also become enriched in uranium over time due to the extraction of dissolved uranium from groundwater by organic matter.

It is generally assumed that uranium, thorium and actinium series exists, within the bounds of experimental errors, in circular equilibrium in coal, except for radon and thoron

which, according to UNSCEAR (1982), and Corbett (1983), can in some cases escape due to their mobility and inertness. Anthropogenic activities such as coal mining and processing as well as coal combustion, releases the parent radionuclides and their decay daughters from the original coal matrix, thereby distorting their existing equilibrium. These industrial processes also create a significant mass reduction of raw coal and thus produce huge volumes of mine tailings and drainage water with high radioactivity levels (IAEA, 2003; Michalik, 2008). Mining activities thus, distorts the overlying geological strata thereby creating ways of escape for radon gas which finally enters the human dwellings. Wastes that results from mining and cleaning of mined coals are also stock piled always in free access areas almost without protection, which according to Charro and Pena (2013), can be affected by meteorological conditions leading to leaching of radionuclides into the surrounding soil and streams. Coal combustion on the other hand, causes the redistribution of radionuclides within combustion products (Pandit et al., 2011). The redistribution is however, governed by the volatility and chemistry of the individual elements (Zielinski & Finkelman, 1997).

Radionuclides and trace elements in coals are concentrated in their organic and especially the mineral fractions (Duliu et al., 2005), by geochemical or biochemical reactions during the coalification process. Papastefanou (2010) reported that potassium as well as thorium and its decay daughters are concentrated in the inorganic coal matrix, while uranium and its decay daughters are associated with organic materials. Tadmor (1986) stated that during coal combustion process, elemental components of organic compounds in coal are released into the gaseous phase which are eliminated through the air stream and eventually re-condense on the fly ash particles (Tso & Leung, 1996), thereby enhancing ash radioactivity.

Coal is generally known to contain a wide variety of elements, minerals and organic constituents in its original matrix. Coal combustion process results in the elimination of almost all the organic components and the combustible elements and a significant enrichment of about 5-10 times of all non-combustible elements in the combustion residues, among which are all the natural radionuclides found in coal (Flues et al., 2006). Pandit et al. (2011) reported that substantial amount of uranium and thorium together with their decay daughters are liberated from coal by combustion and get enriched in the combustion residue, which therefore, characterize coal ash as Technologically Enhanced Naturally Occurring Radioactive Materials (TENORM). Great amount of combustion residues therefore continues to be formed which may be enriched in radionuclides and other toxic elements. Tadmor (1986) and Durgun and Genc (2009) broadly classified these combustion residues as:

- (a) Bottom ash. These are larger particles of ash that collects at the bottom of the boiler, and
- (b) Fly ash, fine ash aggregates captured from the flue gas existing in the boiler.

Coal combustion is a known principal TENORM generating source. Coal contains trace amounts of natural radionuclides which are released by combustion processes into flue gases and fly ash and thus dispersed into the atmosphere. Spaits et al. (2007) reported radionuclides contained in coal becomes concentrated in the ash and fly ash during coal combustion. These by-products, when used as supplementary materials in building construction, can enhance the potential for human exposure to radiation. In the United Kingdom, the highest dose rate for a critical group as reported by Penfold et al. (1998) was 250 μSv , which was due to the use of fly ash in building materials. Thomas et al. (1990) undertook similar measurements in former Czechoslovakia and gave values approaching 1000 nGyh^{-1} , for walls built by coal slag. Additionally, coal-fired power plants generates huge volumes of fly ash which liberate ^{222}Rn into the environment (Kobal

et al., 1990), thereby radiologically contaminating the atmosphere and enhancing human exposure (Beck et al., 1980; Yaprak, 1999)

As coal is therefore burnt up, these combustion residues are either deposited permanently or temporarily stored at the combustion plant sites which are finally converted for commercial use. Karangelos et al. (2004) reported that nuclides like ^{238}U , ^{226}Ra and ^{210}Pb in uranium decay chain, and ^{232}Th , have different physicochemical properties which control their levels of enrichment and behaviours during coal combustion. Furthermore, ^{238}U can become enriched in coal ash due to the operating conditions of the combustion chambers, coupled with the physical and chemical and physical properties of coal (Coles et al., 1978). Hence a secular radioactive disequilibrium will exist in the decay chain in the ashes due to this difference in enrichment owing to the different chemical and physical characteristics of the daughter radionuclides. Flues et al. (2006) also added that refractory elements such as ^{232}Th and ^{226}Ra becomes more attracted to fine particles of fly ash as they remain in the ash matrix, while the more volatile, gaseous ^{210}Pb escapes the combustion chamber with the flue gases and eventually condenses as temperature of the flue gas drops. Thus, volatilization at coal combustion temperature enhances the enrichment of trace elements on small particles of relatively high specific surface area (Smith, 1980; Tadmor, 1986).

Numerous documented researches have been undertaken worldwide to assess the radiological components of coal and its by-products with the sole aim of protecting the general public from over exposure due to coal use. Alvarez and Vivero (1998) assessed the natural radionuclide contents in Spanish coals of different rank. About 120 different samples of washed coal, run off mine and wastes from coal washing plants were assessed using gamma spectrometer with NaI(Tl) crystal. Their results indicated mean values for uranium, thorium and potassium concentrations in Asturias rom coal to be 3.1, 9.6 and

1.6 ppmw respectively; and 0.7, 3.5 and 0.2 ppmw respectively for the lignite of P. Garcia Rodriguez mine. Their assessment suggested generally that highest values of activity concentrations are found in coal wastes.

Cam et al. (2010) investigated the natural radioactivity contents in feed coals from the lignite-fired power plants in western Anatolia, Turkey. Specific activities of ^{226}Ra , ^{232}Th and ^{40}K were measured in 112 lignite samples from seven lignite-power plants using scintillation gamma-ray spectrometry. The range of the values obtained were 23-291 Bq kg^{-1} for ^{226}Ra , 12-68 Bq kg^{-1} for ^{232}Th and 67-284 Bq kg^{-1} for ^{40}K , while the mean dose rate due to external gamma radiation in the coal handling areas were found to be 40-117 nGy h^{-1} with about 95% confidence interval. Their conclusions showed that the obtained values falls within the safety range specified in UNSCEAR (2000) report. Radiological evaluation of pulverized coal and ashes from Catalagzi coal-fired power plant (CFPP) by Aytekin and Baldik (2012), showed the measured activity concentrations of all the samples studied to be above the world average values. The $R_{\text{a,eq}}$ values calculated for all the fly ash samples were however below the recommended limit, which therefore permitted the use of fly ash wastes as roadbeds and road pavements with no radiological consequence. The enrichment factors (EF) calculated by them for the radioactivity of ^{232}Th , ^{226}Ra and ^{40}K from coal to fly ash were 1.7, 2.24 and 2.0 respectively, which thus necessitated a continuous monitoring of the environmental impact of the power plant.

In their measurement of natural radioactivity of coal, soil and water samples collected from Barapukuria coal mine in Dinajpur district of Bangladesh, Hasan et al. (2013) found out that the activity concentrations of primordial radionuclides were relatively below world mean values for coal, but higher in soil samples. Their calculated mean dose rate, outdoor annual effective dose and $R_{\text{a,eq}}$, were all lower than the global average values, with the calculated hazard indices below one. Their conclusion was that there was no

probability of immediate radiological health challenges of workers and the public and that the environment adjacent the mine area was free from contamination by mining activities.

Amin et al. (2013) investigated the radionuclide emissions from the Sultan Salahuddin Abdul Aziz power station. It is a 220 MW coal-fired power plant located at the west coast of Peninsula Malaysia. From their investigations, the ash/slag from Kapar plant contained high level of TENORM than the world average. The specific activities of ^{238}U , ^{232}Th and ^{40}K , measured in soil samples outside Kapar showed a level of contamination due to the fly ash, which decreases with distance from the power plant. The contamination was found to be however, higher inside the town, which suggested the use of TENORM contaminated soils by the villagers for landfills. They also found that the committed dose from ingestion and inhalation of fly ash was $4.2\ \mu\text{Sv}$ and $220\ \mu\text{Sv}$, respectively, after one year of exposure, while that from contaminated soil was $4.4\ \mu\text{Sv}$ and $190\ \mu\text{Sv}$, respectively. Their conclusion was that a more detailed study of the radiological impact of bottom ash be done to justify the emission control system efficiency of the power plant. In a similar study, Cevik et al. (2007) discussed the radiological characterization of Cayirhan coal-fired power plant in Turkey, using gamma spectrometric technique. Measured mean activities for ^{40}K , ^{226}Ra and ^{232}Th were respectively 322.21, 57.82 and $30.45\ \text{Bq kg}^{-1}$, while the calculated dose rate, annual effective dose, and external hazard index for all samples studied were within stipulated safety limits, while the R_{eq} value was found to be lower than the limit of $370\ \text{Bq kg}^{-1}$. Their results compared well with reported data of other countries.

Balogun et al. (2003), while investigating the radiological consequences of coal mining in Nigeria, used the gamma spectrometric technique to determine the natural radioactivity associated with bituminous coal mining in Nigeria. Their investigation showed that ^{214}Bi was the greatest contributor to natural radioactivity of the studied

environment, with about 49.5% of the overall radioactivity attributable to coal tailings. Absorbed dose rate and the annual effective dose equivalent estimated for the particular Nigerian mining environment studied were in good agreement with the global average values.

Lu et al. (2012) carried out a survey of natural radioactivity and an assessment of associated radiation hazards in soils around Baoji second coal-fired thermal power plant (CFTPP) in China, using NaI(Tl) gamma ray spectrometer. Mean activity concentrations of 751.2 ± 12.4 , 40.3 ± 3.5 and 59.6 ± 3.1 Bq kg⁻¹ were recorded respectively for ⁴⁰K, ²²⁶Ra and ²³²Th in the studied soil samples. These values were higher than the corresponding average values reported for Shaanxi, Chinese, and world soils. The values for absorbed dose rate, and effective dose rates in air, were also above the world mean values for outdoor exposure. Their calculated mean for Ra_{eq} was however lower than the internationally reported value, with the hazard indices less than unity. Their conclusion, therefore, was that though the vicinity of Baoji second CFTPP has normal background radiation, there existed a tendency of increased natural radioactivity level, and enhanced natural radiation in the surrounding soil environment due to the CFTPP. The environment and the CFTPP should thus be monitored periodically.

Turhan et al. (2010) analysed the radiological characteristics of pulverized fly ashes (PFA) collected from 15 coal-fired thermal power plants (TPPs) in operation in Turkey, using gamma spectrometric technique. Their assessment showed that the Turkish PFA have relatively high natural radioactivity content which, according to them, was a function of its origin. The calculated values for the external exposure indices for the PFA were all within the recommended safety limits. Estimated mean total annual effective dose for both workers and the public were significantly lower than the recommended annual limit for safety.

Turhan et al. (2011) assessed the radiological implication of using fly ash as main constituent in the production of cement in Turkey. The activity concentrations of ^{226}Ra , ^{232}Th and ^{40}K in samples of PFA and Portland cement containing 15%, 20% and 25% by mass of PFA were measured, using gamma ray spectrometry with HPGe detector. The calculated mean values for Ra_{eq} , hazard indices and annual effective dose for the cement samples, were all below the recommended upper level, and so they concluded that the examined Portland cement products with PFA complies with the national and international regulatory limits set for radionuclide activity concentrations in building materials.

Radionuclide concentration has been found to be significantly increased in coal ash through coal combustion process. Flues et al. (2006) reported mean activity concentrations in the escaping fly ash as 265 Bq kg^{-1} for ^{40}K , 200 Bq kg^{-1} for ^{238}U , 240 Bq kg^{-1} for ^{226}Ra , 930 Bq kg^{-1} for ^{210}Pb , and 70 Bq kg^{-1} for ^{232}Th . Mandal and Sengupta (2003), Mahur et al. (2008) and Mondal et al. (2006), all reported that fly ash particles have a greater tendency to absorb natural radionuclides, and other trace elements during coal combustion due to their relatively small size and large surface area.

2.7 Potentially Hazardous Trace Elements in Coal

Coal, whose seam usually originates from peat deposited in swamps (Tsai et al., 2005), is a complex, combustible rock which contains most of the naturally occurring elements. These elements are either organically bound to the coal matter (macerals), and coal's pore water or inorganically associated with the discrete minerals (Ward, 2002). Kortenski and Sotirov (2002) and Rađenović (2006) underscored the possibility of these elements to sometimes be found in both forms simultaneously in coals. Several researches (Belkin et al., 2009; Dai et al., 2008a; Dai et al., 2008b; Dai et al., 2010; Dai et al., 2012; Hower et al., 2005a; Hower et al., 2007; Querol et al., 1997b; Querol, Whateley et al., 1997a;

Shibaoka & Smyth, 1975; Ward, 2002) have proved that the concentrations of these elements along with their enrichments in coals, depend primarily on the coal's depositional environments and geological factors, interactions between the organic matter and basinal fluids as well as sediment diagenesis. Similar researches suggested that properties of the source rock, marine environment, hydrological conditions, hydrothermal processes, and coalification processes are additional factors controlling the concentrations and contents of these trace elements (Belkin et al., 2009; Clarke & Sloss, 1992; Cohen et al., 1984; Dai et al., 2008a; Dai et al., 2008b; Dai et al., 2010; Dai et al., 2012; Filippidis et al., 1996; Gluskoter et al., 1977; Hower et al., 2005a; Hower et al., 2007; Querol et al., 1997b; Querol et al., 1997a; Shibaoka & Smyth, 1975; Swaine, 1990; Valkovic, 1985; Ward, 2002). Hence, elemental concentrations appear not to be uniform but differ within coal seams and between coalfields (Gurdal, 2011; Sia & Abdullah, 2011).

Some elemental constituents of coal have been found to be dangerous to human beings and the environment. Lists of potentially hazardous elements have been documented in different literatures. The US National Research Council (NRC), classified trace elements which are of concern in coal study based on known adverse health effects, and relative abundances. Their classification resulted in four major groups which are:

- **Major concern:** arsenic (As), boron (B), cadmium (Cd), lead (Pb), mercury (Hg), molybdenum (Mo), and selenium (Se).
- **Moderate concern:** chromium (Cr), vanadium (V), copper (Cu), zinc (Zn), nickel (Ni), and fluorine (F). These elements are toxic and are present in coal combustion residues at elevated levels.
- **Minor concern:** barium (Ba), strontium (Sr), sodium (Na), manganese (Mn), cobalt (Co), antimony (Sb), lithium (Li), chlorine (Cl), bromine (Br), and germanium (Ge).

- **Radioactive elements:** uranium (U), and thorium (Th) and their decay products- radium (Ra), polonium (Po) and radon (Rn).

Panel on the Trace Element Geochemistry of Coal Resource Development Related to Health, (PECH), (1980), subsequently, placed trace elements in coal and coal residues into five groups:

- **Of great concern:** As, B, Cd, Hg, Mo, Pb, Se
- **Of moderate concern:** Cr, Cu, F, Ni, V, Zn
- **Of minor concern:** Ba, Br, Cl, Co, Ge, Li, Mn, Sr
- **Radioactive elements:** Po, Ra, Rn, Th, U
- **Of concern** but with insignificant concentrations in coal and residues: Ag, Be, Sn, Tl.

With respect to environmental relevance of trace elements in coal, Swaine and Goodarzi (1995) suggested four groups:

- **Group I:** As, Cd, Cr, Hg, Se; known to be hazardous in some circumstances,
- **Group IIA:** B, Cl, F, Mn, Mo, Ni, Pb; and
- **Group IIB:** Be, Cu, P, Th, U, V, Zn, includes B, Mn, and Mo. These concerns leachates from mining wastes.
- **Group III:** Ba, Co, Sb, Sn, Tl: these are not expected to pose any hazardous effects

Fifteen trace elements have been identified according to US public law (1990), by the United States Environmental Protection Agency (US EPA), as potentially hazardous trace elements (PHTEs) (Sia and Abdullah, 2011). These include: As, Be, Cd, Cl, Co, Cr, F, Hg, Mn, Ni, Pb, Sb, Se, Th, and U.

Residues produced during coal combustion are released into the environment either as waste gases which are released into the air or as industrial ash, an extremely disposed dusty powder formed when coal is burned at a temperature over 800⁰C in a thermo-power plant (Liu et al., 2004). The industrial ash from coal combustion is classified into two: Fly ash, which is captured by electrostatic precipitators or other particle filtration equipment before the flue gases reach the chimneys of the coal fired plants (Patra et al., 2012), and Bottom ash which stays at the bottom of the boiler after the coal is burned. Fly ash particles are however, the major combustion residues (Ctvrtnickova et al., 2009), which when released into the environment, provides a matrix for the interactions of great variety of substances during the combustion and emission processes (Borm, 1997).

Coal, in comparison to most geologic materials, have high concentration of trace elements. During coal combustion, these numerous persistent and bio-accumulative trace elements become concentrated in the ashes to between 3-10 times their concentrations in the original coal matrix (Beck, 1989; Block & Dams, 1976; Coles et al., 1979). Their concentration always increases with decreasing particle size, because, according to Patra et al. (2012) and Bogdanović et al. (1995), the concentration of elements depends on availability of surface area.

The chemical composition of the ashes depend on geological and geographic factors that govern the coal deposit, conditions and methods of coal burning as well as the precipitation technique (Patra et al., 2012). Upon combustion in the furnace, trace elements that are organically bound in coal vaporizes and escapes into the atmosphere, while some are adsorbed on the fly ash particles (Sia & Abdullah, 2011). Other inorganically bound elements generally have very low volatility and are thus retained in the bottom ash (Dai et al., 2010b; Finkelman, 1994; Huang et al., 2004; Liu, et al., 2004; Querol et al., 1995; Smriti Singh et al., 2011; Spears & Zheng, 1999). Affinity of the toxic

trace elements to fly ash thus make fly ash disposal a potential source of environmental pollution, more so that the cumulative build-up, long life and high toxicity of these elements pose health risk to humans, plants and animals. Furthermore, trace elements can easily leach out from acid ashes leading to soil contamination and surface and groundwater pollution (Polic et al., 2005; Roy et al., 1984; Swaine, 2000; Theis & Wirth, 1977).

Environmental and health challenges from potentially hazardous elements contained in coal and coal ash has stimulated a lot of research in many parts of the world. Wagner and Hlatshwayo (2005), investigated the occurrence of potentially hazardous trace elements in five Highveld coals, South Africa. 32 coal samples were analyzed for their trace element constituents using the ICP-AES, and CVAA techniques. Based on the general perception that coal combustion can release some PHTEs that can threaten human health and environment, 14 trace elements including As, Pb, Cd, Hg and V were investigated. Their results showed that the elemental concentrations in the studied coal samples correlated well with the values obtained in literatures for other South African coals, except for Cr, and Mn. There was also a good agreement of their findings with the elemental concentrations data from the United States Geological Survey. They concluded, however, that though the reported values were low, there existed the tendency of release of high levels of toxic elements into the atmosphere upon coal utilization, especially when the elements like As, Cd, Pb, and Mn were likely to become bound to fly ash and get emitted through the stacks.

Gurdal (2011) studied the abundances and modes of occurrence of trace elements in the lignite to subbituminous Can coals (Miocene) from Canakkale-Turkey. About 20 trace elements of environmental and human health concerns were studied using the ICP-MS, and ICP-OES techniques. Results of his analysis showed that all the elements were within

the Swaine's worldwide concentration range, except for As, Th, U, and V. He also compared his results with the data on world coals, and discovered that Can coals were enriched in As, B, Cu, Co, Mo, Pb, Th, U, V, and Zn. He thus concluded that there was a high tendency for the elements and the radioactive U, Th, and V to be concentrated in the coal waste after combustion which made the enriched fly ash, and slag materials of urgent attention in the region.

Trace element contents in composited samples of three lignite seams from the central part of the Drama lignite deposit in Macedonia, Greece were analysed by Filippidis et al. (1996), using the instrumental neutron activation (INAA), and inductively couple plasma (ICP) analysis techniques. Their investigation showed that elements from the surrounding rocks, and mineralization of the Drama basin have influenced the organic constituents of the lignite such that As, Br, Mo, and Sb have become enriched in the lignite samples compared with their crustal abundances. They concluded that though uranium in the lignite might have some potential economic values, trace elements like As, Cd, Mo, and Sb have potential environmental implications especially at the combustion and gasification of the Drama lignite. In a similar investigation of trace element contents of coal samples from Taiwan, Tsai et al. (2005) discovered that the investigated coals were high volatile bituminous coals in rank, with high percentage of vitrinites and mean vitrinite reflectance less than 0.8%. Wukeng mine samples, from their analysis has appreciable contents of Fe_2O_3 (29.5%), Tl (54.8ppm), Zn (140ppm), and As (697ppm) in ash, and Hg (2.3ppm) in coal. They however concluded that the studied coal samples presented no health hazards if used properly.

Fu et al. (2013) studied the minerals and potentially hazardous elements in the Late Triassic coals from the Qiangtang basin in China. According to their findings, the Fumen coal mine which has been developed, and utilized as important energy source in Tibet,

has raised some health problems during its exploitation, and utilization. The Late Triassic coals, according to their reports, were enriched in several trace elements compared with their world average abundances. As, Hg, Pb, and Se were however identified as potentially hazardous trace elements in the samples, and their elevation in concentration may partly be attributed to their erosion, and leaching from the underlying shale bed and subsequent accumulation in the coal forming peat swamps.

Sia and Abdullah (2011) investigated the concentration, and association of minor and trace elements in Mukah coal from Sarawak, Malaysia, with special attention on the potentially hazardous trace elements. Perkin-Elmer Inductively Coupled Plasma Optical Emission Spectrometer (ICP-OES) was used to analyse the elemental concentrations of the studied coal samples. The elemental concentrations of the studied samples were found to be below their respective Clarke values except for As, Cr, Pb, Sb, and Th that have high values and so deserved some attention from the environmental and health perspective. According to the researchers, organically bound As, Pb, and Sb could escape as vapours during coal combustion into the atmosphere or could get absorbed into the fly ash particle. They therefore emphasized the application of effective coal cleaning processes to reduce the PHTEs to levels of minimum health effects. Similar investigation on the distribution of potentially hazardous trace elements in coals from Shanxi Province, China, was conducted by Zhang et al. (2004). About 110 peat and coal samples were collected from the drilling cores, main and small coal mines in the province. 20 potentially hazardous trace elements were determined using the INAA, AAS, CVAAS, ICS, and WCA techniques. Their results showed an enrichment of F, Cd, Ba, Cr, Zn, Cu, and As in brown coals; Cl, Hg, V and U in anthracite; while Hg, Cl and B were abundant in bituminous coals. When compared with the world averages, and Clarke's values, middle Jurassic coals, Early Permian coals, and late Carboniferous coals have high concentration of Hg, while the quaternary peat was enriched with As, and Mo, and tertiary brown coals

with Cd. The concentrations of Cd, F, Hg, and Th in the studied coals were found to be more than their world arithmetic mean.

In their studies of the mineral matter and potentially hazardous trace elements in coals from Qianxi Fault Depression Area (QFDA), south western Guizhou, China, Zhang et al. (2004) found out that QFDA was an area strongly affected by low temperature hydrothermal activity in its geologic history. Their investigation involved the analysis of potentially hazardous trace elements, coal chemistry and mineralogy of 44 coal samples. Coal samples from QFDA were found to be enriched in volatile PHTEs probably due to the low temperature hydrothermal activity associated with tectonic faulting. Comparison with the coal Clarke values showed that QFDA coals have higher elemental concentrations than other Guizhou coals and so may need careful attention.

Vijayan et al. (1997) investigated the elemental composition of fly ash from a coal-fired power plant at the National thermal power corporation, Talcher, India, using the particle-induced x-ray emission (PIXE) and energy dispersive x-ray fluorescence (EDXRF) techniques. Very high agreement within experimental errors was seen in the two techniques for the sixteen elements that were characterized. The K/Rb ratio for the studied fly ash samples was 136, which was in good agreement with the average ratio (128) reported by other researchers. Their conclusion was that these techniques can effectively be used to generate data for trace elements concentrations in fly ash samples that can be helpful in developing pollution control approach for various applications of fly ash. In a similar investigation, Patra et al. (2012) used the PIXE to analyse the elemental composition of coal, and coal ash collected from NALCO thermal power plant in Orissa, India. Sixteen elements were quantified in which K, Ca, Ti, and Fe were present as major elements, while V, Cr, Mn, Co, Ni, Cu, Zn, As, Rb, Sr, and Pb were at trace levels, and the highest enrichment ratio (ER) of the elements with respect to coal was

witnessed in the pond ash. The concentrations of most of the elements were found to be low when compared with that of the European fly ashes. Their conclusion was that PIXE can be an effective tool for elemental analyses in coal and ash with high precision.

Bogdanović et al. (1995) studied the trace element distribution in Greek lignites, and their ashes using the XRF, PIXE, RBS and STIM techniques. Their results classified the elements into two groups based on the dependence of elemental concentrations on the ash grain size: the first group (Ca, S, Cl, Zn, As, Se, Br, and Pb) exhibited increasing elemental concentration with decreasing grain size, while the second group of elements, which showed decrease in concentration with grain size, formed nucleation sites on which volatile elements tends to solidify after combustion. They concluded, therefore, that finer fractions of ash were expected to carry high levels of trace elements, especially the volatile elements.

In their investigation of toxic element mobility in coal, and ashes, Flues et al. (2013) determined the major, and trace elements in coal, and ashes from the Figueira coal power plant in Brazil, and also evaluated their mobility, through total, and available metal concentration ratio. The total elemental concentration was evaluated by WDXRF technique, while the ICP-OES was employed in evaluating the available concentration after extraction from EDTA. Their results indicated a high total concentration of As, and Zn in both coal and fly ash. Elemental mobility studies showed As to be the most critical element of concern in ashes disposal on soil. They concluded that the high mobility of As (> 70%), followed by Mo (> 55%) in ash could have serious environment consequences. In similar investigation, Sia and Abdullah (2012a) studied the enrichment of arsenic (As), lead (Pb) and antimony (Sb) in Belingian coal from Sarawak, Malaysia. These elements were mostly organic which vaporizes during coal combustion, and get released into the atmosphere. Their results showed values of arithmetic mean which were much higher

than their respective coal Clarke values. Thus from their conclusion, Belingian coal should be placed on high alert.

Medina et al. (2010) studied the mineralogical, and physicochemical properties of fly ash from the “Jose Lopez Portillo” coal fired power plant in Mexico (MFA). Their conclusion was that the morphological properties as well as the structural, and thermal stability of MFA makes it suitable for use in thermal isolation materials, refractory products, and as a solid support for high temperature heterogeneous catalysts. The high pozzolanic reactivity of MFA also makes it useful as raw material for cement making. Furthermore, the MFA can be suitable for synthesis of low Si/Al ratio zeolites, judging from their chemical and mineralogical composition.

To maximize coal usage efficiently, and effectively, therefore, there is the need to assess the environmental, and health impacts of the entire coal fuel cycle. Coal samples need to be analysed intensively in order to generate enough information on the occurrence, concentration and distribution of the PHTEs, especially for environmental, and human protection purposes.

2.8 Gamma-ray Spectrometry

The evaluation of environmental radioactivity including the monitoring, and assessment of the radiation environment is achieved mainly through the gamma ray spectrometry technique. Gamma ray surveys over the years have enjoyed numerous applications in several fields of science. Of particular interest to this research is its application in estimating, and assessing the terrestrial radiation dose to human population due to coal exploitation and utilization.

Gamma ray spectrometers use the direct proportionality between the energy of an incoming gamma ray, and the pulse amplitude at the output of the detector. Radiation

with the highest penetrating potential, from both natural and anthropogenic sources are the gamma-rays. Their detection is a function of their interaction with the medium such that all or most part of their energy is transferred to an electron in the absorbing medium. Gamma-ray detector therefore, must act as a conversion medium for the incident gamma rays to have a high interaction probability to produce fast electrons, and also function as a conventional detector for these secondary electrons (Knoll, 2010). Figure 2.2 show a block diagram of a gamma-ray spectrometer. Pulse amplitudes are analyzed after the amplification, and digitization. The output of the spectrometer thus represents the energy spectrum of detected radiation.

High-resolution gamma-spectrometry is one of the commonly applied, non-destructive radioactivity assessment methods that give low detection limits for many radioactive nuclides. A gamma-ray spectrometer is an instrument that provides information on both the energy, and intensity of radiation that is emitted from a gamma-ray source (or energetic X-rays).

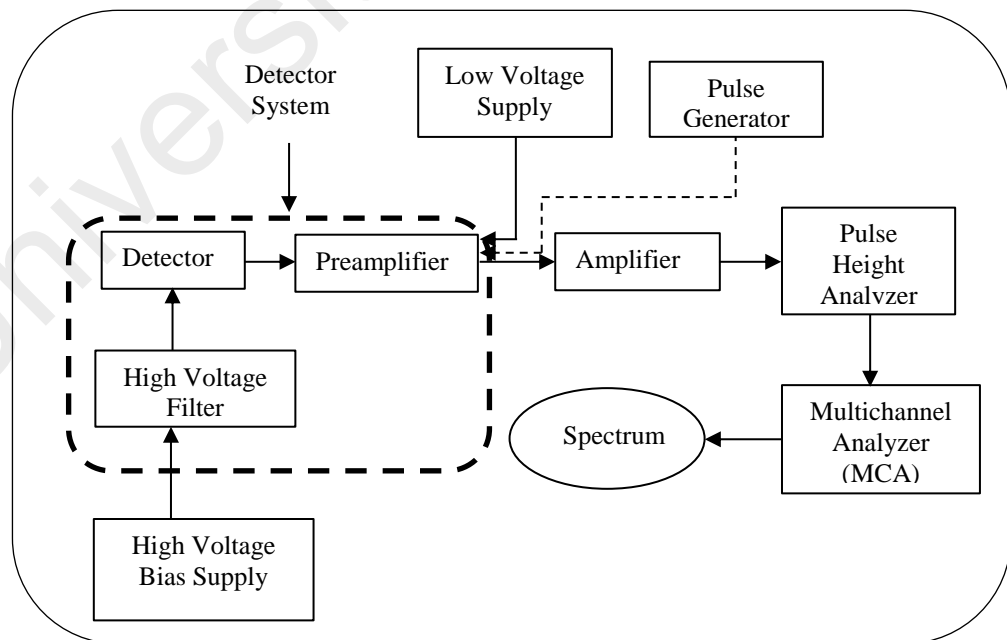


Figure 2.2: Block diagram of a gamma-ray spectrometer

Two basic detectors are commonly employed in gamma-ray spectrometric technique: thallium-doped sodium-iodide (NaI (Tl)), and high purity germanium (HPGe), which is characterized by low impurity concentration, high atomic number, and low ionizing energy required to produce electron-hole pair. Readily available detectors commonly used in radioactivity surveys are the NaI (Tl) scintillation crystals, especially that they can be operated at room temperature. The crystal suffers various excitations by the incident radiation, which is followed by series of de-excitations within the same crystal. This process results in the production of light photons which are captured on the photocathode of a photomultiplier tube and eventually released as electrical charge that is amplified along a dynode chain to produce electrical signal which is finally processed.

High Purity Germanium detector (HPGe), has however, become the major and appropriate device for photon detection (in ≈ 0.1 to ≈ 10 MeV) due to the high energy resolution of the semi-conductor (Ge) material, high conductivity, compact size, first time response, and the full-energy efficiency of large detector (Khandaker, 2011). HPGe detectors are semi-conductor diodes which are reverse biased. Electron-hole pairs that are produced in the semi-conductor crystal by the incident radiation drifts under an electric field towards the electrodes where they are collected as electrical pulses (Khandaker, 2011). The magnitude of the resulting electrical signal, is proportional to the amount of energy deposited in the detector. The signals from the detector are finally processed by a multichannel analyzer (MCA).

2.8.1 Detector characterization

Three basic parameters which are all dependent upon the energy of the incoming photon, characterize the effective operation of a gamma-ray detector: the energy resolution, energy calibration, and detector efficiency calibration.

2.8.1.1 Energy resolution

Energy resolution is a measure of the quality of detector performance. It defines the accuracy of any given spectrometer to measure gamma-ray energy. It is a measure of the width of pulse height distribution (energy peaks) in a gamma-ray spectrum obtained from monoenergetic particles. Energy resolution is expressed as a dimensionless percentage ratio of full width at half the maximum amplitude (FWHM) of a photopeak, to the energy value E_0 at the centroid of the peak; i.e.

$$R = \frac{FWHM}{E_0} \times 100\% \quad (2.6)$$

The smaller the width, the better the detector, and the easier it is for two gamma rays of very close energy to be distinguished (Gilmore, 2008; Khandaker, 2011).

2.8.1.2 Energy calibration

The spectrometer's sensitivity to detecting any element in a given energy window is dependent upon the instrument calibration (IAEA, 2003). Instrument calibration guarantees the effectual functioning of the detector, and ensures the reliability, and accuracy of the measurements in all energy ranges. Whenever a detector is correctly calibrated, it becomes easier to interpret gamma-ray spectrum in terms of energy (qualitative analysis), and the amount of radionuclides rather than the number of pulses (quantitative analysis) (Gilmore, 2008). Energy calibration is usually done with known standard sources before the commencement of any measurement, in order to establish the connection between specific gamma-ray energy, and the corresponding channel number or peak position in the spectrum.

2.8.1.3 Efficiency calibration

Efficiency of a detector, as a basic detector parameter, independent of detector geometry, is the proportionality constant which relates the activity of the source being

counted to the number of the observed counts (Khandaker, 2011). It relates the peak area of the spectrum to the activity concentration of the radionuclide it represents. Thus accurate efficiency calibration is necessary to quantify the radionuclides present in a given sample. The absolute full energy peak efficiency of a detector, relates the peak area at a particular energy to the number of gamma rays emitted by the source. It is therefore defined as the ratio of the number of counts detected in a peak to the number emitted by the source (Gilmore, 2008; Khandaker, 2011), and expressed as

$$\varepsilon = \frac{R}{A_t \times P_\gamma} \times 100\% \quad (2.7)$$

where R is the full energy peak count rate in counts per second, A_t is the present activity of the source in Bq, and P_γ the probability of emission of particular γ -ray being measured.

Generally, the comparison of observed photo-peaks to a library of known gamma emitting source energies, enables a qualitative interpretation of gamma ray spectra, while a good quantitative interpretation involves the relationship of the net energy peak to the activity concentration of a given nuclide (IAEA, 2003). The calibration standards used must therefore be of similar matrix, and identical container geometry as that of the samples to be analyzed, and the calibration energies must cover the entire range over which the spectrometer is to be used (Gilmore, 2008).

2.8.2 Minimum detectable activity (MDA)

In gamma spectrometry measurements, it is expected that the activity concentrations measured for radionuclides in a given sample be reliable, and acceptable. A detection limit is therefore introduced for the minimum activity expected in a sample, such that a measurement can be expected to represent the presence, and quantitatively assay the activity with some degree of confidence.

MDA represents the least quantity of a particular gamma-emitting radionuclide measurable at 95% confidence at the time of measurement. It expresses the activity concentration in a sample that is practically achievable by the overall method of measurement. For gamma spectrometry measurements, the MDA, measured in Becquerel (Bq), is given to be (Gilmore, 2008; Knoll, 2010):

$$MDA = \frac{L_D}{\varepsilon_\gamma \times P_\gamma \times T_c} \quad (2.8)$$

where L_D is the limit of detection (in counts), ε_γ is the efficiency of the detector at the energy of the measured gamma ray, P_γ is the gamma ray probability, and T_c is the live time of the count. With the 95% certainty for detection, the limit of detection L_D is expressed as (Gilmore, 2008):

$$L_D = 2.71 + 3.29\sigma_0 \quad (2.9)$$

Where $\sigma_0 = \sqrt{2B}$ is the uncertainty of the background count, B. MDA is therefore the activity equivalent of L_D .

Potassium, and the uranium, and thorium decay series are the only relatively abundant naturally occurring radioactive elements in the natural environment with radioisotopes that produces gamma rays of sufficient intensity and commensurate energy that could be measured by gamma-ray spectroscopy. Others such as vanadium-50, do exist but contribute insignificantly (Ibeanu, 2002), which may be due to their very low isotopic abundance.

2.9 Elemental Analysis of Coal using the ICP-MS Technique

Coal mining industry as well as coal combustion facilities and electricity generation from coal based power plants have become recognized sources of environmental pollution and health challenge to man. Apart from the distortions of the general aesthetics

of the environment, a number of trace elements which are hazardous to human beings and environment have been dispersed in the atmosphere owing to coal mining operations and coal combustion processes. Heavy metals and other toxic contaminants are leached from coal disposal sites or directly from coal in the mines (Fadda et al., 1995), into surface and groundwater sources thereby contaminating the water bodies. Flow of toxic elements between coal, bottom ash, fly ash and flue gases constitute a health challenge to man through atmospheric inhalation (Fadda et al., 1995; Rodushkin et al., 2000; Swaine, 1990). According to Huggins (2002) and Fadda et al. (1995), technical and environmental challenges associated with coal exploitation are mostly due to non-combustible inorganic chemical composition of coal which varies widely, particularly with respect to the trace element assemblage. This, therefore, make a complete chemical characterization of coal a primary concern in all its industrial and geological applications (Rodushkin et al., 2000).

To effectively evaluate the potential environmental impact and minimize the problems, and health challenges posed by coal mining and utilization, there is the need to accurately determine the concentration of toxic elements at all levels in coal and coal by-products, to understand their modes of occurrence, and their behaviour in all coal exploitation processes (Huggins, 2002). This obviously requires accurate and precise analytical techniques that are versatile, highly sensitive, and able to provide accurate and reliable data, and information on concentrations of coal associated elements (Ammann, 2007; Fadda et al., 1995).

Many analytical techniques have been developed over the years with the aim of quantifying elements associated with coal and coal by-products in all ranges of their concentrations. Of all the techniques currently available, plasma source mass spectrometry (PS MS) have proved to be undoubtedly superior, with long lasting and unbroken record of excellent analytical performance (Ammann, 2007). This, according

to Rodushkin et al. (2000), is due to their combination of multi-element capability, wide dynamic range and low instrumental detection limits. Inductively coupled plasma mass spectrometry (ICP-MS), the most widely used PS-MS, is an efficient technique for very rapid multi-element analysis, and reliable in detecting and quantifying elements of solutions of a wide variety of biological and environmental samples (Ammann, 2007; Beauchemin, 2006; Voellkopf et al., 1992). In the ICP mass spectrometry, the inductively coupled plasma which acts as a powerful ionization source, is coupled to a quadrupole mass spectrometer which detects and analyses the ions produced. ICP-MS has the ability to accommodate a broad range of sample types, and is highly sensitive to measuring majority of elements in the periodic table simultaneously with high spectral resolution. It is a fairly inexpensive, highly sensitive, and high-throughput analytical tool with the capability of providing such basic chemical information as single elemental contents or elemental isotope ratios (Ammann, 2007).

There are five basic steps involved in the operations of ICP-MS, which are represented in Fig 2.3 below. These steps are:

- Aerosol generation of the sample
- Ionization of the sample in the ICP source
- Ions extraction in the sampling interface
- Ions separation by mass
- Ions detection and calculation of concentrations

ICP-MS analyses samples fundamentally, and in good quantitative precision, as solutions or in liquid form. A more rapid and safe sample digestion method is the microwave assisted acid dissolution. This method is less prone to contaminations and requires only small amounts of acids for sample digestion. The prepared solution for analysis is nebulized, and the aerosol of the sample thus formed is carried into the high

frequency plasma for subsequent atomization and ionization. In the plasma, ions are generated as the electrons are removed from the analyte atoms. The excellent properties of the ICP as an atomic vaporization process makes it an excellent ion generation source (Huggins, 2002).

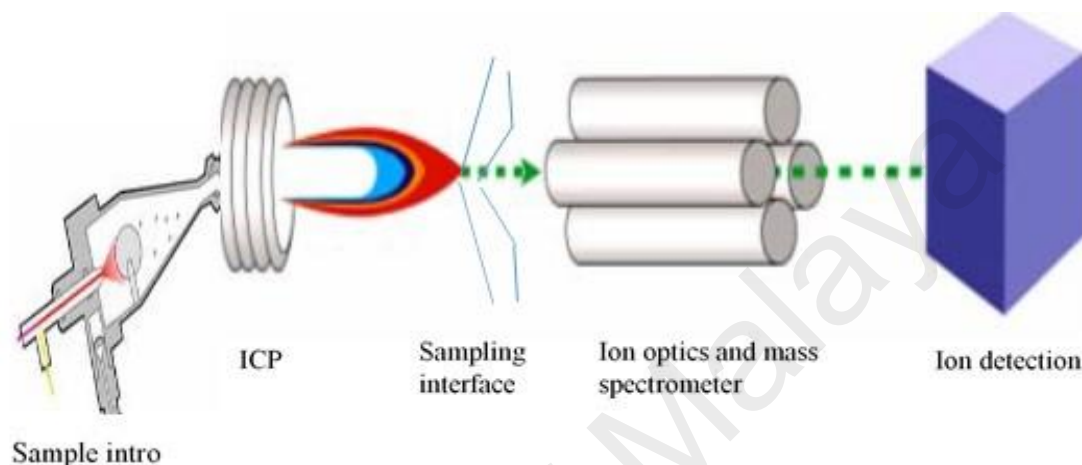


Figure 2.3: Block diagram of ICP-MS

Positive ions from plasma are sampled through a sampling interface (a cone), and directed into the mass spectrometer where they are separated according to their mass-to-charge ratio. The ions are finally measured using an electron multiplier, and are collected by a counter for each mass number. A correct instrument calibration with known standard solutions establishes a linear relation between the intensity of the ion signals and the concentration of an element. Quantitative analysis is therefore achieved by analysing standards of known concentration for each of the isotopes of interest, and comparing the peak intensities of the standards and the samples.

Fadda et al. (1995) determined 48 trace elements in 8 international coal standards using the ICP-MS technique. Their investigation proved that the use of microwave oven acid digestion is a very attractive tool for obtaining solutions suitable for ICP-MS trace analysis of powdered coal samples. The precision of the analysis, as well as the

repeatability of the sample preparation procedure and precision of instrumental measurements were evaluated, and their overall results showed a good agreement with certified and /or available published values. Following the same procedure, Gupta and Bertrand (1995), conducted a direct ICP-MS determination of trace and ultra-trace elements in geological materials (silicate rocks and lake, stream and river sediments). Their findings also proved the advantages of microwave digestion method to include, not only the rapidity of sample dissolution procedure, but also the economy of reagents and equipment, and negligible environmental pollution. A very satisfactory correlation (about 95-100%) of their results with the recommended or consensus values was established which proved the accuracy and precision of this technique. Booth et al. (1999), on the other hand, used the laser ablation ICP-MS to determine low level trace elements in three South African certified bituminous coal samples. Their results showed a good agreement with the certificate values even at low concentrations. Their conclusion was therefore that laser ablation ICP-MS could be a very useful analytical tool for rapid screening of coal samples, and for determining accurate concentrations at whatever levels, of a wide range of environmentally important trace elements in coal.

2.10 Geology of Coal

Coal is an organic rock generally formed from accumulation, and preservation of dead plant materials. These plant remains that are usually buried, and settled in swampy environments, undergo physical, and chemical alterations under anoxic conditions, as a result of heat, and pressure, which after long period of coalification processes, is transformed into coal (Figure 2.4). This organic-rich rock can consist of significant amount of inorganic components (Riepe, 1993). The inorganic constituents of coal are usually expressed by its ash yield, mineral matter, sulphur contents, and trace element contents. The organic components are the several biologically formed materials, called macerals, with a range of distinct chemical, and physical characteristics that are

fundamental to many coal properties. Coal is a combustible sedimentary rock, and a versatile fossil fuel with a wide variety of industrial and domestic uses.

Coal is generally classified into three major types, based on its heating value and fixed carbon content. These are the Lignite coal, the Bituminous coal and the Anthracite (Figure 2.4). These two parameters of coal classification have an inverse relationship with other coal parameters such as coal moisture and volatile matter content.



Figure 2.4: Schematic presentation of coalification process and coal classification (www.uky.edu/KGS/coal/coalkinds.htm)

In between this major classification is the sub-bituminous coal with less moisture content and high heating value than the lignite and the semi-anthracite, whose carbon content and volatile matter composition are higher than that of the bituminous coal but lower than that of anthracite.

2.10.1 Lignite

This is the youngest coal from geological perspective, considered to be immature, and of course, the lowest in coal rank. It is a soft coal, commonly referred to as brown coal.

It is characterized by high moisture, and volatile matter contents, low heating value and low carbon content. It represents the first step in coal metamorphosis from peat.

2.10.2 Bituminous coal

This is generally black, and blocky with low moisture content compared with the lignite. It is higher in rank compared to lignite, and has high carbon content, and high heating value.

2.10.3 Anthracite

This is commonly the oldest coal from geological stand point and the highest in coal rank. It is a hard coal composed mainly of carbon, black and brittle with a glassy appearance, with practically no moisture. It has slightly lower heating value than the bituminous coal owing to its low volatile matter content.

2.11 Coal Petrography

Coal petrographic study deals with the origin, formation, composition, occurrence, and physical and chemical properties of coal. It is a versatile tool in understanding the nature and characteristics of coal (Scott, 2002). It gives an insight into the kind and distribution of various coal macerals, and very fundamental in predicting coal behaviour and utilization.

Coal is a heterogeneous sedimentary rock material made up of various basic organic components called macerals. Macerals are optically homogeneous components of organic substances with distinct physical and chemical properties. These basic and relatively homogeneous organo-petrographic coal entities which are functions of the depositional environment against the vegetal conditions that prevailed in the coal forming environment (Obaje & Ligouis, 1996), are the determining factors for coal properties and utilization.

Coals are composed of a number of macerals which can be separated into three basic groups: the liptinites, which are relatively rich in hydrogen and show the least reflectance property; the vitrinites, which have high oxygen content and medium reflectance, and the inertinite, which have high reflectance with high carbon content.

2.11.1 The Vitrinite (Huminite) Group

They are the most common and dominant maceral in most coals, and a common constituent of hydrocarbon source rocks. The vitrinite is the coalified remains of cell walls, woody tissue of stems, branches, leaves, roots of plants and their precipitated gels, which have been subjected to humification of varying intensity. They are generally composed of carbon, hydrogen and oxygen, with trace amounts of sulphur and nitrogen. Vitrinites have a pale-grey to grey colour in white light and has very poor reflectance in ultraviolet (UV) light.

2.11.2 The Liptinite (Exinite) Group

These are derived from hydrogen-rich plants, and composed of waxy, lipid-rich and resinous parts of plants. During coking, these macerals devolatilize to produce gases and oily tars, which make it the highest potent oil and gas producing maceral. Liptinites have a dark mid-grey colour in white light, and has a bright yellow to green fluorescence in UV light. Liptinites have the lowest reflectivity of all the maceral groups.

2.11.3 The inertinite Group

This maceral group is made of plant material (bark, stem, leaves, roots etc) which have undergone oxidation during the early peat stages of burial diagenesis. Inertinite is characterized by high reflectance, high carbon, but low hydrogen contents and a strong aromatisation with generally no fluorescence (Teichmuller, 1989).

2.11.4 The vitrinite reflectance (R_0 %)

Vitrinite reflectance is extensively used in the assessment of coal maturity in hydrocarbon exploration (Speight, 2005; Sia and Abdullah, 2012b). It is independent of coal maceral composition, but rather dependent upon the level of coalification, thus, a parameter for estimating the degree of diagenesis. It is a petrographic parameter used to express or measure the rank, maturation of coals, and sedimentary organic matter. Maceral reflectance under incident light along with morphology is the main property that distinguishes macerals and maceral groups under the microscope.

Numerous scholars have discussed the petrographic properties of coals from different coal formations. Alias et al. (2012), discussed the organic geochemical characteristics and depositional environment of the Tertiary Tanjong Formation coals in the Pinangah area, onshore Sabah, Malaysia. Their results showed that the studied coal samples have a humic composition, dominated by vitrinite macerals with low inertinite and significant liptinite up to around 20% of the whole rock. According to their investigation, the coals were of sub-bituminous B-A and high volatile bituminous C rank, and were at most marginally mature in conventional terms. The studied samples, according to the researchers, have entered immature to early mature stage of the oil window, judging from their mean vitrinite reflectance of 0.42-0.66 R_0 %. Also the significant liptinitic content (>15%) of the studied coals supported their good liquid hydrocarbon generation potential. All other parameters studied according to them, indicated that the organic matter was derived from terrestrial inputs and deposited under oxic conditions.

Singh et al. (2010) analysed the petrographic characteristics of coal from the Latin Formation, Tarakan basin, east Kalimantan, Indonesia. Their study revealed that the coals from this basin have high moisture and high volatile matter content. They were sub-bituminous/low-rank A coals, mostly dominated by telohuminite macerals with low

concentrations of liptinite and inertinite macerals. They deciphered that the high telovitrinite concentration and low inertinite content gave an indication of the absence of severe oxidation/dehydration during peat formation.

Sia and Abdullah (2012b) investigated the geochemical and petrographic characteristics of low rank Belingian coal from Sarawak, Malaysia, with emphasis on its implication on depositional conditions and thermal maturity. Their investigation revealed that the studied coal was petrographically dominated by huminite macerals, with low to moderate amounts of liptinite and inertinite. The studied coals were chemically characterized by high moisture content with low ash yield and sulphur content. Most of the studied coals have random huminite reflectance values between 0.26 and 0.35%, suggesting a lignite coal rank.

Costa et al. (2010) studied the importance of thermal behaviour and petrographic composition of Portuguese perhydrous Jurassic coal. Their investigation revealed that the huminite maceral group is the main component (96%) of the studied coal samples, with a huminite reflectance of 0.33%. The studied coals were characterized by high H/C atomic ratio and judging from the calorific value (moist ash free basis) obtained, and the studied coals were considered as sub bituminous A coal. Their studies showed also that the presence of resinite influences the technological and thermal behaviour of the coal samples.

Obaje and Ligouis (1996) investigated the depositional environments and petrographic composition of the cretaceous Obi/Lafiya coal deposits in the Benue trough, Nigeria. Their investigation delineated three petrographic facies with distinct depositional environments: the vitrinite-fusinite coal facies lies underneath the stratigraphic sequence and have high percentage of vitrinite, low percentage of liptinite with varying amounts of inertinite and poor mineral matter content. The second was the trimaceritic coal facies at

the top, which have substantial percentages of vitrinite, liptinite, inertinite, with little content of mineral matter. Sandwiched between these two facies was the shaly coal facies which plotted generally in an area of increasing groundwater influence. The mineral matter content of this facies is appreciably high, with varying vitrinite, liptinite, and inertinite percentages. They concluded that the vitrinite-fusinite coal facies was deposited in a telmatic wet forest swamp sub-environment along with lagoons; while the trimaceritic coal facies was deposited in a limno-telmatic clastic marsh sub-environment in lower delta plains.

Gurba and Ward (2000) used light element electron microprobe technique to analyse the elemental composition of coal macerals of Gunnedah basin, Australia. Their evaluation was in relation to the maximum vitrinite reflectance trends in vertical section, including the effects of marine influences and igneous intrusions on the coal bearing sequence. Their results showed the mean vitrinite reflectance of coal samples to be between 0.63% to 0.99%, and 2.2% for coals affected by igneous intrusion. The carbon content of the vitrinite ranged from 79.74% to 86.07%, and up to 89.06% for heat affected coals; while the oxygen content was between 15% to about 17%. They could however, not establish a direct correlation between the reflectance of the vitrinite and the vitrinite carbon content within the obtained vitrinite reflectance range.

Tsai et al. (2005) showed from their detailed petrographic and chemical characterization of coal samples from Taiwan that the samples were high volatile bituminous coals in rank, whose moisture and ash contents varied from 4.2-14.4% to 2.7-4.6% respectively. The studied coals were highly enriched in vitrinite macerals and have vitrinite reflectance value below 0.8%.

Obaje et al. (1996) investigated the cretaceous Awgu formation in the middle Benue trough of Nigeria for its coal-derived hydrocarbon potential, organic maturation and

maceral associations. Their investigations revealed that the coal beds have attained a rank of high to medium volatile bituminous coal. From the maceral analysis, three distinct petrographic facies were identified: the vitrinite-fusinite coal facies, the trimaceritic coal facies, and the shaly coal facies. Vitrinite macerals dominates the organic matter content of the studied coal beds, with measured reflectance values ranging between 0.76-1.25%. Similar investigations were carried out by Wuyep and Obaje (2012) on some coal deposits in Anambra basin and the middle Benue trough in Nigeria. Their field mapping and sampling exercise were undertaken in Enugu, Okaba, Ogboyaga, Orukpa, and Obi/Lafiya coalfields which span through the basin. Their petrographic studies showed that the composition of coals in Anambra basin was dominated by huminites with vitrinite reflectance values between 0.4-0.63 R₀%, while vitrinite macerals with R₀ values between 0.81-1.25% predominated the petrographic composition of coals from middle Benue trough. Their conclusion showed that the sub-bituminous coals of Anambra basin, by virtue of their petrographic composition and rank were optimum for combustion and electric power generation but sub-optimum for liquefaction. The coals from the middle Benue trough were, however, high-volatile bituminous coals optimum for liquefaction and suitable as raw materials for carbonization in steel manufacturing operations.

Sarate (2010) carried out a survey of the petrographic characteristics of coals from Mailaram coalfield, Godavari valley, Andhra Pradesh. The quantitative maceral studies showed alternate coal beds rich in vitrinite/liptinite or inertinite. The random vitrinite reflectance of the studied coals for the top part ranged between 0.50 and 0.64%, and 0.47 to 0.52% for the bottom, indicating that the studied coals have attained a high volatile bituminous C rank. Being high in liptinite and vitrinite contents with low mineral matters, he concluded the coals to be of high economic potential.

Ogala et al. (2012) studied the petrography, mineralogy and geochemistry of lignite samples from the Ogwashi-Asaba formation in Nigeria. The lignite samples investigated displayed low ash yield, low telohuminite, high detrohuminite and liptinite contents, with most samples found to be low-rank coals C to B. Their results showed that the lignite samples originated in peat derived from herbaceous plants and/or tropical angiosperm trees, and accumulate in topogenous mires located in a continental basin. Small amounts of clastic minerals, mainly quartz and clay were noticed in the samples. With these outcrops distributed over a distance of about 60 km, they projected that this good quality lignite reserves can constitute a very promising exploration target.

University of Malaya

CHAPTER 3: MATERIALS AND METHODS

3.1 Sample Site

Maiganga coalfield is one of the recently discovered coal deposits that has attracted lots of attention from the federal government of Nigeria, and from coal investors. This deposit is one of the prime targets for the establishment of coal-fired power plant to boost energy generation in Nigeria, yet, very limited information is available on the quality, and inherent properties of the deposit. Exploration work is currently on-going at the mine to ascertain the quantity and quality of the coal. Maiganga is a local community located between latitude $10^{\circ} 02'$ to $10^{\circ} 05'$ and longitude $11^{\circ} 06'$ to $11^{\circ} 08'$ in Akko local government area of Gombe, Northeast Nigeria (Figure 3.1). Coal from this deposit is currently the primary energy source (on trial) for firing the cement kilns of a leading cement factory in northeast Nigeria, the Ashaka Cement Factory (AshakaCem). This study is therefore aimed at characterizing the deposit in terms of its maceral composition, carbon content, and thermal maturity. The study also attempt to discuss the natural radioactivity and trace elements compositions from the point of view of human health, and environmental protection. Data generated will form a baseline for further studies.

3.2 Sample Collection and Processing

Coal samples were collected from Maiganga coal mine for analysis. The samples were carefully collected using grab method, to satisfactorily represent the entire coal mine. The samples, each about 1.00 kg were neatly packed in well labelled polyethylene bags, properly sealed, and transported to the laboratory for analysis.

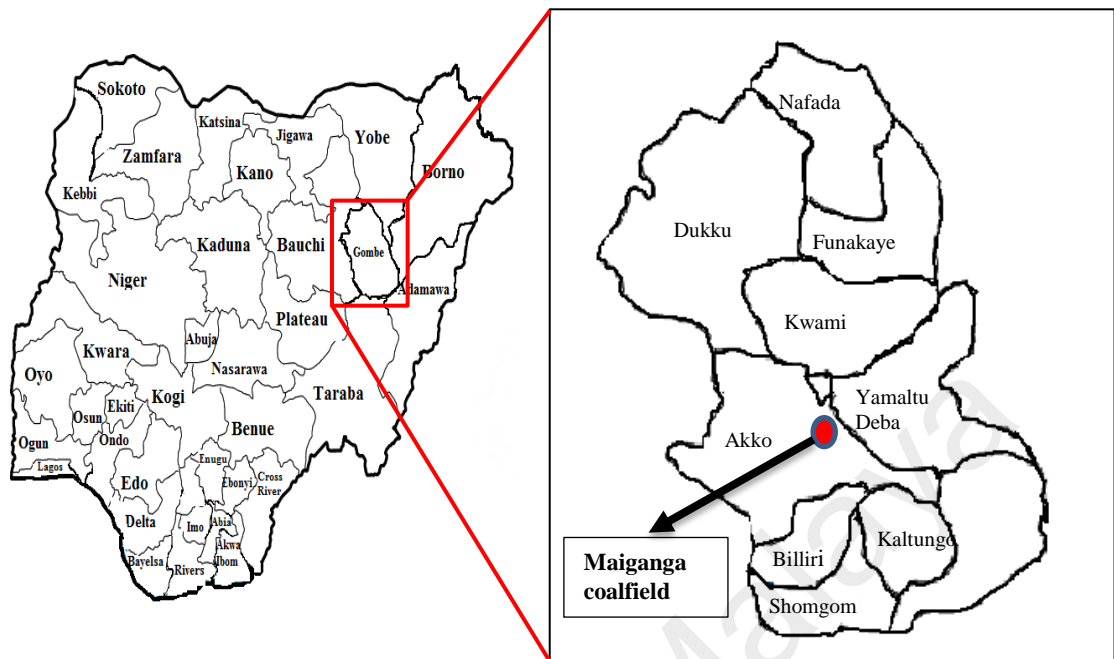


Figure 3.1: Map of Nigeria showing the sample site

Open-cast mining is a surface mining technique employed for coal mining in Maiganga coalfield. This technique involves the removal of large volumes of overburden waste rock (mine tailings) which consists of relatively loose, non-compacted debris (Figure 3.2), and dumped indiscriminately on the surface within the vicinity of the mine. Waste from the coal mining process (mine tailings) was also collected, and processed for radiological and trace elements analyses. The analysed mine tailings were code named CMW 01 to CMW 20.



(a)



(b)

Figure 3.2: Maiganga coal mine tailings: (a) panoramic view (b) close up view

3.3 Sample Preparation and Analysis

3.3.1 Radiological Analysis

Coal samples were air-dried at ambient temperature in the laboratory for 72 hours to ensure completely moisture free samples (Asgharizadeh et al., 2013; Surinder Singh et al., 2005; Sroor et al., 2001). This becomes necessary because, according to IAEA (2003), moisture content constitutes error in the desired spectrum. The samples were further oven dried in the laboratory to attain constant weight. The dried samples were thoroughly pulverized, sieved, and homogenized (Figure 3.3a). 375 ± 1.0 g of the homogenized samples were carefully packed into well-labelled marinelli beakers (Figure 3.3b), and properly sealed to prevent escape of radon (Figure 3.3c). The sealed samples were stored for six weeks to attain radiological equilibrium, where the decay rates of the daughter nuclides and their respective long-lived parents become equal (Agbalagba & Onoja, 2011; Amekudzie et al., 2011; Cevik et al., 2007; Hasan et al. 2014; Mehra et al., 2010).

Samples of the mine wastes (tailings) were also prepared following the procedure outlined above and stored for analysis (Figure 3.3d).

3.3.1.1 Gamma spectrometric measurement

The gamma counting was done using a P-type Coaxial ORTEC, GEM-25P (Serial No. 46-TP22121A) HPGe gamma-ray detector with 57.5 mm crystal diameter and 51.5 mm thickness. The detector is shielded in a cylindrical lead shield with a fixed bottom in order to minimize interference of background radiation from terrestrial and extra-terrestrial sources with the measured spectrum (Asaduzzaman et al., 2014; Khandaker et al., 2012). The detector, which has relative efficiency of 28.2% and 1.67 keV FWHM energy resolution at 1.33 MeV peak of ^{60}Co , was coupled to ADCM data acquisition system with PCAII multi-channel analyzer and set at operating voltage of +2800 V (Figure 3.4).



(a) Dry, pulverized coal samples



(b) 530G-E 500 ml Marinelli beakers



(c) Sealed and stored coal



(d) Sealed and stored mine tailings

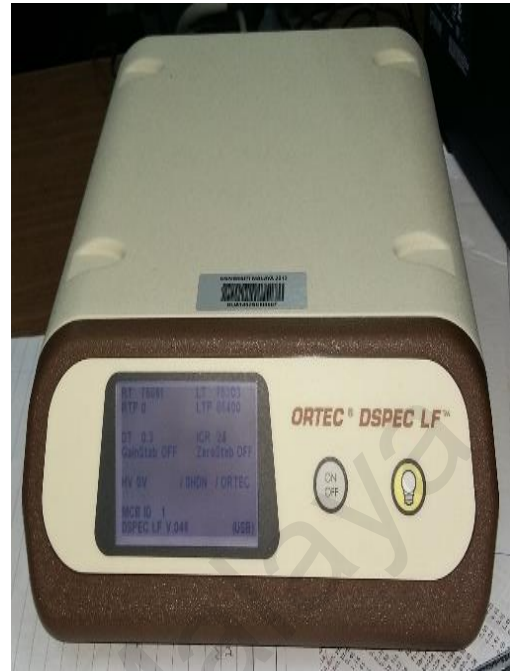
Figure 3.3: Coal and tailings samples preparation and packaging for the current study

Before the radiometric measurement of the samples, the detector was calibrated for energy and efficiency using a cylindrical multi-nuclide gamma-ray calibration source with homogeneously distributed activity in the same container geometry as the samples. The calibration source which was supplied by Isotopes Products Laboratories, Valencia, CA 91355, has initial activity of $5.109\mu\text{Ci}$ (Figure 3.5). The nuclides contained in the calibration source, along with their respective energies are presented in Table 3.1.

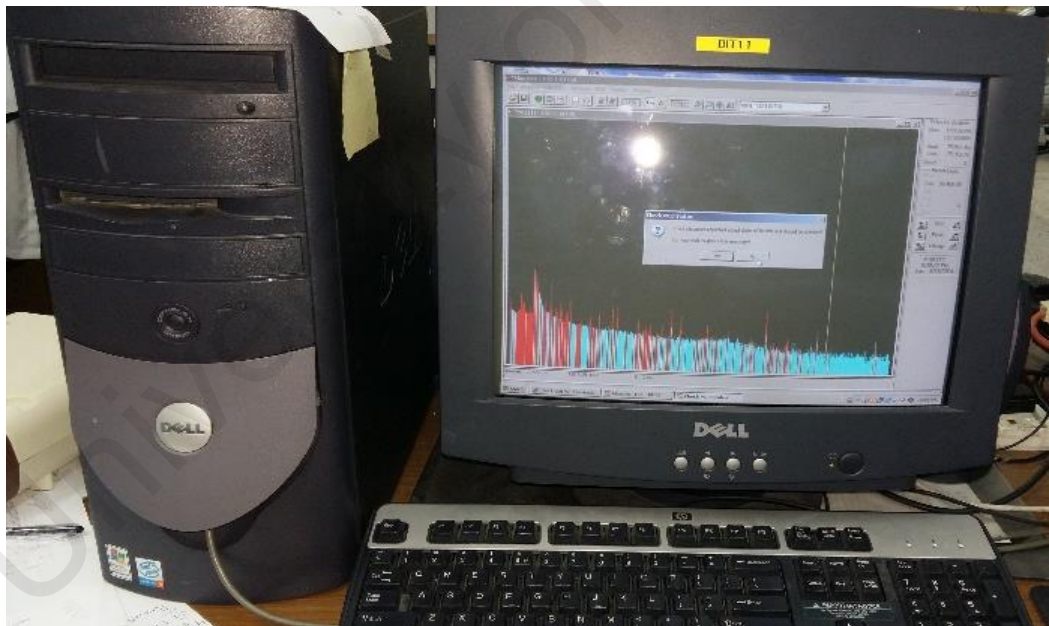
Background radiation in the surrounding environment of the detector was obtained by counting an empty sealed beaker with the same geometry as the samples. Each sample and the background were counted for 86,400 seconds to achieve reasonable counting statistics. The net count rate of the primordial radionuclides was obtained by subtracting the respective count rate from the background spectrum acquired for the same counting time (Amin et al., 2013; Kolo, 2014; Uosif & El-Taher, 2008).



(a) Lead shielded HPGe detector



(b) Multi channel analyser



(c) Spectrum display unit

Figure 3.4: High purity germanium detector system used in the present study



Figure 3.5: Standard gamma-ray calibration source

Table 3.1: Nuclides contained in the standard calibration source with their respective energies

Nuclide	Energy (keV)	Emission probability (%)
^{241}Am	59.541	35.78
^{109}Cd	88.04	36.26
^{57}Co	122.061, 136.474	85.51, 10.71
^{203}Hg	279.195	81.48
^{113}Sn	391.698	64.94
^{85}Sr	514.007	
^{137}Cs	661.657	84.99
^{88}Y	898.042, 1836.063	93.90, 99.38
^{60}Co	1173.22, 1332.492	99.85, 99.98

The minimum detectable activity (MDA) at 95% confidence level for the detector was estimated using following the equation (Khandaker et al., 2012):

$$MDA(Bq\ kg^{-1}) = \frac{K_{\alpha}\sqrt{N_B}}{\eta(E)P_{\gamma}T_cM} \quad (3.1)$$

where K_{α} is the statistical coverage factor equivalent to 1.645, N_B is the background count (cps), $\eta(E)$ the photo-peak efficiency, P_{γ} is the probability of gamma emission, T_c the counting time(s), and M is the sample mass (kg). The characteristic gamma lines used to obtain the net activities of the respective nuclides, along with their respective minimum detectable activity (MDA), calculated from Eq. 3.1 are presented in Table 4.1

Activity concentrations of ^{226}Ra , ^{232}Th and ^{40}K , in all the samples investigated were calculated using the expression (Amekudzie et al., 2011; Dabayneh et al., 2008; Khandaker et al., 2012):

$$A(Bq\ kg^{-1}) = \frac{CPS \times 1000}{\varepsilon_{\gamma} \times I_{\gamma} \times W} \quad (3.2)$$

where, A ($Bq\ kg^{-1}$) is the specific activity, CPS is the net counts per second for each sample investigated, $\varepsilon_{\gamma}(E)$ is the detector photo-peak efficiency at respective gamma-ray peak, I_{γ} is the corresponding gamma-ray intensity, and W the mass of sample in gram (g).

Activity concentrations of natural radionuclides in environmental samples are geologically interpreted in terms of their elemental mass fractions. Elemental mass concentrations of ^{226}Ra and ^{232}Th , in parts per million (or $mg\ kg^{-1}$), and percentage (%) by weight of ^{40}K in coal samples from Maiganga coalfield, were calculated from their respective specific activities (in $Bq\ kg^{-1}$) following the equation (Ali et al., 2013; Dabayneh et al., 2008; Isinkaye, 2013; Tzortzis et al., 2004):

$$F_E = \frac{A_E M_E}{\lambda_E f_{A,E} N_A} \xi \quad (3.3)$$

where, F_E is the fraction of element E in the sample, A_E is the measured activity concentration in $Bq\ kg^{-1}$ of radionuclides considered (^{226}Ra , ^{232}Th and ^{40}K), M_E is the

atomic mass (kg mol^{-1}) and λ_E the decay constant (s^{-1}) of element E, $f_{A,E}$ is the fractional atomic abundance of element E in nature, and N_A is the Avogadro's number (6.023×10^{23} atoms mol^{-1}), ξ is a constant with value of 1,000,000 for ^{226}Ra and ^{232}Th , or 100 for ^{40}K .

3.3.1.2 Radiation hazard indices

(a) Radium equivalent activity (Ra_{eq})

^{226}Ra , ^{232}Th and ^{40}K are not uniformly distributed virtually in all environmental samples. A single radiation index which represents the weighted sum of individual activities of ^{226}Ra , ^{232}Th and ^{40}K in any environmental sample is therefore defined with respect to radiation exposure. This single entity, called the Radium equivalent activity (Ra_{eq}), is measured in Bq kg^{-1} , and defined based on the assumption that 370 Bq kg^{-1} of ^{226}Ra , 259 Bq kg^{-1} of ^{232}Th , and 4810 Bq kg^{-1} of ^{40}K produce the same gamma ray dose (Agbalagba & Onoja, 2011; Dabayneh et al., 2008). It is quantitatively expressed as (UNSCEAR, 2000):

$$Ra_{eq}(\text{Bq kg}^{-1}) = A_{Ra} + A_{Th} + A_K \quad (3.4)$$

where A_{Ra} , A_{Th} , and A_K are the respective specific activities of ^{226}Ra , ^{232}Th , and ^{40}K , measured in Bq kg^{-1} .

(b) Absorbed dose rate (D_R)

Absorbed dose rate (D_R) at 1m above the ground is estimated using the conversion factors published by UNSCEAR (2008). D_R is calculated based on assumption that the contribution to background dose from other radionuclides outside the three primordial nuclides is insignificant (Jacob et al., 1986; Leung et al., 1990). It is quantitatively expressed as:

$$D_R(\text{nGy h}^{-1}) = 0.462A_{Ra} + 0.604A_{Th} + 0.0417A_K \quad (3.5)$$

where, A_{Ra} , A_{Th} , and A_K are the specific activity measured in $Bq\ kg^{-1}$ for ^{226}Ra , ^{232}Th , and ^{40}K respectively.

(c) **Annual effective dose equivalent (AEDE)**

Annual effective dose equivalent is calculated from the absorbed dose rate by applying the two conversion coefficients provided by UNSCEAR (2000). These are the conversion coefficient from absorbed dose in air to effective dose, given to be $0.7\ Sv\ Gy^{-1}$; and the outdoor occupancy factor of 0.2. The outdoor occupancy factor presupposes that an individual spends an average of 80% of his time indoors. The annual effective dose equivalent (AEDE) in outdoor air, measured in $mSv\ y^{-1}$ is therefore calculated as (UNSCEAR, 2000):

$$AEDE \left(\frac{mSv}{y} \right) = D_R \left(\frac{10^{-9}Gy}{h} \right) \times 24 \left(\frac{h}{day} \right) \times 365 \frac{day}{y} \times \frac{10^{-6}mGy}{10^{-9}Gy} \times 0.7 \left(\frac{Sv}{Gy} \right) \times 0.2$$

or

$$AEDE (mSv\ y^{-1}) = D_R \times 1.21 \times 10^{-3} \quad (3.6)$$

(d) **Annual gonadal dose equivalent (AGDE)**

The genetic relevance of the dose equivalent received each year by the reproductive organs (gonads) of the exposed population is represented by the annual gonadal equivalent dose (Morsy et al., 2012). Within this context also, the activity of bone marrow, and the bone surface cells are inclusive by UNSCEAR (1988), as organs of interest. Thus, the annual gonadal dose equivalent (AGDE) due to the specific activities of ^{228}Ra , ^{232}Th , and ^{40}K in the studied samples was estimated using the formula (Chandrasekaran et al., 2014; Ravisankar et al., 2014):

$$AGDE(\mu Sv\ y^{-1}) = 3.09A_{Ra} + 4.18A_{Th} + 0.314A_K \quad (3.7)$$

(e) **Activity utilization index (AUI)**

The dose rate in air from different combinations of the three primordial radionuclides in the studied samples is expressed by the activity utilization index (AUI). Application of appropriate conversion factors to the measured specific activities of respective radionuclides enable AUI to be calculated from the equation (Ramasamy et al., 2011; Ravisankar et al., 2014):

$$AUI = \left(\frac{A_{Ra}}{50 \text{ Bq/kg}} \right) f_U + \left(\frac{A_{Th}}{50 \text{ Bq/kg}} \right) f_{Th} + \left(\frac{A_K}{500 \text{ Bq/kg}} \right) f_K \quad (3.8)$$

where, A_{Ra} , A_{Th} , and A_K are the measured specific activities of ^{226}Ra , ^{232}Th , and ^{40}K respectively, and f_K (0.041), f_{Th} (0.604), and f_U (0.462), are the respective fractional contributions from the actual activities of these radionuclides to the total gamma radiation dose rate in air (Chandrasekaran et al., 2014). Typical activities per unit mass of ^{40}K , ^{232}Th , and ^{226}Ra (A_K , A_{Th} , and A_{Ra}), are reported by NEA-OECD (1979), to be 500, 50, and 50 Bq kg⁻¹ respectively.

(f) **External hazard index (H_{ex})**

Radiation hazard incurred due to external exposure to gamma rays from environmental samples is quantified in terms of the external hazard index (H_{ex}) given by UNSCEAR (2000):

$$H_{ex} = \frac{A_{Ra}}{370} + \frac{A_{Th}}{259} + \frac{A_K}{4810} \quad (3.9)$$

(g) **Internal hazard index (H_{in})**

Respiratory organs are in danger of radiation exposure from radon and its short-lived daughter radionuclides. The internal radiation exposure is quantified by the internal hazard index (H_{in}) given by UNSCEAR (2000):

$$H_{in} = \frac{A_{Ra}}{185} + \frac{A_{Th}}{259} + \frac{A_K}{4810} \quad (3.10)$$

where, A_{Ra} , A_{Th} , and A_K are the specific activities of ^{226}Ra , ^{232}Th , and ^{40}K respectively. UNSCEAR (2000) provided that the value of the above indices must be less than unity for the radiation hazard to be regarded as insignificant.

(h) **Representative gamma index ($I_{\gamma r}$)**

The gamma radiation hazard due to the respective concentrations of the investigated natural radionuclides is assessed by the representative gamma index ($I_{\gamma r}$). This index, according to Jibiri and Okeyode (2012), is a screening parameter for materials of possible radiation health challenge. It is calculated using the equation (El-Gamal et al., 2007; NEA-OECD, 1979; Ravisankar et al., 2014):

$$I_{\gamma r} = \frac{A_{Ra}}{150} + \frac{A_{Th}}{100} + \frac{A_K}{1500} \quad (3.11)$$

where, A_{Ra} , A_{Th} , and A_K are the respective specific activities of ^{226}Ra , ^{232}Th , and ^{40}K in Bq kg^{-1} . Manigandan and Shekar (2014), stated that to satisfy the dose criteria, the value of representative gamma index should be ≤ 1 , which corresponds to an annual effective dose of ≤ 1 mSv (Ravisankar et al., 2014).

(i) **Excess lifetime cancer risk (ELCR)**

Consequent upon the evaluation of annual effective dose equivalent, excess lifetime cancer risk (ELCR) was estimated using the equation (Ravisankar et al., 2014; Taskin et al., 2009):

$$ELCR = AEDE \times DL \times RF \quad (3.12)$$

where AEDE, DL, and RF are the annual effective dose equivalent, duration of life (70 years), and risk factor (0.05Sv^{-1}), respectively. Ravisankar et al. (2014), defined risk factor as fatal cancer risk per Sievert, which according to Taskin et al. (2009), is assigned

a value of 0.05 by International Commission on Radiological Protection, for the public for stochastic effects.

3.3.2 Trace Elements Analysis

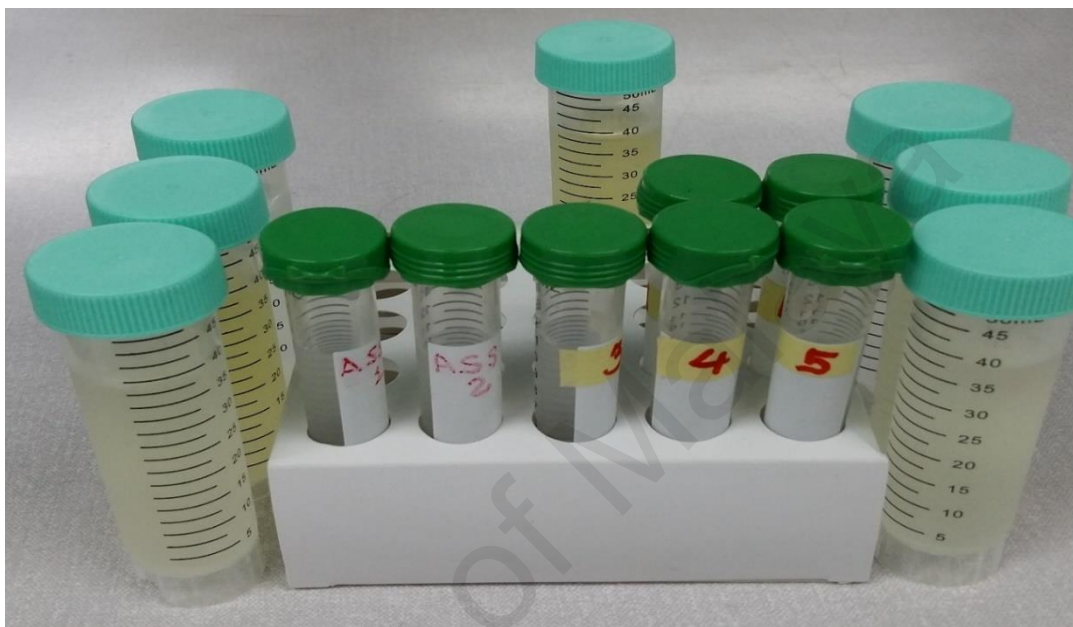
0.50 g of dry, pulverized coal sample was moistened with deionized water in a 60 ml Teflon beaker. 5 ml of concentrated HNO₃ was slowly added, and the solution evaporated to near dryness at 150⁰C on a hotplate. It was left to cool to room temperature, after which 10 ml of HF and 4 ml of HClO₄ were slowly added, and allowed to decompose at 200⁰C to near dryness. 10 ml of 5M HNO₃ was then added to the slurry, and carefully digested without excessive evaporation on hotplate. The sample was then allowed to cool to room temperature, and filtered through Whatman NO. 41 filter. The filtered digestate was diluted to 50 ml with deionized water in a volumetric flask, and the final solution stored at 4⁰C for analysis.

The digested coal samples were analysed for their trace elements concentrations using 7500 series inductively coupled plasma mass spectrometry (ICP-MS), supplied by Agilent Technologies, USA (part No. 8500-6940). The instrument was calibrated prior to analysis with multi element calibration standard 2A solution with analyte concentration of 10 mg kg⁻¹. The elemental detection limit for the equipment was below 1 ppb. Digested samples and the ICP-MS spectrometer are shown in Figure 3.6.

Enrichment/depletion factor (EDF) of all the measured trace elements in coal from Maiganga coalfield were computed as the ratio of elemental concentrations in coal to their respective Clarke values (Sia and Abdullah, 2011). That is:

$$EDF = \frac{\text{concentration of trace element in Maiganga coal}}{\text{trace element Clarke value}} \quad (3.12)$$

EDF is a parameter that expresses the degree of enrichment or depletion of any measured trace element in coal samples from Maiganga coalfield. $EDF > 1$ for any element indicates its level of enrichment, while $EDF < 1$ gives the degree of depletion of the element in coal.



(a)



(b)

Figure 3.6: (a) Digested coal samples (b) Agilent Technologies 7500 series ICP-MS used for trace elements analysis

3.3.3 Proximate Analysis

Proximate analysis is a chemical analytical process which involves the determination of moisture, volatile matter, fixed carbon, and ash contents in the coal samples. Proximate analysis was carried out on pulverized coal samples ($< 150 \mu\text{m}$ in size) using PerkinElmer Diamond Thermogravimetric-Differential Thermal Analyser (TG-DTA) shown in Figure 3.7



Figure 3.7: Perkin Elmer Diamond Thermogravimetric-Differential Thermal Analyser (TG-DTA) used in this study

3.3.4 Petrographic Analysis

Fine particles (2-4 mm) of coal samples were tightly bound together into coal blocks using a resin mixture and hardener. Each coal block was polished thoroughly using fine abrasives to obtain absolutely scratch-free smooth coal surface (Speight, 2005). Samples of prepared coal blocks are shown in Figure 3.8



Figure 3.8: Polished coal blocks

Petrographic analysis which involves determination of coal macerals and random vitrinite reflectance measurements was carried out on the polished coal blocks using LEICA CTR DM6000 Orthoplan microscope (Figure 3.9). Maceral analysis was done using single scan method under sample illumination by a combination of white and ultraviolet lights. Three basic maceral groups identified on the studied coal samples were the vitrinite, the liptinite, and the inertinite. Vitrinite reflectance measurements were carried out under light of single wavelength. The measurements were done using immersion oil of refractive index 1.518 at 23⁰C, and microscope oil immersion objective of $\times 50$. Before the measurements, the microscope was calibrated using a sapphire glass calibration standard of 0.589% reflectance value. Vitrinite reflectance was measured in random mode with at least 50 measurements per sample, and the mean recorded for the sample.



Figure 3.9: LEICA CTR DM6000 Orthoplan Microscope used in this study

University of Malaya

CHAPTER 4: RESULTS

4.1 Detector Efficiency Curve

Broad range of gamma-ray transition energies ranging from ~100 keV to about 2 MeV were analysed for the absolute photo-peak efficiency calibration of the HPGe detector. The absolute photo-peak efficiency was evaluated using a cylindrical multi-nuclide gamma-ray calibration source with an initial activity of 5.109 μCi , which was supplied by Isotopes Products Laboratories, Valencia, CA 91355. Photo-peak efficiency calibration curve as a function of photon energy used in the present study is shown in Figure 4.1.

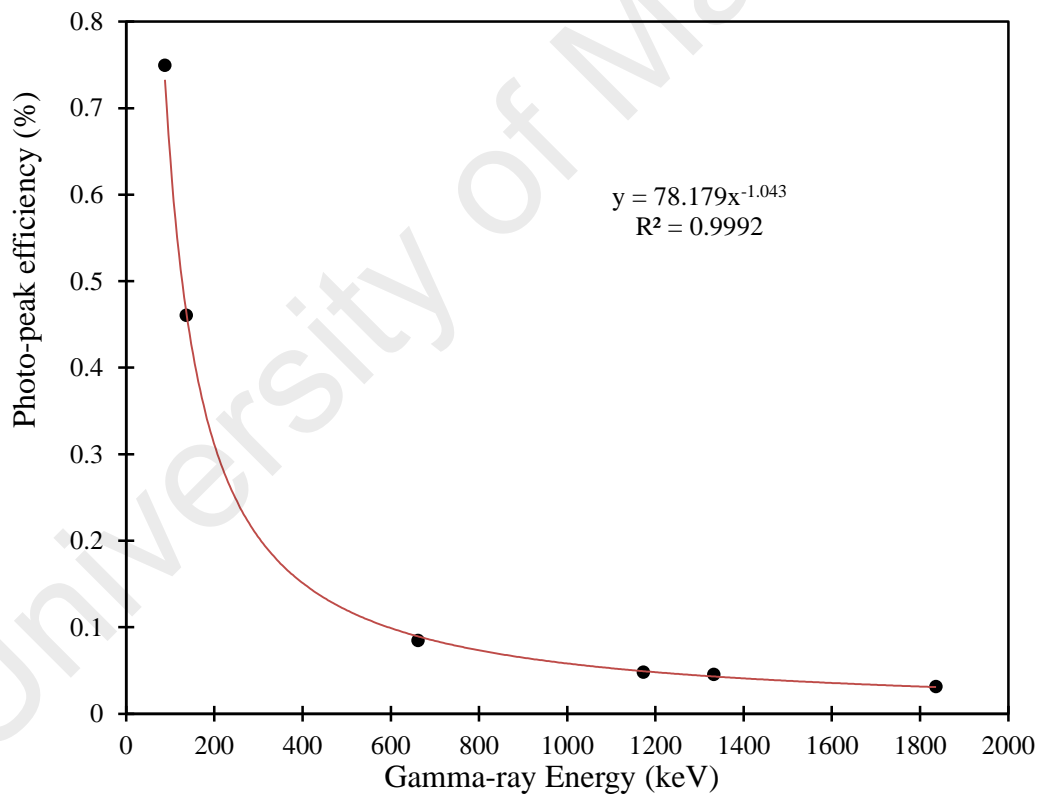


Figure 4.1: Efficiency calibration curve of the HPGe gamma-ray detector used in this study

4.2 Minimum Detectable Activity (MDA)

An empty Marinelli beaker was counted for the same counting time as the coal samples (86, 400 seconds), in order to obtain the radiation background. Minimum detectable activity (MDA) for each radionuclide of concern was then evaluated from the obtained background spectrum using Equation 3.1. The calculated MDA values are presented in Table 4.1. MDA, which is a function of detector efficiency and emission probability of the gamma lines of concern, ranged from 0.11 Bq kg⁻¹ for ²⁰⁸Tl to 2.16 Bq kg⁻¹ for ⁴⁰K.

Table 4.1: Decay data for radionuclides and the respective gamma lines and MDA (Bq kg⁻¹) used for activity determination

Nuclides of interest	Detected nuclides	Half-life	Decay mode (%)	γ -ray energy, E _{γ} (keV)	γ -ray intensity, I _{γ} (%)	Sources/ origin	MDA
²³⁸ U (²²⁶ Ra)	²¹⁴ Pb	26.80 m	β^- (100)	295.22	18.42	²³⁸ U (²²⁶ Ra) series	0.36
				351.93	35.6	²³⁸ U (²²⁶ Ra) series	0.55
	²¹⁴ Bi	19.90 m	α (0.02); β^- (99.98)	609.32	45.49	²³⁸ U (²²⁶ Ra) series	0.99
²³² Th (²²⁸ Ra)	²²⁸ Ac	6.15 h	$\alpha+\beta^-$ (100)	911.21	29	²³² Th series	0.75
				968.97	17.4		0.69
	²⁰⁸ Tl	3.053 m	β^- (100)	583.187	85	²³² Th (²²⁸ Ra) series	0.11
⁴⁰ K	⁴⁰ K	1.248×10 ⁹ y	EC (10.72); β^- (89.28)	1460.822	10.66	Primordial/terrestrial	2.16

4.3 Natural Radioactivity in Coal from Maiganga Coalfield

Thirty three coal samples (MCS 01 to MCS 33) were collected from Maiganga coalfield, and analysed for their radioactivity contents using high purity germanium (HPGe) gamma-ray spectrometer. Specific activities of ²²⁶Ra, ²³²Th, and ⁴⁰K in the samples were computed from the measured gamma ray photo-peaks using Equation (3.2). The results of the computed activity concentrations which comprises the minimum and maximum values, the arithmetic mean (AM) and standard deviation (SD), are presented in Table 4.2. Activity concentration of ²²⁶Ra in coal samples from Maiganga coalfield

ranged from 3.7 ± 0.1 to 16.3 ± 0.3 Bq kg⁻¹ with average value of 8.2 ± 3.5 Bq kg⁻¹, while ²³²Th activity varied between 2.0 ± 0.1 and 11.3 ± 0.3 Bq kg⁻¹ with a mean value of 7.0 ± 2.4 Bq kg⁻¹. The activity concentration of ⁴⁰K was found to lie between 6.7 ± 0.1 and 44.1 ± 0.7 Bq kg⁻¹ with a mean value of 27.4 ± 11.4 Bq kg⁻¹. Mean activity concentrations of ²²⁶Ra, ²³²Th, and ⁴⁰K in coal samples from Maiganga coalfield were found to be lower than their respective world average values of 20, 20, and 50 Bq kg⁻¹ for coal reported by UNSCEAR (1982). These results indicate the non-hazardous nature of Maiganga coalfield.

Radiation hazard indices, which include the radium equivalent activity (R_{eq}), gamma absorbed dose rate (D_R), annual effective dose equivalent (AEDE), annual gonadal dose (AGDE), external hazard index (H_{ex}), internal hazard index (H_{in}), gamma index (I_{γ}), and excess life cancer risk (ELCR) were computed from the specific activities of ²²⁶Ra, ²³²Th, and ⁴⁰K using Equations (3.4 – 3.12), and the results are presented in Table 4.3. The calculated values for radium equivalent activity index for coal samples from Maiganga coalfield were in the range of 8.92 to 35.30 Bq kg⁻¹ with a mean value of 20.26 Bq kg⁻¹, and standard deviation of 6.62 Bq kg⁻¹. The corresponding external hazard index was found to vary between 0.02 and 0.10, with an average value of 0.05 for the studied coal samples. These values were found to be lower than the respective safety limits of 370 Bq kg⁻¹ and 1, recommended by UNSCEAR (2000). External absorbed gamma dose at 1 m above ground level from exposure to ²²⁶Ra, ²³²Th, and ⁴⁰K in coal samples from Maiganga coalfield ranged from 4.19 to 15.90 nGy h⁻¹ with a mean value of 9.13 nGy h⁻¹. Assuming a 20 % outdoor occupancy factor, the corresponding annual effective dose equivalent was found to vary between 0.010 and 0.020 mSv y⁻¹ with an average value of 0.012 mSv y⁻¹. This value was found to be significantly lower than the world average annual effective dose limit of 0.07 mSv y⁻¹ documented in UNSCEAR (2000) report.

Table 4.2: Activity concentrations (Bq kg⁻¹) of ²²⁶Ra, ²³²Th, and ⁴⁰K, in coal samples from Mainganga coalfield

Sample ID	²²⁶ Ra	²³² Th	⁴⁰ K
MCS 01	12.7±0.6	11.0±0.6	17.9±1.0
MCS 02	12.8±0.7	10.5±0.6	19.1±1.0
MCS 03	7.0±0.4	3.5±0.3	7.7±1.0
MCS 04	10.8±0.6	9.1±0.5	13.3±1.0
MCS 05	6.6±0.4	3.3±0.3	9.2±1.0
MCS 06	10.8±0.6	8.3±0.5	12.9±1.0
MCS 07	11.4±0.6	9.3±0.5	15.1±1.0
MCS 08	10.5±0.6	9.1±0.5	12.1±1.0
MCS 09	13.1±0.3	8.1±0.2	36.6±0.6
MCS 10	13.0±0.2	8.1±0.2	34.4±0.5
MCS 11	9.4±0.2	8.3±0.2	29.8±0.5
MCS 12	8.3±0.5	7.2±0.4	16.2±0.9
MCS 13	7.4±0.4	6.1±0.4	15.0±0.8
MCS 14	16.3±0.3	11.3±0.3	37.6±0.6
MCS 15	15.9±0.3	11.3±0.3	38.5±0.6
MCS 16	6.2±0.4	7.1±0.4	15.5±0.9
MCS 17	8.5±0.2	9.4±0.2	6.7±0.1
MCS 18	8.8±0.2	7.4±0.2	34.3±0.6
MCS 19	7.6±0.2	5.8±0.2	41.3±0.7
MCS 20	8.0±0.1	7.3±0.1	44.1±0.7
MCS 21	5.0±0.1	6.9±0.1	36.1±0.6
MCS 22	4.5±0.1	4.0±0.1	31.9±0.5
MCS 23	3.7±0.1	2.0±0.1	29.9±0.5
MCS 24	6.0±0.1	7.6±0.2	35.7±0.6
MCS 25	5.8±0.1	7.3±0.2	38.5±0.6
MCS 26	5.3±0.1	5.9±0.1	35.3±0.6
MCS 27	4.8±0.1	5.7±0.1	36.3±0.6
MCS 28	4.4±0.1	4.4±0.1	38.9±0.6
MCS 29	5.4±0.1	5.1±0.2	39.2±0.7
MCS 30	4.7±0.3	4.1±0.3	31.3±1.6
MCS 31	5.1±0.3	4.9±0.4	31.0±1.6
MCS 32	4.9±0.3	4.9±0.3	30.3±1.6
MCS 33	5.2±0.3	5.4±0.4	31.6±1.7
Minimum	3.7±0.1	2.0±0.1	6.7±0.1
Maximum	16.3±0.3	11.3±0.3	44.1±0.7
Mean	8.2	7.0	27.4
SD	3.5	2.4	11.4

SD = standard deviation

Similarly, calculated annual gonadal dose varied between 29.35 and 109.23 $\mu\text{Sv y}^{-1}$ with average value of 63.01 $\mu\text{Sv y}^{-1}$ for the studied coal samples. The internal hazard index, H_{in} , which describes the degree of internal exposure to radon and its decay products, varied from 0.03 to 0.14 with an average value of 0.08. Furthermore, calculated gamma index, I_{gr} , for coal samples from Maiganga coalfield varied in the range of 0.06 to 0.25 with a mean value of 0.14. These values were less than the safety limit of one stipulated by UNSCEAR (2000).

Excess lifetime cancer risk (ELCR), calculated for Maiganga coalfield, varied between 0.2×10^{-4} and 0.7×10^{-4} , with a mean value of 0.04×10^{-3} . This value was found to be less than the precautionary limit of 0.29×10^{-3} set by UNSCEAR (2000) and 0.05 prescribed by the International Commission on Radiological Protection (ICRP) for low-level radiations. Generally, the estimated radiation hazard indices presented in Table 4.3 for coal samples from Maiganga coalfield were found to be lower than their respective safety limits prescribed by UNSCEAR. The results of this current work thus, showed that the exploitation and utilization of Maiganga coal, either for power generation or other industrial and domestic uses does not pose any significant radiological impact to the coal workers, the coal users, and the general environment.

Table 4.3: Radiation hazard indices of coal samples from Maiganga coalfield

Sample ID	R _{eq} (Bq kg ⁻¹)	D _R (nGy h ⁻¹)	AEDE (mSv y ⁻¹)	AGDE (μSv y ⁻¹)	AUI	H _{ex}	H _{in}	I _{yr}	ELCR (× 10 ⁻³)
MCS 01	29.83	13.27	0.02	90.91	0.25	0.08	0.11	0.21	0.06
MCS 02	29.38	13.09	0.02	89.71	0.25	0.08	0.11	0.20	0.06
MCS 03	12.65	5.69	0.01	38.84	0.11	0.03	0.05	0.09	0.02
MCS 04	24.88	11.06	0.01	75.72	0.21	0.07	0.10	0.17	0.05
MCS 05	12.11	5.46	0.01	37.31	0.10	0.03	0.05	0.08	0.02
MCS 06	23.73	10.57	0.01	72.32	0.20	0.06	0.09	0.16	0.04
MCS 07	25.88	11.52	0.01	78.90	0.22	0.07	0.10	0.18	0.05
MCS 08	24.40	10.83	0.01	74.15	0.21	0.07	0.09	0.17	0.05
MCS 09	27.46	12.45	0.02	85.70	0.22	0.07	0.11	0.19	0.05
MCS 10	27.22	12.33	0.01	84.81	0.22	0.07	0.11	0.19	0.05
MCS 11	23.56	10.60	0.01	73.09	0.19	0.06	0.09	0.17	0.04
MCS 12	19.89	8.88	0.01	60.97	0.17	0.05	0.08	0.14	0.04
MCS 13	17.30	7.74	0.01	53.14	0.14	0.05	0.07	0.12	0.03
MCS 14	35.30	15.90	0.02	109.23	0.29	0.10	0.14	0.25	0.07
MCS 15	35.01	15.77	0.02	108.44	0.29	0.09	0.14	0.24	0.07
MCS 16	17.48	7.77	0.01	53.51	0.14	0.05	0.06	0.12	0.03
MCS 17	22.46	9.88	0.01	67.66	0.19	0.06	0.08	0.16	0.04
MCS 18	22.08	9.99	0.01	69.05	0.17	0.06	0.08	0.16	0.04
MCS 19	19.12	8.76	0.01	60.84	0.14	0.05	0.07	0.14	0.04
MCS 20	21.86	9.95	0.01	69.15	0.17	0.06	0.08	0.16	0.04
MCS 21	17.65	7.99	0.01	55.64	0.13	0.05	0.06	0.13	0.03
MCS 22	12.71	5.84	0.01	40.75	0.09	0.03	0.05	0.09	0.02
MCS 23	8.92	4.19	0.01	29.35	0.06	0.02	0.03	0.06	0.02
MCS 24	19.62	8.85	0.01	61.54	0.15	0.05	0.07	0.14	0.04
MCS 25	19.26	8.72	0.01	60.70	0.15	0.05	0.07	0.14	0.04
MCS 26	16.52	7.51	0.01	52.33	0.12	0.04	0.06	0.12	0.03
MCS 27	15.75	7.18	0.01	50.09	0.12	0.04	0.06	0.11	0.03
MCS 28	13.66	6.30	0.01	44.13	0.10	0.04	0.05	0.10	0.03
MCS 29	15.73	7.22	0.01	50.36	0.11	0.04	0.06	0.11	0.03
MCS 30	12.97	5.95	0.01	41.48	0.10	0.04	0.05	0.09	0.03
MCS 31	14.52	6.62	0.01	46.04	0.11	0.04	0.05	0.10	0.03
MCS 32	14.22	6.48	0.01	45.08	0.11	0.04	0.05	0.10	0.03
MCS 33	15.31	6.96	0.01	48.43	0.12	0.04	0.06	0.11	0.03
Minimum	8.92	4.19	0.01	29.35	0.06	0.02	0.03	0.06	0.02
Maximum	35.30	15.90	0.02	109.23	0.29	0.10	0.14	0.25	0.07
Mean	20.26	9.13	0.01	63.01	0.16	0.05	0.08	0.14	0.04

4.4 Natural Radioactivity in Coal Mine Tailings from Maiganga Coalfield

Twenty samples of coal mine tailings were collected from Maiganga coalfield and analyzed for their radioactivity contents using HPGe gamma-ray detector. Activity concentrations of ^{226}Ra , ^{232}Th , and ^{40}K in the investigated mine tailings were computed from the measured gamma ray photo-peaks using Equation (3.2). Statistical description comprising the minimum and maximum values, the mean, and standard deviation (SD) of activity concentrations of ^{226}Ra , ^{232}Th , and ^{40}K in coal mine tailings from Maiganga coalfield together with their respective concentration ratios are presented in Table 4.4. The activity concentration of ^{226}Ra ranged between 4.6 ± 0.2 and 16.3 ± 0.8 Bq kg^{-1} with a mean concentration value of 11.9 ± 3.0 Bq kg^{-1} . For ^{232}Th , the activity concentration varied from 8.5 ± 0.4 to 23.2 ± 1.1 Bq kg^{-1} with an average concentration of 17.7 ± 3.6 Bq kg^{-1} . ^{40}K , however, showed a high mean concentration value of 70.4 ± 20.4 Bq kg^{-1} within the standard deviation compared to those of ^{226}Ra , and ^{232}Th . Mean activities of ^{226}Ra , ^{232}Th and ^{40}K in the tailings from Maiganga coal mine were found to be lower than their respective world averages of 32, 45 and 412 Bq kg^{-1} .

Table 4.4: Descriptive statistics of activity concentrations, and concentration ratios of ^{226}Ra , ^{232}Th , ^{40}K , in coal mine tailings from Maiganga coalfield

Sample ID	^{226}Ra (Bq kg ⁻¹)	^{232}Th (Bq kg ⁻¹)	^{40}K (Bq kg ⁻¹)
CMW 01	13.3±0.6	18.6±0.9	87.4±4.1
CMW 02	12.9±0.6	21.4±1.0	69.4±3.3
CMW 03	11.0±0.5	19.5±1.0	66.0±3.1
CMW 04	10.0±0.5	13.0±0.6	65.0±3.1
CMW 05	15.1±0.7	19.8±1.0	84.8±4.0
CMW 06	10.8±0.5	18.9±1.0	64.1±3.1
CMW 07	13.5±0.6	17.9±0.9	70.9±3.3
CMW 08	10.7±0.5	18.2±0.9	53.6±2.6
CMW 09	4.6±0.2	8.5±0.4	26.7±1.3
CMW 10	10.7±0.5	17.6±0.9	45.8±2.2
CMW 11	14.3±0.7	23.2±1.1	96.5±4.5
CMW 12	6.5±0.3	12.4±0.6	54.3±2.6
CMW 13	12.3±0.6	19.6±1.0	81.1±3.8
CMW 14	13.7±0.7	20.3±1.0	98.0±4.6
CMW 15	14.3±0.7	20.1±1.0	66.5±3.2
CMW 16	12.2±0.6	18.4±0.9	114.1±5.3
CMW 17	13.7±0.7	20.4±1.0	81.5±3.8
CMW 18	16.3±0.8	15.8±0.8	46.0±2.2
CMW 19	7.4±0.4	12.6±0.6	75.7±3.5
CMW 20	14.6±0.7	18.0±0.9	61.5±2.9
Min	4.6±0.2	8.5±0.4	26.7±1.3
Max	16.3±0.8	23.2±1.1	114.1±5.3
Mean±SD	11.9±3.0	17.7±3.6	70.4±20.4

Similarly, radiation hazard indices which include radium equivalent activity (Ra_{eq}), external dose rate (D_R), annual effective dose (AEDE), excess lifetime cancer risk (ELCR), and other radiation hazard indices were calculated from the specific activities of ^{226}Ra , ^{232}Th , and ^{40}K using Equations (3.4 – 3.12), and the results are presented in Table 4.5.

The results obtained for Ra_{eq} varied from 18.77 to 54.98 Bq kg⁻¹ with a mean value of 42.67 Bq kg⁻¹. The mean value was lower than the world precautionary limit of 370 Bq kg⁻¹ set by the Organization of Economic Cooperation and Development (NEA-OECD, 1979). Gamma absorbed dose rate in air at 1 m above ground level estimated for the

tailings ranged between 8.35 and 26.67 nGy h⁻¹ with an average value of 19.14 nGy h⁻¹. This value was lower than the world average value of 58 nGy h⁻¹ provided by UNSCEAR (2008). Similarly, the estimated mean annual effective dose equivalent of 0.02 mSv y⁻¹ was recorded for the studied mine tailings, which was lower than the mean worldwide outdoor effective dose of 0.07 mSv reported by UNSCEAR (2000).

Average values calculated for AUI, H_{ex}, H_{in} and I_{yr} were 0.33, 0.12, 0.15 and 0.30, respectively. These values were below the internationally approved safety limit of one, for radiation protection (UNSCEAR, 2000). Generally, the radiation hazard to the general public due to exposure to natural radionuclides in mine tailings from Maiganga coalfield is insignificant, thus, the use of coal mine tailings from Maiganga coalfield, either for landfills, agricultural purposes, or as aggregates of building material does not pose any radiological threat to the general public. Furthermore, the computed average AGDE was 132.97 μSv y⁻¹ with a corresponding mean ELCR of 0.08 × 10⁻³. This value was found to be below the world average ELCR value of 0.29 × 10⁻³ contained in UNSCEAR (2000) report, and also lower than 0.05 low-level radiation limit set by the International Commission on Radiation Protection. The probability of cancer effects in the general public from the use of coal mine tailings from Maiganga coalfield, is therefore negligible.

Table 4.5: Radiological hazard indices of coal mine tailings from Maiganga coalfield

Sample ID	R _{aeq} (Bq kg ⁻¹)	D _R (nGy h ⁻¹)	AEDE (mSv yr ⁻¹)	AGDE (μSv yr ⁻¹)	AUI	H _{ex}	H _{in}	I _{yr}	ELCR (×10 ⁻³)
CMW 01	46.64	21.03	0.03	146.32	0.36	0.13	0.16	0.33	0.09
CMW 02	48.94	21.82	0.03	151.40	0.38	0.13	0.17	0.35	0.09
CMW 03	43.99	19.62	0.02	136.29	0.34	0.12	0.15	0.31	0.08
CMW 04	33.54	15.16	0.02	105.48	0.25	0.09	0.12	0.24	0.06
CMW 05	49.89	22.45	0.03	155.90	0.39	0.13	0.18	0.35	0.10
CMW 06	42.77	19.08	0.02	132.53	0.33	0.12	0.14	0.30	0.08
CMW 07	44.62	20.03	0.02	138.98	0.35	0.12	0.16	0.32	0.08
CMW 08	40.85	18.17	0.02	125.97	0.32	0.11	0.14	0.29	0.08
CMW 09	18.77	8.35	0.01	58.00	0.15	0.05	0.06	0.13	0.04
CMW 10	39.49	17.52	0.02	121.29	0.32	0.11	0.14	0.28	0.07
CMW 11	54.98	24.67	0.03	171.67	0.42	0.15	0.19	0.39	0.10
CMW 12	28.48	12.79	0.02	89.17	0.22	0.08	0.09	0.20	0.05
CMW 13	46.62	20.92	0.03	145.53	0.36	0.13	0.16	0.33	0.09
CMW 14	50.24	22.66	0.03	157.85	0.38	0.14	0.17	0.36	0.10
CMW 15	48.17	21.52	0.03	149.11	0.38	0.13	0.17	0.34	0.09
CMW 16	47.32	21.52	0.03	150.51	0.34	0.13	0.16	0.34	0.09
CMW 17	49.14	22.05	0.03	153.17	0.38	0.13	0.17	0.35	0.09
CMW 18	42.49	19.02	0.02	131.02	0.35	0.11	0.16	0.30	0.08
CMW 19	31.33	14.22	0.02	99.55	0.23	0.08	0.10	0.23	0.06
CMW 20	45.10	20.19	0.02	139.74	0.36	0.12	0.16	0.32	0.09
Min	18.77	8.35	0.01	58.00	0.15	0.05	0.06	0.13	0.04
Max	54.98	24.67	0.03	171.67	0.42	0.15	0.19	0.39	0.10
Mean	42.67	19.14	0.02	132.97	0.33	0.12	0.15	0.30	0.08

4.5 Natural Radioactivity in Soil Samples around Ashaka Cement Factory

Ashaka cement factory Plc (AshakaCem) is located at 10°55'49''N and 11°28'34''E in Bajoga, Funakaye Local Government Area of Gombe State, North-eastern Nigeria. AshakaCem, which assumed full continuous operation since 1979, is currently the largest cement producing factory in Northern Nigeria. About 90 % of the energy requirements of the factory, especially in firing the cement kiln, is realised from combustion of coal supplied directly from Maiganga coalfield. Coal combustion has been identified as a potential source of enhanced soil radioactivity in the environment.

Twenty soil samples (ASS 01 to ASS 20) which satisfactorily represents AshakaCem environment were collected and analyzed for their radioactivity content. Four sub-

samples were collected around a sampling point, and thoroughly mixed together to obtain one bulk sample that represents a particular sampling point. Activity concentrations of ^{226}Ra , ^{232}Th , and ^{40}K , in soil samples around AshakaCem were computed from the measured gamma ray photo-peaks using Equation (3.2). Statistical description comprising the minimum and maximum values, the mean, and standard deviation (SD) of specific activities of ^{226}Ra , ^{232}Th , and ^{40}K , in the soil samples are presented in Table 4.6.

Table 4.6: Activity concentrations (Bq kg⁻¹) of ^{226}Ra , ^{232}Th , and ^{40}K , in soil samples around AshakaCem

Sample ID	^{226}Ra	^{232}Th	^{40}K
ASS 01	8.8±0.4	15.6±0.8	216.3±10.0
ASS 02	7.0±0.4	15.5±0.8	174.9±8.1
ASS 03	7.4±0.4	15.7±0.8	192.3±8.9
ASS 04	6.5±0.4	13.9±0.7	222.9±10.3
ASS 05	5.7±0.3	11.5±0.6	189.2±8.7
ASS 06	7.0±0.4	15.5±0.7	180.7±8.3
ASS 07	5.2±0.3	11.7±0.6	95.3±4.4
ASS 08	3.7±0.3	9.1±0.5	74.8±3.6
ASS 09	6.7±0.4	15.2±0.8	157.8±7.3
ASS 10	5.9±0.4	12.7±0.6	168.9±7.8
ASS 11	7.4±0.4	16.1±0.8	191.0±8.8
ASS 12	9.0±0.5	19.2±1.0	233.3±10.8
ASS 13	8.7±0.5	17.7±0.9	245.6±11.3
ASS 14	7.5±0.4	14.6±0.8	193.9±9.0
ASS 15	8.3±0.5	18.1±0.9	252.8±11.7
ASS 16	11.5±0.6	35.9±1.7	221.7±10.3
ASS 17	6.5±0.4	15.4±0.8	203.3±9.4
ASS 18	9.6±0.5	19.4±1.0	248.0±11.5
ASS 19	8.1±0.5	16.5±0.8	229.9±10.6
ASS 20	7.5±0.4	16.1±0.8	229.5±10.6
Min	3.7±0.3	9.1±0.5	74.8±3.6
Max	11.5±0.6	35.9±1.7	252.8±11.7
Mean	7.4	16.3	196.1
SD	1.7	5.3	46.8

Mean activity concentration of ^{226}Ra was $7.4\pm 0.4 \text{ Bq kg}^{-1}$, with concentration values varying between 3.7 ± 0.3 and $11.5\pm 0.6 \text{ Bq kg}^{-1}$. Average activities of ^{232}Th and ^{40}K were 16.3 ± 0.8 and $196.1\pm 9.1 \text{ Bq kg}^{-1}$ respectively, with concentration values ranging from 9.1 ± 0.5 to $35.9\pm 1.7 \text{ Bq kg}^{-1}$, and 74.8 ± 3.6 to $252.8\pm 11.7 \text{ Bq kg}^{-1}$, in sequence. Variations noticed in activity values may not be unconnected with the physical, chemical and geochemical properties of the radionuclides, coupled with their respective presence in soil samples of the study area (El Mamoney & Khater, 2004; Ravisankar et al., 2014). Data obtained in this investigation for specific activities of primordial radionuclides were below their respective world average values of 35, 30, 400 Bq kg^{-1} for normal soils documented by UNSCEAR (2000).

Results of radiological dose parameters, including R_{eq} , D_{R} , AEDE, AGDE, and the hazard indices are presented in Table 4.7. Studied soil samples showed R_{eq} values in the vicinity of AshakaCem to range from 22.52 to 79.94 Bq kg^{-1} , with an average value of 45.77 Bq kg^{-1} . This value is lower than the prescribed limit for safety of 370 Bq kg^{-1} (UNSCEAR, 2000). Calculated average value for D_{R} at 1 m above ground level was 21.43 nGy h^{-1} , with corresponding average AEDE of 0.03 mSv y^{-1} (Table 4.7). These values were below their respective world precautionary limits of 57 nGy h^{-1} and 0.07 mSv y^{-1} respectively, for external exposure (UNSCEAR, 2000). Similarly, the overall mean value of AGDE was 152.48 $\mu\text{Sv y}^{-1}$, with variations spanning from 73.10 to 255.32 $\mu\text{Sv y}^{-1}$ in the vicinity of AshakaCem. Furthermore, all the calculated hazard indices including AUI, H_{ex} , H_{in} and I_{yr} , as seen in Table 4.7, have values lower than 1, which corresponds to annual effective dose $\leq 1 \text{ mSv}$ (Ravisankar et al., 2014). Additionally, estimated average ELCR was 0.9×10^{-4} , which was below the world average value of 0.29×10^{-3} for normal soils documented by UNSCEAR (2000), and also lower than 0.05 safety limit for low-level radiations set by the International Commission for Radiological Protection. Generally, gamma dose received by factory workers and the general public from the

operations of AshakaCem are below the safety limits set by UNSCEAR (2000), for radiation protection. The risk of cancer among the general population was also found to be insignificant. The results of this study showed that the impacts of coal combustion during AshakaCem operations on human health and the environment, are negligible from radiation protection perspective.

Table 4.7: Radiological hazard indices of soil samples around AshakaCem

Sample ID	R _{eq} (Bq kg ⁻¹)	D _R (nGy h ⁻¹)	AEDE (mSv y ⁻¹)	AGDE (μSv y ⁻¹)	AUI	H _{ex}	H _{in}	I _{yr}	ELCR (×10 ⁻³)
ASS 01	47.83	22.54	0.03	160.52	0.29	0.13	0.15	0.36	0.10
ASS 02	42.62	19.88	0.02	141.31	0.27	0.12	0.13	0.32	0.08
ASS 03	44.63	20.91	0.03	148.79	0.27	0.12	0.14	0.33	0.09
ASS 04	43.51	20.68	0.03	148.08	0.25	0.12	0.14	0.33	0.09
ASS 05	36.64	17.44	0.02	124.88	0.21	0.10	0.11	0.28	0.07
ASS 06	43.08	20.13	0.02	143.18	0.27	0.12	0.14	0.32	0.09
ASS 07	29.34	13.48	0.02	95.12	0.20	0.08	0.09	0.22	0.06
ASS 08	22.52	10.35	0.01	73.10	0.15	0.06	0.07	0.17	0.04
ASS 09	40.56	18.85	0.02	133.72	0.26	0.11	0.13	0.30	0.08
ASS 10	37.07	17.44	0.02	124.35	0.22	0.10	0.12	0.28	0.07
ASS 11	45.07	21.08	0.03	149.96	0.28	0.12	0.14	0.34	0.09
ASS 12	54.38	25.47	0.03	181.20	0.33	0.15	0.17	0.41	0.11
ASS 13	52.96	24.97	0.03	178.09	0.31	0.14	0.17	0.40	0.11
ASS 14	43.37	20.40	0.02	145.27	0.26	0.12	0.14	0.33	0.09
ASS 15	53.77	25.36	0.03	181.03	0.32	0.15	0.17	0.41	0.11
ASS 16	79.94	36.26	0.04	255.32	0.56	0.22	0.25	0.58	0.15
ASS 17	44.09	20.75	0.03	148.05	0.26	0.12	0.14	0.33	0.09
ASS 18	56.40	26.48	0.03	188.52	0.34	0.15	0.18	0.42	0.11
ASS 19	49.49	23.33	0.03	166.46	0.29	0.13	0.16	0.37	0.10
ASS 20	48.21	22.77	0.03	162.60	0.28	0.13	0.15	0.36	0.10
Min	22.52	10.35	0.01	73.1	0.15	0.06	0.07	0.17	0.04
Max	79.94	36.26	0.04	255.32	0.56	0.22	0.25	0.58	0.15
Mean	45.77	21.43	0.03	152.48	0.28	0.12	0.14	0.34	0.09
SD	11.53	5.27	0.01	37.24	0.08	0.03	0.04	0.08	0.02

4.6 Trace Elements Concentrations in Coal Samples from Maiganga Coalfield

Trace elements concentrations of fifteen coal samples (MCS 10 to MCS 15) from Maiganga coalfield were analysed using inductively coupled plasma mass spectrometer (ICP-MS). Results of trace elements concentrations (mg kg^{-1}) are presented in Table 4.8. The concentration of Cd was below detection limit in all the samples while Zn was detected in less than 50% of the samples, thus they were not discussed in details in this study. Potentially hazardous trace elements (PHTEs) are bolded and underlined.

Table 4.8: Trace elements concentrations (mg kg^{-1}) of coal samples from Maiganga coal-field. PHTEs are bold and underlined

Sample ID	<u>Cr</u>	<u>Cd</u>	Cu	<u>Pb</u>	<u>Ni</u>	V	Co	Zn	<u>Mn</u>	Ba	<u>Be</u>	Sr
MCS 01	13.54	bdl	10.15	6.10	8.50	28.50	3.71	3.88	120.44	59.37	1.13	8.85
MCS 02	7.28	bdl	7.16	4.74	4.15	15.57	2.56	1.14	189.83	50.42	1.46	8.41
MCS 03	9.79	bdl	8.26	5.19	5.08	20.38	2.65	3.54	216.00	52.76	1.54	8.32
MCS 04	1.45	bdl	1.24	0.66	3.19	1.84	0.43	bdl	128.56	30.17	0.33	14.43
MCS 05	0.93	bdl	1.52	0.74	3.19	0.78	0.83	bdl	69.91	39.78	0.27	11.54
MCS 06	6.43	bdl	5.83	3.83	5.54	5.60	3.45	1.27	130.76	57.82	0.96	12.55
MCS 07	1.75	bdl	1.98	0.86	2.10	2.20	0.07	bdl	121.25	43.49	0.30	16.07
MCS 08	1.36	bdl	2.02	0.53	2.52	1.82	1.84	0.64	46.45	24.49	1.26	20.04
MCS 09	0.32	bdl	0.87	0.29	3.61	0.72	0.85	bdl	76.17	20.19	0.46	18.20
MCS 10	1.27	bdl	1.72	0.72	2.25	1.78	0.89	0.61	107.02	24.64	0.65	34.08
MCS 11	0.81	bdl	1.50	0.18	1.45	1.18	0.34	bdl	58.56	19.47	0.32	15.19
MCS 12	0.98	bdl	1.43	0.50	0.23	1.42	bdl	bdl	47.17	86.94	0.53	95.60
MCS 13	0.56	bdl	1.23	0.38	bdl	0.86	bdl	bdl	21.81	35.44	0.17	36.33
MCS 14	0.34	bdl	0.55	0.34	bdl	0.76	bdl	0.10	11.36	42.84	0.13	46.12
MCS 15	0.38	bdl	1.05	0.45	0.07	0.82	bdl	bdl	17.84	65.29	0.28	73.94

bdl = below detection limit

Descriptive statistics of elemental concentrations including the maximum, minimum, mean, and standard deviation, along with their respective Clarke values and calculated enrichment/depletion factor (EDF) are presented in Table 4.9. The Clarke values for trace elements in low rank coals were adopted from Ketris and Yudovich (2009).

Concentration of Cr in coal samples from Maiganga coalfield varied between 0.32 and 13.54 mg kg⁻¹ with an average of 3.15 mg kg⁻¹ (Table 4.9). Estimated EDF with respect to its Clarke value for low-rank coals was 0.2. This showed that Cr is highly depleted in Maiganga coal, and therefore, does not pose any environmental or health challenge to the workers and the community.

The range of concentration for Pb was from 0.18 to 6.10 mg kg⁻¹ with a mean concentration value of 1.70 mg kg⁻¹. Average concentration of Pb was lower than its Clarke value for low-rank coals, thus the estimated EDF of 0.3 (Table 4.9) showed the level of depletion of Pb in coal samples from Maiganga coalfield.

Ni in the studied coal samples from Maiganga coalfield was found to be very low compared to the average value for Ni in world low-rank coals provided by Ketriss and Yudovich (2009). Ni recorded an average concentration of 3.22 mg kg⁻¹ with calculated EDF of 0.4 (Table 4.9).

Mn was found to be the most abundant element in coal samples from Maiganga coalfield as seen in Table 4.8. Its concentration span through wide variations, ranging from 11.36 to 216.00 mg kg⁻¹. The mean concentration value of 90.88 mg kg⁻¹ for Mn is comparable to the average concentration of Mn in world low-rank coals (100 mg kg⁻¹) reported by Ketriss and Yudovich (2009).

Table 4.9: Descriptive statistics including minimum, maximum, mean and standard deviation of trace elements concentrations (mg kg⁻¹) in coal samples from Maiganga coalfield, along with their respective Clarke values and enrichment/depletion factors

Element	Cr	Cd	Cu	Pb	Ni	V	Co	Zn	Mn	Ba	Be	Sr
Min	0.32	bdl	0.55	0.18	bdl	0.72	bdl	bdl	11.36	19.47	0.13	8.32
Max	13.54	bdl	10.15	6.10	8.50	28.50	3.71	3.88	216.00	86.94	1.54	95.60
Mean	3.15	bdl	3.10	1.70	3.22	5.62	1.60	1.60	90.88	43.54	0.65	27.98
SD	4.11	bdl	3.11	2.09	2.28	8.66	1.30	1.50	61.25	18.99	0.49	25.93
CV^a	15±1	0.24±0.04	15±1	6.6±0.4	9±0.9	22±2	4.2±0.3	18±1	100±6	150±20	1.2±0.1	120±10
EDF	0.2	nc	0.2	0.3	0.4	0.3	0.3	0.1	0.9	0.3	0.5	0.2

bdl = below detection limit

CV^a = Clarke value (after Ketris and Yudovich, 2009)

EDF = enrichment/depletion factor

nc = not calculated

PHTEs are bold

Generally, the concentration of all the studied trace elements in coal samples from Maiganga coalfield were found to be below the world average values for low-rank coals provided by Ketris and Yudovich (2009). Furthermore, the EDF for all the elements relative to their Clarke values were found to be less than one (Table 4.9). It is evident from the obtained results, therefore, that coal samples from Maiganga coalfield are depleted in trace elements including those termed potentially hazardous. Hence, the exploitation and utilization of coal from Maiganga coalfield does not constitute any threat from the perspective of human health and environmental protection.

4.7 Proximate and Petrographic Analysis of Coal from Maiganga Coalfield

Proximate and petrographic analyses were undertaken on coal samples from Maiganga coalfield in order to determine the traditional parameters of the deposit. Proximate analysis of fifteen coal samples was carried out using PerkinElmer Diamond Thermogravimetric-Differential Thermal Analyser (TG-DTA), and the results are presented in Table 4.10.

Graphical representation of proximate analysis of Maiganga coal using the TG-DTA is shown in Figure 4.2. Three temperature zones were clearly delineated. In Zone I, the temperature was ramped to 105⁰C and held isothermally. Weight loss in coal sample experienced in this zone was directly due to loss of total moisture content of the coal sample.

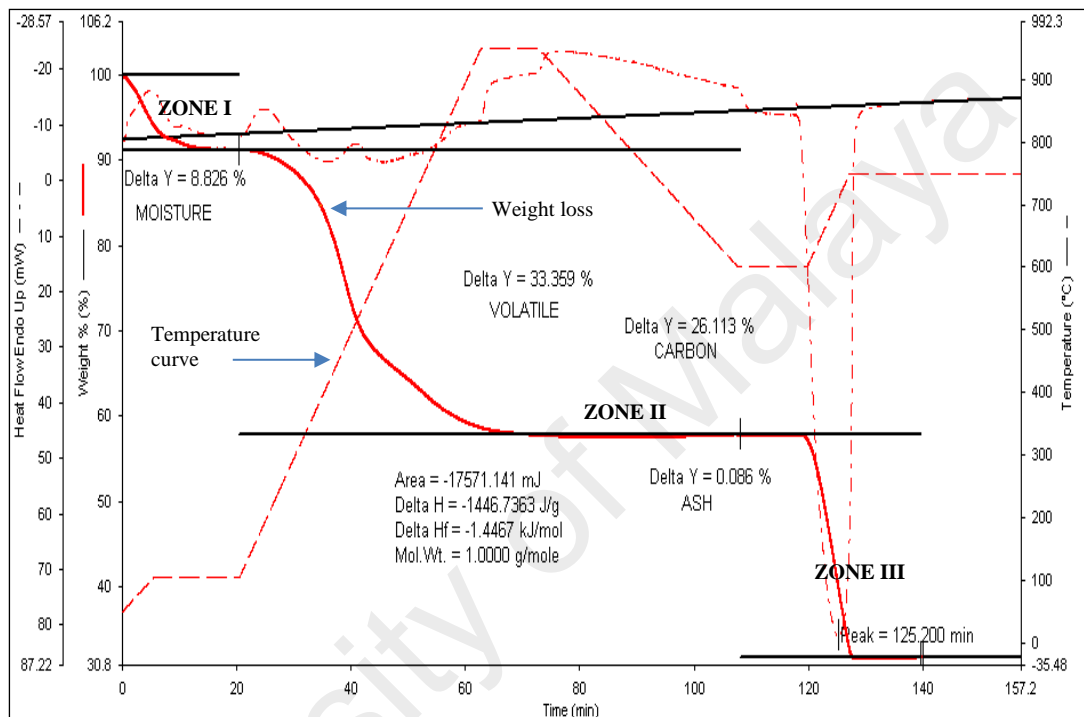


Figure 4.2: Proximate analysis of Maiganga coal using TGA

The furnace temperature was then ramped to 950⁰C and held isothermally (Zone II) until constant weight was achieved in the coal sample. The weight loss experienced in this zone was a direct result of loss of total volatile matter component of the sample. Zones I and II took place under nitrogen (N₂) atmosphere. In Zone III, the atmosphere of operation automatically switched to air (O₂), creating a conducive environment for rapid and complete combustion of organic carbon content of the studied coal sample at 950⁰C. The residue left behind due to complete combustion of the coal sample represents the ash content of the sample.

The percentage by weight (wt%) of moisture content in coal samples from Maiganga coalfield ranged from 7.90 to 15.19 % with mean value of 11.03 %. Volatile matter and fixed carbon contents varied from 33.65 to 38.48 %, and from 41.48 to 48.71 % respectively with average values of 36.10 % and 45.98 %, in sequence. Coal samples from Maiganga coalfield showed low ash content ranging from 3.94 to 9.88 % (Table 4.10). The values are comparable to those documented for Indonesian coals (Belkin et al., 2009) and eastern Malaysian coals (Hakimi et al., 2013). The low ash contents of coal from Maiganga coalfield gave an indication of potentially good quality coal for power generation. It also show high prospect for exportation as thermal coal to other countries to boost Nigeria foreign exchange earnings.

Table 4.10: Proximate analysis of coal samples from Maiganga coalfield

sample	Moisture (%)	Volatile (%)	Carbon (%)	Ash (%)
MCS 01	8.83	38.36	43.11	9.70
MCS 02	9.73	36.84	45.60	7.83
MCS 03	9.00	37.02	46.95	7.03
MCS 04	10.64	35.93	46.31	7.12
MCS 05	8.61	35.71	47.00	8.68
MCS 06	7.90	35.89	46.33	9.88
MCS 07	9.10	35.93	45.76	9.21
MCS 08	11.61	36.85	45.88	5.66
MCS 09	12.32	38.48	45.26	3.94
MCS 10	12.75	36.06	41.48	9.71
MCS 11	11.58	37.51	44.82	6.09
MCS 12	12.67	33.65	48.39	5.29
MCS 13	13.00	33.73	48.71	4.56
MCS 14	15.19	33.65	46.60	4.56
MCS 15	12.52	35.88	47.18	4.42
Min	7.90	33.65	41.48	3.94
Max	15.19	38.48	48.71	9.88
Mean	11.03	36.10	45.96	6.91

Petrographic analysis, which comprises maceral composition analysis and measurement of vitrinite reflectance, were carried out to establish the rank (thermal

maturity) of coal from Maiganga coalfield. Macerals are the petrographic entities and the organic constituents of coals (Obaje & Ligouis, 1996). The nature of organic source materials and the prevailing conditions during peat accumulation, determines the maceral composition of any given coal (Sia & Abdullah, 2012b). Table 4.11 presents the results of petrographic analysis and vitrinite reflectance measurements of four coals samples (CS 01 to CS 04) from Maiganga coalfield performed in this study. Photomicrographs of maceral composition of the studied coal samples are shown in Appendix F.

Table 4.11: Mean random vitrinite reflectance (R_{om}) and maceral composition of coal samples from Maiganga coal-field

SAMPLE	Vitrinite (%)	Liptinite (%)	Inertinite (%)	Mineral Matter (%)	Mean R_{om} (%)
CS 01	43	25	30	2	0.52
CS 02	39	15	40	6	0.46
CS 03	45	28	24	3	0.25
CS 04	39	20	37	4	0.32
AVE	41.5	22.0	32.8	3.8	0.39

4.7.1 Maceral Composition

Although the three maceral groups were well represented, vitrinite macerals dominated the studied coal samples with an average percentage composition of 41.50 %. Percentage composition of inertinite varied between 24 and 40 % with mean composition of 32.75 %. Liptinite on the other hand occur commonly in the studied coal samples with average composition of 22 %. Photomicrographs of maceral composition of studied coal are shown in Appendix F. Mineral matter, which may be due to the presence of clay minerals in the studied coal samples from Maiganga coalfield, was found to be generally low in composition varying from 2 to 6 %. In general, the results showed that Maiganga coal is a low rank coal deposit which belongs to the humic type.

4.7.2 Vitrinite Reflectance

Mean random vitrinite reflectance of coal samples from Maiganga coalfield varied from 0.25 to 0.52 % (Table 4.11). Following the results of vitrinite reflectance measurements (Sia & Abdullah, 2012b; Životić et al., 2013), Maiganga coalfield can be classified as thermally immature lignite to subbituminous coal rank. The low mean vitrinite reflectance values of 0.25% may be a consequence of bitumen impregnation, associated with relatively high abundance of liptinite macerals.

University of Malaya

CHAPTER 5: DISCUSSIONS

5.1 Natural Radioactivity Contents of Coal Samples from Maiganga Coalfield

Coal is an indispensable fuel for power generation and a base industrial raw material in many developed and developing countries including Nigeria. It is therefore important that the radiological health effects associated with its exploitation and utilization be assessed. Descriptive statistical results of activity concentrations, in Bq kg^{-1} , of ^{226}Ra , ^{232}Th and ^{40}K , with their respective uncertainty levels of $\pm\sigma$, involving the minimum, maximum, mean and standard deviation of coal samples from Maiganga coalfield are presented in Table 5.1. The range of activities obtained for the studied coal showed very low concentrations. Mean activity concentration of ^{226}Ra , ^{232}Th , and ^{40}K , in coal samples from Maiganga coalfield are $8.18\pm 3.5 \text{ Bq kg}^{-1}$, $6.97\pm 2.4 \text{ Bq kg}^{-1}$, and $27.38\pm 11.4 \text{ Bq kg}^{-1}$ respectively. Skewness, which defines the degree of asymmetry of real valued random variables around its mean have positive values for the studied nuclides (Table 5.1). This implies asymmetric distribution of the radionuclides within the studied coal samples. Kurtosis on the other hand, is a comparative parameter that shows the relative peakedness or flatness of any given distribution relative to the normal distribution. Relatively peaked distribution is represented by positive kurtosis, while negative kurtosis connotes a relatively flat distribution. Results presented in Table 5.1 for the present investigation recorded negative values of kurtosis, which indicates a relatively flat distribution of the radionuclides in the studied coal samples.

Table 5.1: Descriptive statistics of radiological parameters of coal samples from Maiganga coalfield

	Activity concentrations (Bq kg ⁻¹)				Dose			Radiation hazard indices (≤ 1)				ELCR (×10 ⁻³)
	²²⁶ Ra	²³² Th	⁴⁰ K	Ra _{eq}	D _R (nGy h ⁻¹)	AEDE (mSv y ⁻¹)	AGDE (μSv y ⁻¹)	AUI	H _{ex}	H _{in}	I _{yr}	
Minimum	3.73	2.02	6.69	8.92	4.19	0.010	29.35	0.06	0.02	0.03	0.06	0.02
Maximum	16.26	11.29	44.08	35.30	15.90	0.020	109.23	0.29	0.10	0.14	0.25	0.07
Mean	8.18	6.97	27.38	20.26	9.13	0.012	63.01	0.16	0.05	0.08	0.14	0.04
SD	3.50	2.41	11.42	6.62	2.93	0.004	19.94	0.06	0.02	0.03	0.05	0.01
Skewness	0.79	0.04	-0.48	0.58	0.62	2.038	0.62	0.55	0.53	0.73	0.49	0.73
Kurtosis	-0.34	-0.63	-1.30	-0.22	-0.12	2.287	-0.08	-0.47	0.04	0.06	-0.19	0.14
N	33	33	33	33	33	33	33	33	33	33	33	33

The bell-shaped distribution illustrated by the frequency distribution histograms shown in Figure 5.1, attests to the even distribution of ²²⁶Ra, ²³²Th, and ⁴⁰K in the studied coal samples.

Mean activity concentrations of ²²⁶Ra, ²³²Th, and ⁴⁰K, measured in coal samples from Maiganga coal field were compared with world average activity values documented by UNSCEAR (2000), and those of similar studies from other parts of the world. The results of the comparison are plotted in Figure 5.2.

Mean activity concentrations of ²²⁶Ra, ²³²Th, and ⁴⁰K, in coal samples from Maiganga coalfield were found to be lower than those obtained for similar studies around the world as seen in Figure 5.2. The values were also below the world average values for coal provided by UNSCEAR (1982). This showed that the mean concentrations of natural radionuclides in coal samples from Maiganga coalfield were generally lower than their respective mean values in the earth crust (UNSCEAR, 2000). Uranium is present mainly in the carbonaceous components of sedimentary rocks and accumulates in both mineral and organic fractions of coal during coalification, while thorium is contained in common phosphate minerals and accumulates in inorganic phases (Lu et al., 2012; Mandal & Sengupta, 2003; Mondal et al., 2006).

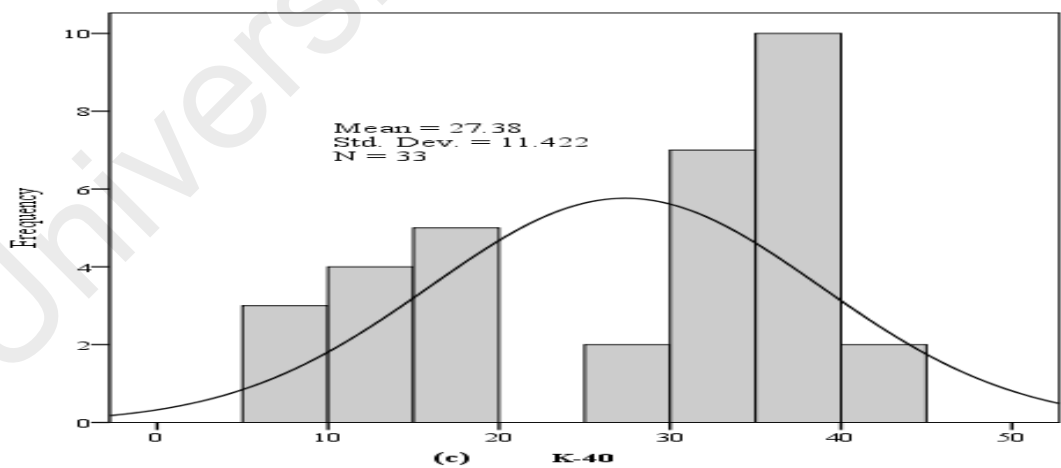
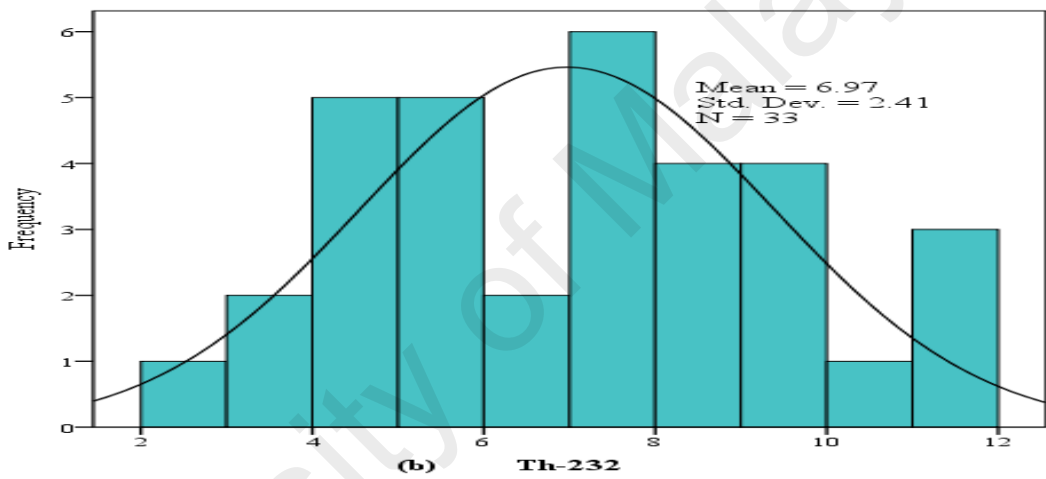
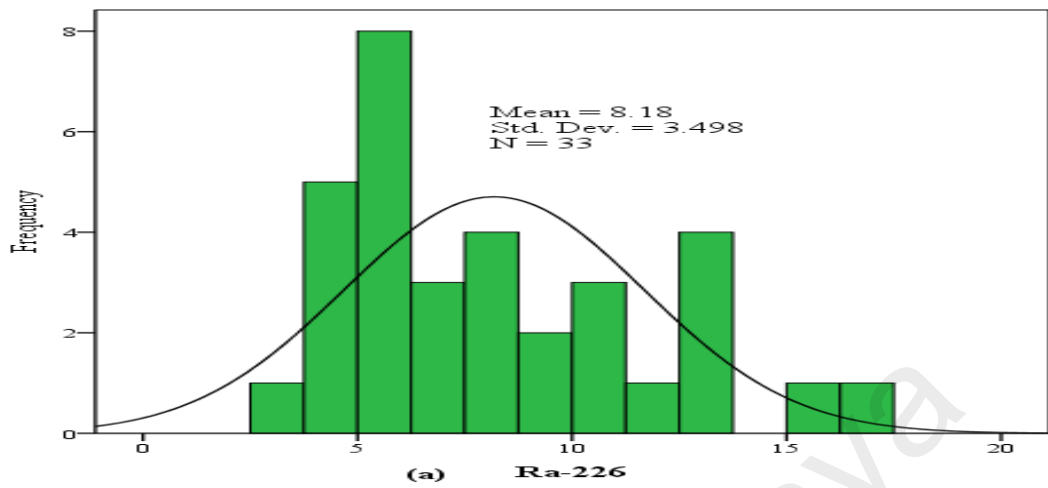


Figure 5.1: Frequency distribution histograms of (a) ^{226}Ra , (b) ^{232}Th , (c) ^{40}K in coal samples from Maiganga coalfield

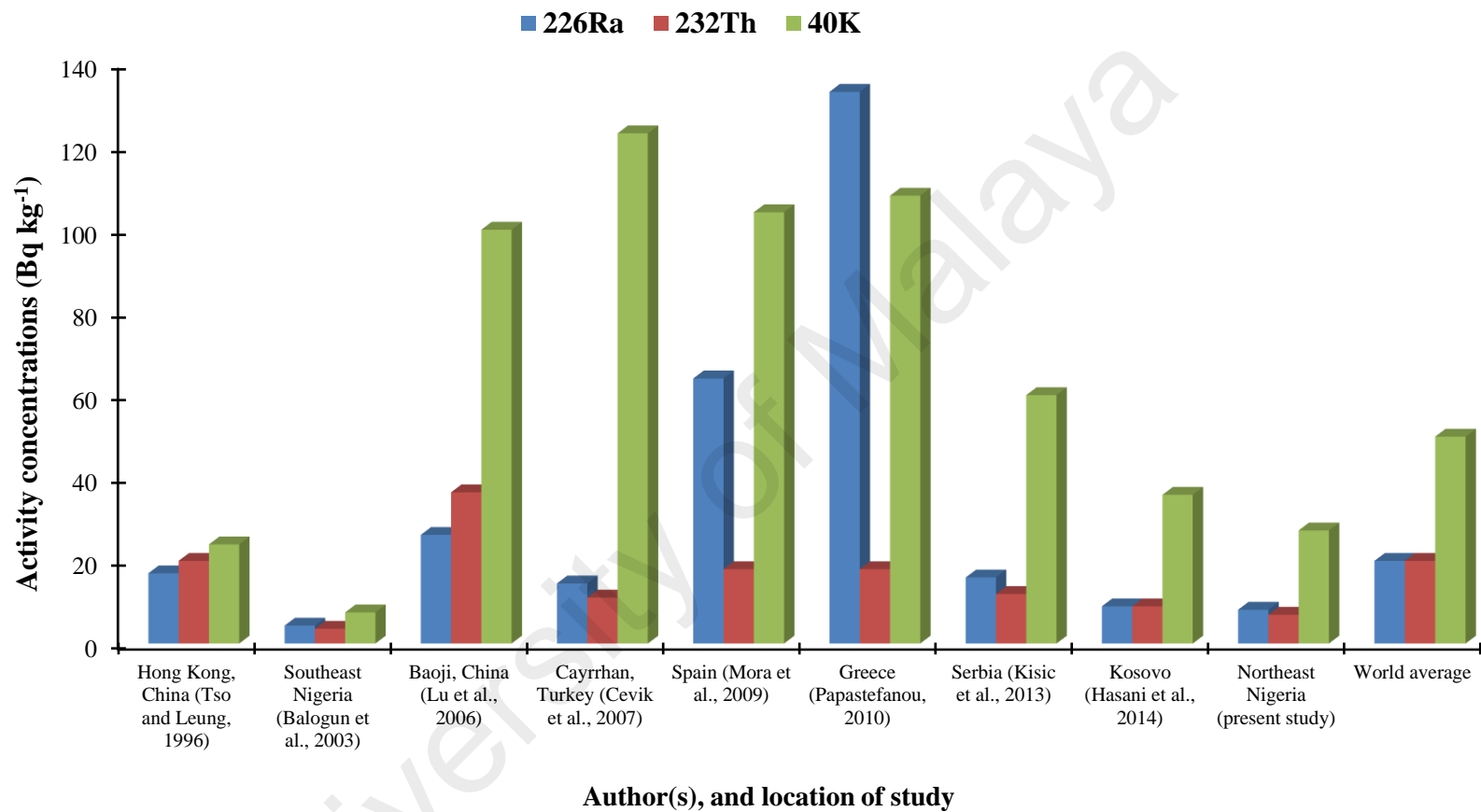


Figure 5.2: Comparison of activity concentrations (Bq kg^{-1}) of ^{226}Ra , ^{232}Th and ^{40}K in coal samples from Maiganga coalfield with the World average values and those of other published works

Elemental mass fraction of ^{226}Ra , ^{232}Th (mg kg^{-1}) and ^{40}K (% by weight), in coal samples from Mainganga coalfield were calculated from Equation (3.3), and the results are plotted in Figure 5.3.

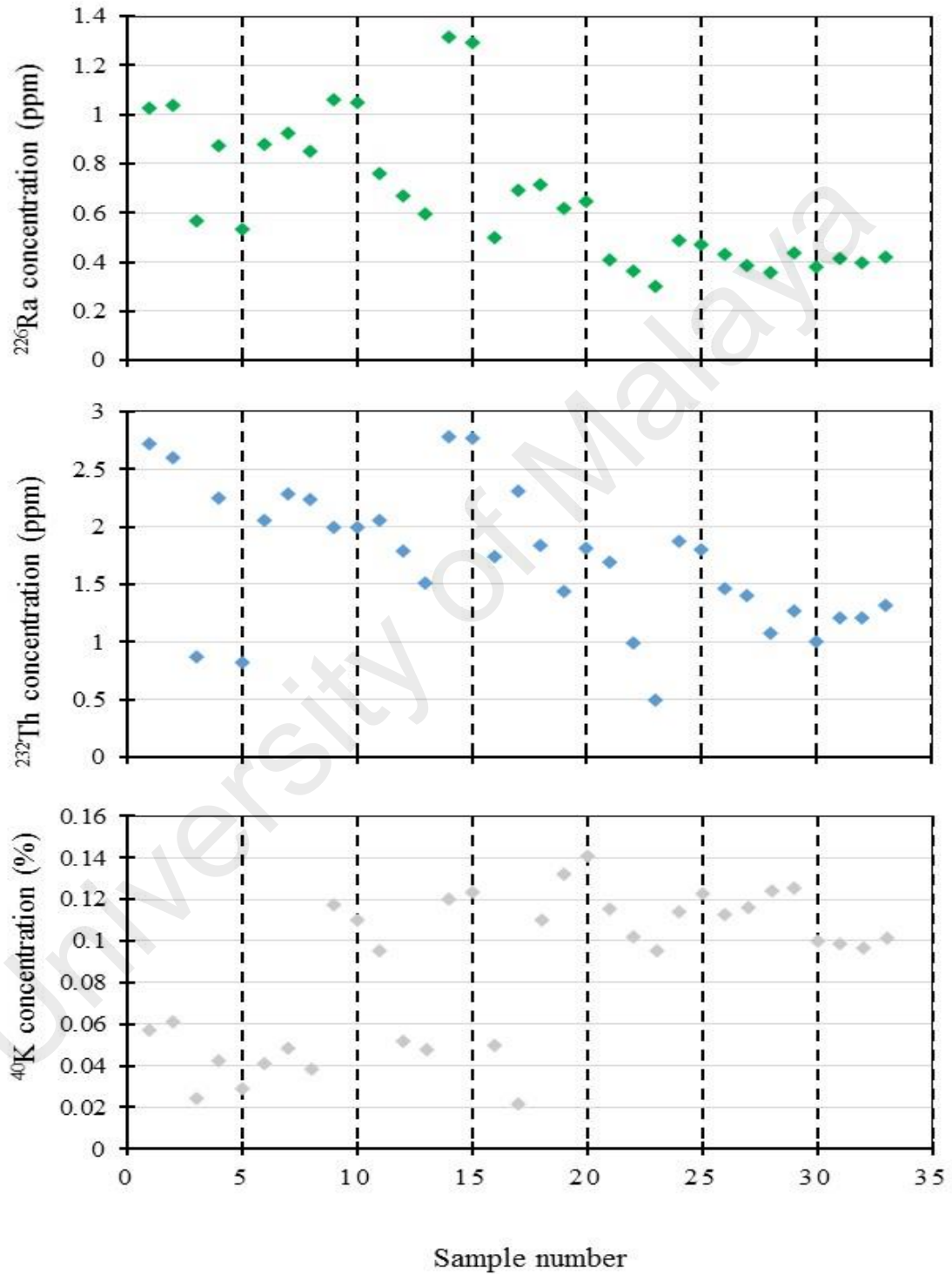


Figure 5.3: Elemental concentration of ^{226}Ra , ^{232}Th (ppm) and total ^{40}K (%) in coal samples from Mainganga coalfield

Elemental concentrations of ^{226}Ra , ^{232}Th , and ^{40}K ranged as 0.30 - 1.32 mg kg⁻¹, 0.50 - 2.78 mg kg⁻¹, and 0.02 - 0.14 %, respectively, with average values of 0.66 mg kg⁻¹, 1.72 mg kg⁻¹, and 0.09 % in sequence. World average activity values of 20, 20 and 50 Bq kg⁻¹ for ^{226}Ra , ^{232}Th , and ^{40}K provided by UNSCEAR (1982) were converted into mass concentrations using Equation (3.3) and obtained the world mean elemental concentrations as 1.62 mg kg⁻¹, 4.93 mg kg⁻¹, and 0.16 %, respectively. Comparison of the results from this study with their computed world average values showed that mean concentrations of radioactive elements of ^{226}Ra and ^{232}Th in the studied coal samples were 5-7 times lower than their corresponding world average values. Elemental concentration of ^{40}K was found to be about 5 times lower than the world mean value.

5.1.1 Correlation Coefficients of Radiological Parameters of Coal Samples from Maiganga Coalfield

Data generated in this study were subjected to multivariate statistical analysis using the Statistical software package: Statistical Program for Social Science (SPSS 22.0). The essence is to understand the interdependency and natural relationships between the samples and/or determined variables that will enable valid judgements on the nature, significance of radionuclide and trace elements distributions from the point of view of environmental protection (Kolo et al., 2015; Laaksoharju et al., 1999; Liu et al., 2003).

The degree of association and possible natural relationships that may exist among the measured radiological variables for coal samples from Maiganga coalfield were evaluated by Pearson's correlation matrix with the alpha testing level at $P < 0.05$ for coal samples. Based on the strength of relationship between the radiological variables, the correlation coefficient values in this study were grouped as "very weak" ($r < 0.36$), "weak" ($0.36 < r < 0.49$), "strong" ($0.50 < r < 0.75$), and "very strong" ($r > 0.75$), while maintaining the alpha testing level at $p < 0.05$ for coal samples ($n = 33$). The calculated correlation

coefficients are presented in Table 5.2. Very strong positive relationship was found to exist between ^{226}Ra and ^{232}Th ($r = +0.85$), while very weak negative degree of association existed between ^{40}K and ^{232}Th ($r = -0.12$), and ^{226}Ra ($r = -0.15$).

The very strong positive correlation existing between ^{226}Ra and ^{232}Th may not be unconnected with the fact that radium and thorium decay series have a common origin, and exists together in nature (Mustapha et al., 2007). Furthermore, all the estimated radioactive variables were strongly correlated with one another positively ($r \geq +0.70$), and also with ^{226}Ra and ^{232}Th ($r > +0.60$). ^{40}K , on the other hand, exhibited very weak relationship with all the radiological variables ($-0.01 \leq r \leq 0.05$). This indicated that the emission of gamma radiation is principally due to ^{226}Ra and ^{232}Th contents in coal samples from Maiganga coalfield.

Table 5.2: Correlation matrix of radiological variables for coal samples from Maiganga coalfield

Variables	^{226}Ra	^{232}Th	^{40}K	Ra_{eq}	D_R	AEDE	AGDE	AUI	H_{ex}	H_{in}	I_{yr}	ELCR
^{226}Ra	1.00											
^{232}Th	0.85	1.00										
^{40}K	-0.15	-0.12	1.00									
Ra_{eq}	0.95	0.96	-0.01	1.00								
D_R	0.95	0.95	0.02	1.00	1.00							
AEDE	0.73	0.62	0.10	0.72	0.73	1.00						
AGDE	0.95	0.95	0.04	1.00	1.00	0.73	1.00					
AUI	0.96	0.96	-0.11	0.99	0.99	0.71	0.99	1.00				
H_{ex}	0.93	0.96	-0.02	0.99	0.98	0.70	0.98	0.98	1.00			
H_{in}	0.97	0.92	-0.02	0.99	0.99	0.72	0.99	0.99	0.97	1.00		
I_{yr}	0.94	0.96	0.03	1.00	1.00	0.71	1.00	0.98	0.98	0.98	1.00	
ELCR	0.91	0.93	0.05	0.97	0.97	0.74	0.97	0.96	0.97	0.96	0.97	1.00

5.2 Trace Elements Contents of Coal Samples from Maiganga Coalfield

Descriptive statistics of elemental concentrations including the maximum, minimum, mean and standard deviation (SD), along with their respective Clarke values and enrichment/depletion factor (EDF) of coal samples from Maiganga coalfield are

presented in Table 4.7. The calculated EDF for all the studied trace elements were found to be less than one. This means that coal samples from Maiganga coalfield are depleted of trace elements including those that could be of serious environmental concern.

Natural relationships that may exist between the studied trace elements and ash yield in coal samples from Maiganga coalfield were evaluated using the Pearson's correlation matrix. The calculated correlation coefficients are presented in Table 5.3.

Significant positive relationship was witnessed between Cr and ash yield ($r = +0.54$) as seen in Table 5.3, which indicated that Cr is inorganically bound in coal samples from Maiganga coalfield. Cr is one of the elements listed by the U. S. Public Law (1990) as potentially hazardous, and of great environmental concern especially when present in coals in its carcinogenic oxidation state (Clarke & Sloss, 1992; Huggins & Huffman, 1996). Incidence of lung cancer reported in Shengbei coalfield of China was traceable to high concentration of Cr in the lignite. Routine monitoring of Maiganga coal with respect to its Cr content is therefore encouraged.

The average concentration for Pb in coal samples from Maiganga coalfield was 1.70 mg kg^{-1} . Although the value was found to be lower than the world average concentration of Pb in low-rank coals, its accumulation in the environment over long period of coal mining and combustion could pose significant threat to man. Pb is known to be carcinogenic (Epstein et al., 2011), and could become poisonous when inhaled from coal combustion processes (Akinlua et al., 2010). This, according to Fu et al. (2013), Duzgoren-Aydin (2007) and Sia and Abdullah (2011), could result in respiratory problems, kidney disease, hearing loss, impaired cognitive function, pregnancy disorders, and premature death. The positive correlation between Pb and ash ($r = +0.53$) as seen in Table 4.10 imply that Pb is inorganically bound in coal samples from Maiganga coalfield.

Table 5.3: Correlation matrix of elemental composition and ash yield for coal samples from Maiganga coalfield

Variables	Cr	Cu	Pb	Ni	V	Co	Zn	Mn	Ba	Be	Sr	Ash
Cr	1.00											
Cu	0.99**	1.00										
Pb	0.98**	0.99**	1.00									
Ni	0.86**	0.84**	0.83**	1.00								
V	0.97**	0.96**	0.95**	0.80**	1.00							
Co	0.86**	0.88**	0.87**	0.92**	0.78**	1.00						
Zn	0.95**	0.93**	0.91**	0.82**	0.94**	0.83**	1.00					
Mn	0.70**	0.74**	0.76**	0.71**	0.66**	0.70**	0.67**	1.00				
Ba	0.36	0.36	0.38	0.06	0.33	0.11	0.24	0.08	1.00			
Be	0.76**	0.81**	0.80**	0.67**	0.74**	0.85**	0.78**	0.71**	0.18	1.00		
Sr	-0.45	-0.46	-0.45	-.677**	-0.40	-.620*	-0.44	-.604*	0.56*	-0.40	1.00	
Ash	0.54*	0.54*	0.53*	0.65**	0.43	0.61*	0.47	0.61*	0.07	0.35	-0.51	1.00

** . Correlation is significant at the 0.01 level (2-tailed).

* . Correlation is significant at the 0.05 level (2-tailed).

PHTEs are bold

Ni and ash yield exhibited strong positive relationship ($r = +0.65$) as seen in Table 5.3, which points to the inorganic association of Ni in coal samples of Maiganga coalfield. Furthermore, the EDF of 0.4 obtained for Ni in coal samples from Maiganga coalfield is similar to the value obtained for Mukah coals (Sia & Abdullah, 2011), which thus revealed the level of depletion of Ni in Maiganga coal. Although Ni, an anticipated carcinogen and one of the PHTEs is yet to be associated with any environmental or health challenge (Swaine, 1990), its continuous release into the environment during coal combustion can cause severe irritations to human respiratory tracts.

Mn which was found to be the most abundant element in coal samples from Maiganga coalfield exhibited significant positive relationship with the ash yield ($r = +0.61$). This showed that Mn is primarily inorganically bound in coal from Maiganga coalfield.

Significant relationship existed between all the studied trace elements in coal samples from Maiganga coalfield, which was demonstrated by the positive correlation coefficients

among the elements as seen in Table 5.3. This is, however, not the case with Sr, which was negatively correlated with all other elements except Ba ($r = +0.56$). This positive correlation presume that barite exists in Maiganga coal with small amount of strontium, though Ward et al. (1996), in their investigation of Australian coals thought that Sr and Ba may exist as aluminophosphate minerals of the goyazite-gorceixite-crandallite group (Sia & Abdullah, 2011). Furthermore, the relationship between Ba and ash yield was found to be significantly weak ($r = +0.07$) suggesting, therefore, that Ba may be predominantly bound organically in coal samples from Maiganga coalfield.

University of Malaya

CHAPTER 6: CONCLUSION

Radiological, trace elemental, and petrographic analyses were performed on coal samples from Maiganga coalfield in order to determine the intrinsic characteristics of the coal deposit, and to understand the environmental and human health challenges that may be associated with its exploitation and utilization. Radiological investigation showed that activity concentrations of ^{226}Ra , ^{232}Th , and ^{40}K in the coal samples from Maiganga coalfield varied from 3.7 ± 0.1 to 16.3 ± 0.3 Bq kg^{-1} , 2.0 ± 0.1 to 11.3 ± 0.3 Bq kg^{-1} , and 6.7 ± 0.1 to 44.1 ± 0.7 Bq kg^{-1} respectively with mean values of 8.0 ± 3.5 , 7.0 ± 2.4 , and 27.4 ± 11.4 Bq kg^{-1} in sequence. These values were lower than the world average values of 20, 20, and 50 Bq kg^{-1} , respectively, for coals provided by UNSCEAR (1982). The values were also below those obtained for similar studies around the world. Radium equivalent activity (Ra_{eq}) values which were calculated from the measured activity concentrations of ^{226}Ra , ^{232}Th , and ^{40}K in the coal samples were found to lie in the range of 8.92 to 35.30 Bq kg^{-1} , with a mean value of 20.26 Bq kg^{-1} . This value was below the world permissible limit of 370 Bq kg^{-1} . Similarly, the external hazard index (H_{ex}), internal hazard index (H_{in}) and the gamma index (I_{gr}), recorded average values of 0.05, 0.08 and 0.14 respectively, for the studied coal samples. These values were below the precautionary limit of one, set by the UNSCEAR (1982). Furthermore, mean total annual effective dose of 0.012 mSv y^{-1} received by coal workers was found to be below safety criterion of 1.0 mSv y^{-1} set by the International Committee on Radiological Protection. Calculated excess lifetime cancer risk due to constant exposure varied between 0.2×10^{-4} and 0.7×10^{-4} , with a mean value of 0.04×10^{-3} . This value was found to be below the precautionary limit of 0.29×10^{-3} set by UNSCEAR (2000) and 0.05 prescribed by the International Commission on Radiological Protection (ICRP) for low-level radiations.

Coal mine tailings from Maiganga coalfield were investigated for their radiological contents using HPGe gamma-ray detector. Activity concentrations of ^{226}Ra , ^{232}Th , and ^{40}K in the investigated tailing samples varied between 4.58 and 16.32 Bq kg⁻¹, 8.48 and 23.21 Bq kg⁻¹, 26.74 and 114.07 Bq kg⁻¹, respectively with mean concentration values of 11.9±3.0, 17.7±3.6, and 70.4±20.4 Bq kg⁻¹, in sequence. Calculated radium equivalent activity, R_{eq} for the investigated mine tailings varied from 18.77 to 54.98 Bq kg⁻¹ with an average of 42.67 Bq kg⁻¹, and corresponding mean external hazard index (H_{ex}) of 0.12. Gamma absorbed dose rate (D_{R}) in air at 1 m above ground level estimated for the tailings has an average value of 19.14 nGy h⁻¹, and corresponding mean annual effective dose equivalent (AEDE) of 0.02 mSv y⁻¹. Average values calculated for activity utilization index (AUI), internal hazard index (H_{in}), and gamma index ($I_{\gamma\text{r}}$) were 0.33, 0.15, and 0.30, respectively. All the calculated hazard indexes were within the prescribed safety limits.

Concentrations of trace elements in coal samples from Maiganga coalfield were lower than Clarke values. Calculated enrichment/depletion factors for respective trace elements were less than one, indicating that coals from the Maiganga coal-field are depleted in trace elements including those that are potentially hazardous.

Petrographic analysis of coal samples revealed that, although the three basic maceral groups were identified as the organic constituents of coal samples from Maiganga coalfield, vitrinite macerals dominated the studied coal samples with percentage composition varying between 39 and 45 %. Inertinite, whose percentage composition varied between 24 and 40 %, recorded average concentration of 32.8 % in the investigated coal samples. Liptinite, on the other hand, occurred commonly in the studied coal samples with average composition of 22 %. Mean random vitrinite reflectance was found to vary from 0.25 to 0.52%. The results of the vitrinite reflectance measurements suggested that coal from Maiganga coalfield is thermally immature lignite to

subbituminous coal in rank. Furthermore, the studied coal samples were characterized by low ash yield (3.9 to 9.9 %), which justifies government's expectations of good quality coal for power generation. Generally, this study revealed that the exploitation and utilization of coals from Maiganga coalfield, either for power generation, industrial or domestic consumption, is safe from the perspective of human health and environmental protection.

Further works should be focused on:

1. In depth investigation of the geology and the geography, soil origin and type of soil of the study area in order to correlate the data obtained in this study with the geology of Maiganga coalfield.
2. Radiological studies of other surrounding environmental components like the water and air within the vicinity of the minefield.
3. Radiological and trace elemental studies of the coal ash and other waste materials that will be generated from the operations of the coal thermal power plant
4. Investigation of the nature and modes of occurrence of organic and inorganic constituents of Maiganga coal.
5. Study of the nature and modes of occurrence of potentially hazardous trace elements in Maiganga coal and their interrelationships with the organic and inorganic constituents in which they occur in Maiganga coal.
6. Investigation of hydrocarbon generation potential of coal from Maiganga coalfield.

REFERENCES

- Adedosu, T. A., Adedosu, H. O., & Adebisi, F. M. (2007). Geochemical and Mineralogical Significance of Trace Metals in Benue Trough Coal, Nigeria. *Journal of Applied Sciences*, 7(20), 3101-3105.
- Adrovic, F., Ninkovic, M., & Todorovic, D. (1997). *Natural radionuclides and radiation measurements in the vicinity of the Kosovian coal-fired power plants*. Paper presented at the Proceedings of the IRPA Regional Symposium on Radiation Protection, Prague.
- Agbalagba, E., & Onoja, R. (2011). Evaluation of natural radioactivity in soil, sediment and water samples of Niger Delta (Biseni) flood plain lakes, Nigeria. *Journal of Environmental Radioactivity*, 102(7), 667-671.
- Akinlua, A., Adekola, S., Swakamisa, O., Fadipe, O., & Akinyemi, S. (2010). Trace element characterisation of Cretaceous Orange Basin hydrocarbon source rocks. *Applied Geochemistry*, 25(10), 1587-1595.
- Albering, H., Hoogewerff, J., & Kleinjans, J. (1996). Survey of ²²²Rn concentrations in dwellings and soils in the Dutch Belgian border region. *Health physics*, 70(1), 64-69.
- Ali, M., Wasim, M., Iqbal, S., Arif, M., & Saif, F. (2013). Determination of the risk associated with the natural and anthropogenic radionuclides from the soil of Skardu in Central Karakoram. *Radiation Protection Dosimetry*, nct057.
- Alias, F. L., Abdullah, W. H., Hakimi, M. H., Azhar, M. H., & Kugler, R. L. (2012). Organic geochemical characteristics and depositional environment of the Tertiary Tanjong Formation coals in the Pinangah area, onshore Sabah, Malaysia. *International Journal of Coal Geology*, 104, 9-21
- Alvarez, M. C., & Vivero, M. T. D. (1998). Natural radionuclide contents in Spanish coals of different rank. *Fuel*, 77(13), 1427-1430.
- Amekudzie, A., Emi-Reynolds, G., Faanu, A., Darko, E., Awudu, A., Adukpo, O., Quaye, L. A. N., Kporozro, R., Agyemang, B., & Ibrahim, A. (2011). Natural radioactivity concentrations and dose assessment in shore sediments along the coast of Greater Accra, Ghana. *World Applied Sciences Journal*, 13(11), 2338-2343.
- Amin, Y., Uddin Khandaker, M., Shyen, A., Mahat, R., Nor, R., & Bradley, D. (2013). Radionuclide emissions from a coal-fired power plant. *Applied Radiation and Isotopes*, 80, 109-116.
- Ammann, A. A. (2007). Inductively coupled plasma mass spectrometry (ICP MS): a versatile tool. *Journal of Mass Spectrometry*, 42(4), 419-427.
- Arafa, W. (2004). Specific activity and hazards of granite samples collected from the Eastern Desert of Egypt. *Journal of Environmental Radioactivity*, 75(3), 315-327.

- Asaduzzaman, K., Khandaker, M. U., Amin, Y. M., Bradley, D. A., Mahat, R. H., & Nor, R. M. (2014). Soil-to-root vegetable transfer factors for ^{226}Ra , ^{232}Th , ^{40}K , and ^{88}Y in Malaysia. *Journal of Environmental Radioactivity*, *135*(0), 120-127.
- Asgharizadeh, F., Ghannadi, M., Samani, A., Meftahi, M., Shalibayk, M., Sahafipour, S., & Gooya, E. (2013). Natural radioactivity in surface soil samples from dwelling areas in Tehran city, Iran. *Radiation Protection Dosimetry*, *156*(3), 376-382.
- Attix, F. H. (2004). *Introduction to radiological physics and radiation dosimetry*. Germany: Wiley-VCH Verlag GmbH & Co.
- Aytekin, H., & Baldik, R. (2012). Radioactivity of coals and ashes from Catalagzi coal-fired power plant in Turkey. *Radiation Protection Dosimetry*, *149*(2), 211-215.
- Balogun, F. A., Mokobia, C. E., Fasasi, M. K., & Ogundare, F. O. (2003). Natural radioactivity associated with bituminous coal mining in Nigeria. *Nuclear Instruments and Methods in Physics Research A*, *505*(2003), 444-448.
- Beauchemin, D. (2006). Inductively coupled plasma mass spectrometry. *Analytical Chemistry*, *78*(12), 4111-4136.
- Beck, H. L. (1989). Radiation exposures due to fossil fuel combustion. *International Journal of Radiation Applications and Instrumentation. Part C. Radiation Physics and Chemistry*, *34*(2), 285-293.
- Beck, H. L., Gogolak, C. V., Miller, K. M., Lowder, W. M., in: Gesell, T. F., & Lowder, W. M. e. (1980). *Natural radiation environment III*.
- Belkin, H. E., Tewalt, S. J., Hower, J. C., Stucker, J. D., & O'Keefe, J. M. K. (2009). Geochemistry and petrology of selected coal samples from Sumatra, Kalimantan, Sulawesi, and Papua, Indonesia. *International Journal of Coal Geology*, *77*(3-4), 260-268.
- Bell, F. G., Bullock, S. E. T., Halbich, T. F. J., & Lindsay, P. (2001). Environmental impacts associated with an abandoned mine in the Witbank Coalfield, South Africa. *International Journal of Coal Geology*, *45*(2001), 195-216.
- Bell, F. G., & Donnelly, L. J. (2006). *Mining and its Impact on the Environment*: Taylor & Francis.
- Bem, H., Wieczorkowski, P., & Budzanowski, M. (2002). Evaluation of technologically enhanced natural radiation near the coal-fired power plants in the Lodz region of Poland. *Journal of Environmental Radioactivity*, *61*(2), 191-201.
- Bhuiyan, M. A. H., Parvez, L., Islam, M. A., Dampare, S. B., & Suzuki, S. (2010). Heavy metal pollution of coal mine-affected agricultural soils in the northern part of Bangladesh. *Journal of Hazardous Materials*, *173*(2010), 384-392.
- Block, C., & Dams, R. (1976). Study of fly ash emission during combustion of coal. *Environmental Science & Technology*, *10*(10), 1011-1017.

- Bogdanović, I., Fazinić, S., Itskos, S., Jakšić, M., Karydas, E., Katselis, V., Paradellis, T., Tadić, T., Valković, O., & Valković, V. (1995). Trace element characterization of coal fly ash particles. *Nuclear Instruments and Methods in Physics Research Section B: Beam Interactions with Materials and Atoms*, 99(1), 402-405.
- Bonazzola, G. C., Ropolo, R., & Facchinelli, A. (1993). Profiles and downward migration of ¹³⁴Cs and ¹⁰⁶Ru deposited on Italian soils after the Chernobyl accident. *Health physics*, 64(5), 479-484.
- Booth, C. A., Spears, D. A., Krause, P., & Cox, A. G. (1999). The determination of low level trace elements in coals by laser ablation-inductively coupled plasma-mass spectrometry. *Fuel*, 78(14), 1665-1670.
- Borishade, A. B., Hanan, A. H. M. A., Kehinde, L. O., Oluwole, A. F., & Oshin, O. (1985). Elemental composition of Nigerian coals. *Energy*, 10(1), 35-39.
- Borm, P. J. A. (1997). Toxicity and occupational health hazards of coal fly ash (CFA). A review of data and comparison to coal mine dust. *Annals of Occupational Hygiene*, 41(6), 659-676.
- Cam, N. F., Yaprak, G., & Eren, E. (2010). The natural radioactivity contents in feed coals from the lignite-fired power plants in western Anatolia, Turkey. *Radiation Protection Dosimetry*, 142(2-4), 300-307.
- Cember, H., & Johnson, E. (2009). Introduction to Health Physics Department of Environmental and Radiological Health Sciences Colorado State University. *Fort Collins, Colorado*.
- Cevik, U., Damla, N., & Nezir, S. (2007). Radiological characterization of Cayirhan coal-fired power plant in Turkey. *Fuel*, 86(2007), 2509-2513.
- Chandrasekaran, A., Ravisankar, R., Senthilkumar, G., Thillaivelavan, K., Dhinakaran, B., Vijayagopal, P., Bramha, S. N., & Venkatraman, B. (2014). Spatial distribution and lifetime cancer risk due to gamma radioactivity in Yelagiri Hills, Tamilnadu, India. *Egyptian Journal of Basic and Applied Sciences*, 1(1), 38-48.
- Charro, E., & Pena, V. (2013). Environmental impact of natural radionuclides from a coal-fired power plant in Spain. *Radiation Protection Dosimetry*, 153(4), 485-495.
- Cherry, D., Currie, R., Soucek, D., Latimer, H., & Trent, G. (2001). An integrative assessment of a watershed impacted by abandoned mined land discharges. *Environmental Pollution*, 111(3), 377-388.
- Clarke, L. B., & Sloss, L. L. (1992). *Trace elements-emissions from coal combustion and gasification* (Vol. 49): IEA Coal Research.
- Cohen, A. D., Spackman, W., & Dolsen, P. (1984). Occurrence and distribution of sulfur in peat-forming environments of southern Florida. *International Journal of Coal Geology*, 4(1), 73-96.

- Coles, D. G., Ragaini, R. C., & Ondov, J. M. (1978). Behavior of natural radionuclides in western coal-fired power plants. *Environmental Science & Technology*, 12 (4), 442-446.
- Coles, D. G., Ragaini, R. C., Ondov, J. M., Fisher, G. L., Silberman, D., & Prentice, B. A. (1979). Chemical studies of stack fly ash from a coal-fired power plant. *Environmental Science & Technology*, 13(4), 455-459.
- Corbett, J. O. (1983). The radiation dose from coal burning: A review of pathways and data. *Radiation Protection Dosimetry*, 4(1), 5-19.
- Costa, A., Flores, D., Suarez-Ruiz, I., Pevida, C., Rubiera, F., & Iglesias, M. J. (2010). The importance of thermal behaviour and petrographic composition for understanding the characteristics of a Portuguese perhydrous Jurassic coal. *International Journal of Coal Geology*, 84(2010), 237-247.
- Ctvrtnickova, T., Mateo, M.-P., Yanez, A., & Nicolas, G. (2009). Characterization of coal fly ash components by laser-induced breakdown spectroscopy. *Spectrochimica Acta Part B*, 64(2009), 1093-1097.
- Dabayneh, K., Mashal, L., & Hasan, F. (2008). Radioactivity concentration in soil samples in the southern part of the West Bank, Palestine. *Radiation Protection Dosimetry*, 131(2), 265-271.
- Dai, S., Li, D., Chou, C.-L., Zhao, L., Zhang, Y., Ren, D., Ma, Y., & Sun, Y. (2008a). Mineralogy and geochemistry of boehmite-rich coals: new insights from the Haerwusu Surface Mine, Jungar Coalfield, Inner Mongolia, China. *International Journal of Coal Geology*, 74(3), 185-202.
- Dai, S., Tian, L., Chou, C.-L., Zhou, Y., Zhang, M., Zhao, L., Wang, J., Yang, Z., Cao, H., & Ren, D. (2008b). Mineralogical and compositional characteristics of Late Permian coals from an area of high lung cancer rate in Xuan Wei, Yunnan, China: Occurrence and origin of quartz and chamosite. *International Journal of Coal Geology*, 76(4), 318-327.
- Dai, S., Wang, X., Chen, W., Li, D., Chou, C.-L., Zhou, Y., Zhu, C., Li, H., Zhu, X., Xing, Y., Zhang, W., & Zou, J. (2010). A high-pyrite semianthracite of Late Permian age in the Songzao Coalfield, southwestern China: mineralogical and geochemical relations with underlying mafic tuffs. *International Journal of Coal Geology*, 83(4), 430-445.
- Dai, S., Zhang, W., Ward, C. R., Seredin, V. V., Hower, J. C., Li, X., Song, W., Wang, X., Kang, H., Zheng, L., Wang, P., & Zhou, D. (2013). Mineralogical and geochemical anomalies of late Permian coals from the Fusui Coalfield, Guangxi Province, southern China: Influences of terrigenous materials and hydrothermal fluids. *International Journal of Coal Geology*, 105, 60-84.
- Dai, S., Zhao, L., Peng, S., Chou, C.-L., Wang, X., Zhang, Y., Li, D., & Sun, Y. (2010b). Abundances and distribution of minerals and elements in high-alumina coal fly ash from the Jungar Power Plant, Inner Mongolia, China. *International Journal of Coal Geology*, 81, 320-332.

- Duliu, O. G., Culicov, O. A., Radulescu, I., Cristea, C., & Vasiu, T. (2005). Major, trace, and natural radioactive elements in bituminous coal from Australia, Romania, Rissia, South Africa and Ukraine: A comparative study. *Journal of Radioanalytical and Nuclear Chemistry*, 264(3), 525-534.
- Durgun, D., & Genc, A. (2009). Effects of coal properties on the production rate of combustion solid residue. *Energy*, 34(2009), 1976-1979.
- Duzgoren-Aydin, N. S. (2007). Sources and characteristics of lead pollution in the urban environment of Guangzhou. *Science of The Total Environment*, 385(1), 182-195.
- Eisenbud, M., & Gesell, T. F. (1997). *Environmental Radioactivity from Natural, Industrial & Military Sources: From Natural, Industrial and Military Sources*. San Diego, California, USA: Academic Press.
- El-Gamal, A., Nasr, S., & El-Taher, A. (2007). Study of the spatial distribution of natural radioactivity in the upper Egypt Nile River sediments. *Radiation Measurements*, 42(3), 457-465.
- El Mamoney, M., & Khater, A. E. (2004). Environmental characterization and radio-ecological impacts of non-nuclear industries on the Red Sea coast. *Journal of Environmental Radioactivity*, 73(2), 151-168.
- Epstein, P. R., Buonocore, J. J., Eckerle, K., Hendryx, M., Stout Iii, B. M., Heinberg, R., Clapp, W. R., May, B., Reinhart, L. N., Ahern, M. M., Doshi, K. S., & Glustrom, L. (2011). Full cost accounting for the life cycle of coal. *Annals of the New York Academy of Sciences*, 1219(1), 73-98.
- Fadda, S., Rivoldini, A., & Cau, I. (1995). ICP-MS determination of 45 trace elements in whole coal using icrowave oven acid digestion for sample preparation. *Geostandards Newsletter*, 19(1), 41-54.
- Filippidis, A., Georgakopoulos, A., Kassoli-Fournaraki, A., Misaelides, P., Yiakkoupis, P., & Broussoulis, J. (1996). Trace element contents in composited samples of three lignite seams from the central part of the Drama lignite deposit, Macedonia, Greece. *International Journal of Coal Geology*, 29(4), 219-234.
- Finkelman, R. B. (1994). Modes of occurrence of potentially hazardous elements in coal: levels of confidence. *Fuel Processing Technology*, 39(1), 21-34.
- Finkelman, R. B., Orem, W., Castranova, V., Tatu, C. A., Belkin, H. E., Zheng, B., Lerch, H. E., Maharaj, S. V., & Bates, A. L. (2002). Health impacts of coal and coal use: possible solutions. *International Journal of Coal Geology*, 50(2002), 425-443.
- Flues, M., Camargo, I., Silva, P., & Mazzilli, B. (2006). Radioactivity of coal and ashes from Figueira coal power plant in Brazil. *Journal of Radioanalytical and Nuclear Chemistry*, 270(3), 597-602.
- Flues, M., Sato, I. M., Scapin, M. A., Cotrim, M. E. B., & Camargo, I. M. C. (2013). Toxic element mobility in coal and ashes of Figueira coal power plant, Brazil. *Fuel*, 103(2013), 430-436.

- Froehlich, K. (2010). *Environmental radionuclides: tracers and timers of terrestrial processes*. Amsterdam, The Netherlands: Elsevier.
- Fu, X., Wang, J., Tan, F., Feng, X., & Zeng, S. (2013). Minerals and potentially hazardous trace elements in the Late Triassic coals from the Qiangtang Basin, China. *International Journal of Coal Geology*, 116–117(0), 93-105.
- Gilmore, G. (2008). *Practical gamma-ray spectroscopy*: John Wiley & Sons, Ltd
- Gluskoter, H. J., Ruch, R., Miller, W., Cahill, R., & Dreher, G. (1977). *Trace elements in coal: occurrence and distribution. Final report, June 1974--June 1976*. United States of America
- Grashchenko, S. (2005). Naturally Occurring Radionuclides of Uranium and Thorium Series in Nonnuclear Industrial Processes. *Radiochemistry*, 47(6), 614-618.
- Gupta, J. G. S., & Bertrand, N. B. (1995). Direct ICP-MS determination of trace and ultratrace elements in geological materials after decomposition in a microwave oven. Part II. Quantitation of Ba, Cs, Ga, Hf, In, Mo, Nb, Pb, Rb, Sn, Sr, Ta and Tl. *Talanta*, 42(12), 1947-1957.
- Gupta, R. (2007). Advanced coal characterization: A review. *Energy & fuels*, 21(2), 451-460.
- Gurba, L. W., & Ward, C. R. (2000). Elemental composition of coal macerals in relation to vitrinite reflectance, Gunnedah Basin, Australia, as determined by electron microprobe analysis. *International Journal of Coal Geology*, 44(2), 127-147.
- Gurdal, G. (2011). Abundances and modes of occurrence of trace elements in the Can coals (Miocene) Canakkale-Turkey. *International Journal of Coal Geology*, 87(2011), 157-173.
- Hakimi, M. H., Abdullah, W. H., Alias, F. L., Azhar, M. H., & Makeen, Y. M. (2013). Organic petrographic characteristics of Tertiary (Oligocene–Miocene) coals from eastern Malaysia: Rank and evidence for petroleum generation. *International Journal of Coal Geology*, 120, 71-81.
- Hasan, M. M., Ali, M., Paul, D., Haydar, M., & Islam, S. (2013). Measurement of Natural Radioactivity in Coal, Soil and Water Samples Collected from Barapukuria Coal Mine in Dinajpur District of Bangladesh. *Journal of Nuclear and Particle Physics*, 3(4), 63-71.
- Hasan, M. M., Ali, M., Paul, D., Haydar, M., & Islam, S. A. (2014). Natural Radioactivity of Feed Coal and Its by-products in Barapukuria 2× 125 MW Coal Fired Thermal Power Plant, Dinajpur, Bangladesh. *IOSR Journal of Applied Physics*, 5, 32-38.
- Hasani, F., Shala, F., Xhixha, G., Xhixha, M., Hodolli, G., Kadiri, S., Bylyku, E., & Cfaruku, F. (2014). Naturally occurring radioactive materials (NORMs) generated from lignite-fired power plants in Kosovo. *Journal of Environmental Radioactivity*, 138, 156-161.

- Hower, J. C., Eble, C. F., & Quick, J. C. (2005a). Mercury in Eastern Kentucky coals: Geologic aspects and possible reduction strategies. *International Journal of Coal Geology*, 62(4), 223-236.
- Hower, J. C., Ruppert, L. F., & Eble, C. F. (2007). Lateral variation in geochemistry, petrology, and palynology in the Elswick coal bed, Pike County, Kentucky. *International Journal of Coal Geology*, 69(3), 165-178.
- Hu, Z.-q., Yang, X.-h., Bao, Y., & Gao, X.-j. (2005). On the restoration of mine environment. *Science & Technology Review*, 1, 38-41.
- Hu, Z.-q., Zhang, M.-l., Chen, S.-h., Ma, B.-g., Zhao, Y.-l., & Li, J. (2009). Pollution generation, migration and in situ control measures on coal refuses. *Procedia Earth and Planetary Science*, 1(1), 1186-1190.
- Huang, Y., Jin, B., Zhong, Z., Xiao, R., Tang, Z., & Ren, H. (2004). Trace elements (Mn, Cr, Pb, Se, Zn, Cd and Hg) in emissions from a pulverized coal boiler. *Fuel Processing Technology*, 86(1), 23-32.
- Huggins, F., Seidu, L., Shah, N., Backus, J., Huffman, G., & Honaker, R. (2012). Mobility of elements in long-term leaching tests on Illinois# 6 coal rejects. *International Journal of Coal Geology*, 94, 326-336.
- Huggins, F. E. (2002). Overview of analytical methods for inorganic constituents in coal. *International Journal of Coal Geology*, 50(2002), 169-214.
- Huggins, F. E., & Huffman, G. (1996). Modes of occurrence of trace elements in coal from XAFS spectroscopy. *International Journal of Coal Geology*, 32(1), 31-53.
- IAEA. (2003). Guidelines for radioelement mapping using gamma ray spectrometry data. *IAEA-TECDOC-1363*.
- IAEA. (2004). *Application of the Concepts of Exclusion: Exemption and Clearance: Safety Guide. IAEA Safety Standards Series RS-G-1.7. IAEA Safety Standards Series RS-G-1.7*: International Atomic Energy Agency.
- Ibeanu, I. (2002). Tin mining and processing in Nigeria: cause for concern? *Journal of Environmental Radioactivity*, 64(1), 59-66.
- Ibrahiem, N., El Ghani, A. A., Shawky, S., Ashraf, E., & Farouk, M. (1993). Measurement of radioactivity levels in soil in the Nile Delta and Middle Egypt. *Health physics*, 64(6), 620-627.
- Isinkaye, M. O. (2013). Natural radioactivity levels and the radiological health implications of tailing enriched soil and sediment samples around two mining sites in Southwest Nigeria. *Radiation Protection and Environment*, 36(3), 122.
- Izquierdo, M., Font, O., Moreno, N., Querol, X., Huggins, F. E., Alvarez, E., Diez, S., Otero, P., Ballesteros, C. J., & Gimenez, A. (2007). Influence of a modification of the petcoke/coal ratio on the leachability of fly ash and slag produced from a large PCC power plant. *Environmental Science & Technology*, 41(15), 5330-5335.

- Izquierdo, M., Koukouzas, N., Touliou, S., Panopoulos, K. D., Querol, X., & Itskos, G. (2011). Geochemical controls on leaching of lignite-fired combustion by-products from Greece. *Applied Geochemistry*, 26(9), 1599-1606.
- Izquierdo, M., Moreno, N., Font, O., Querol, X., Alvarez, E., Antenucci, D., Nugteren, H., Luna, Y., & Fernández-Pereira, C. (2008). Influence of the co-firing on the leaching of trace pollutants from coal fly ash. *Fuel*, 87(10), 1958-1966.
- Jacob, P., Paretzke, H., Rosenbaum, H., & Zankl, M. (1986). Effective dose equivalents for photon exposures from plane sources on the ground. *Radiation Protection Dosimetry*, 14(4), 299-310.
- Jamil, K., Ali, S., Iqbal, M., Qureshi, A. A., & Khan, H. A. (1998). Measurements of radionuclides in coal samples from two Provinces of Pakistan and computation of external γ -ray dose rate in coal mines. *Journal of Environmental Radioactivity*, 41(2), 207-216.
- Jibiri, N., & Okeyode, I. (2012). Evaluation of radiological hazards in the sediments of Ogun river, South-Western Nigeria. *Radiation Physics and Chemistry*, 81(2), 103-112.
- Karangelos, D. J., Petropoulos, N. P., Anagnostakis, M. J., Hinis, E. P., & Simopoulos, S. E. (2004). Radiological characteristics and investigation of the radioactive equilibrium in the ashes produced in lignite-fired power plants. *Journal of Environmental Radioactivity*, 77(3), 233-246.
- Kathren, R. L. (1998). NORM sources and their origins. *Applied Radiation and Isotopes*, 49(3), 149-168.
- Ketris, M., & Yudovich, Y. E. (2009). Estimations of Clarkes for Carbonaceous biolithes: World averages for trace element contents in black shales and coals. *International Journal of Coal Geology*, 78(2), 135-148.
- Khan, K., Aslam, M., Orfi, S., & Khan, H. (2002). Norm and associated radiation hazards in bricks fabricated in various localities of the North-West Frontier Province (Pakistan). *Journal of Environmental Radioactivity*, 58(1), 59-66.
- Khandaker, M. U. (2011). High purity germanium detector in gamma-ray spectrometry. *International Journal of Fundamental Physical Sciences*, 1(2), 42-46.
- Khandaker, M. U., Jojo, P., Kassim, H., & Amin, Y. (2012). Radiometric analysis of construction materials using HPGe gamma-ray spectrometry. *Radiation Protection Dosimetry*, 152(1-3), 33-37.
- Khandaker, M. U., Jojo, P. J., & Kassim, H. A. (2012). Determination of Primordial Radionuclides in Natural Samples Using HPGe Gamma-Ray Spectrometry. *APCBEE Procedia*, 1, 187-192.
- Kisić, D. M., Miletić, S. R., Radonjić, V. D., Radanović, S. B., Filipovic, J. Z., & Gržetić, I. A. (2013). Natural radioactivity of coal and fly ash at the Nikola Tesla B TPP. *Hemijaska industrija*, 67(5), 729-738.

- Knoll, G. F. (2010). *Radiation detection and measurement*. Unites States of America: John Wiley & Sons Inc
- Kobal, I., Brajnik, D., Kaluza, F., & Vengust, M. (1990). Radionuclides in effluent from coal mines, a coal fired power plant, and a phosphate processing plant in Zasavje, Slovenia (Yugoslavia). *Health physics*, 58(1), 81-85.
- Kolo, M., Aziz, S., Khandaker, M., Asaduzzaman, K., & Amin, Y. (2015). Evaluation of radiological risks due to natural radioactivity around Lynas Advanced Material Plant environment, Kuantan, Pahang, Malaysia. *Environmental Science and Pollution Research*, 22(17), 13127-13136.
- Kolo, M. T. (2014). Natural radioactivity and environmental risk assessment of Sokoto phosphate rock, Northwest Nigeria. *African Journal of Environmental Science and Technology*, 8(9), 532-538.
- Kortenski, J., & Sotirov, A. (2002). Trace and major element content and distribution in Neogene lignite from the Sofia Basin, Bulgaria. *International Journal of Coal Geology*, 52(1), 63-82.
- Korun, M., Likar, A., Lipoglavšek, M., Martinčič, R., & Pucelj, B. (1994). In-situ measurement of Cs distribution in the soil. *Nuclear Instruments and Methods in Physics Research Section B: Beam Interactions with Materials and Atoms*, 93(4), 485-491.
- Krane, K. S. (1987). *Introductory nuclear physics*. New York: John Wiley & Sons Inc
- Laaksoharju, M., Skårman, C., & Skårman, E. (1999). Multivariate mixing and mass balance (M3) calculations, a new tool for decoding hydrogeochemical information. *Applied Geochemistry*, 14(7), 861-871.
- Leung, K., Lau, S., & Poon, C. (1990). Gamma radiation dose from radionuclides in Hong Kong soil. *Journal of Environmental Radioactivity*, 11(3), 279-290.
- Liu, G., Yang, P., Peng, Z., & Chou, C.-L. (2004). Petrographic and geochemical contrasts and environmentally significant trace elements in marine-influenced coal seams, Yanzhou mining area, China. *Journal of Asian Earth Sciences*, 23(4), 491-506.
- Liu, G., Zhang, H., Gao, L., Zheng, L., & Peng, Z. (2004). Petrological and mineralogical characterizations and chemical composition of coal ashes from power plants in Yanzhou mining district, China. *Fuel Processing Technology*, 85(2004), 1635-1646.
- Liu, W., Li, X., Shen, Z., Wang, D., Wai, O., & Li, Y. (2003). Multivariate statistical study of heavy metal enrichment in sediments of the Pearl River Estuary. *Environmental Pollution*, 121(3), 377-388.
- Lu, X., Jia, X., & Wang, F. (2006). Natural radioactivity of coal and its by-products in the Baoji coal-fired power plant, China. *CURRENT SCIENCE-BANGALORE*, 91(11), 1508.

- Lu, X., Li, L. Y., Wang, F., Wang, L., & Zhang, X. (2012). Radiological hazards of coal and ash samples collected from Xi'an coal-fired power plants of China. *Environmental Earth Sciences*, 66(7), 1925-1932.
- Mahur, A. K., Kumar, R., Sengupta, D., & Prasad, R. (2008). Estimation of radon exhalation rate, natural radioactivity and radiation doses in fly ash samples from Durgapur thermal power plant, West Bengal, India. *Journal of Environmental Radioactivity*, 99(2008), 1289-1293.
- Malanca, A., Gaidolfi, L., Pessina, V., & Dallara, G. (1996). Distribution of ²²⁶Ra, ²³²Th, and ⁴⁰K in soils of Rio Grande do Norte (Brazil). *Journal of Environmental Radioactivity*, 30(1), 55-67.
- Malanca, A., Pessina, V., & Dallara, G. (1993). Assessment of the natural radioactivity in the Brazilian state of Rio Grande do Norte. *Health physics*, 65(3), 298-302.
- Mamurekli, D. (2010). Environmental impacts of coal mining and coal utilization in the UK. *Acta Montanistica Slovaca*, 15(2), 134-144.
- Mandal, A., & Sengupta, D. (2003). radioelemental study of Kolaghat thermal power plant, West Bengal, India: possible environmental hazards. *Environmental Geology*, 44(2003), 180-186.
- Manigandan, P., & Shekar, B. C. (2014). Evaluation of radionuclides in the terrestrial environment of Western Ghats. *Journal of Radiation Research and Applied Sciences*, 7(3), 310-316.
- Martin, J. E. (2006). *Physics for radiation protection* (second ed.). Verlag GmbH & Co, KGaA, Weinheim: Wiley-VCH.
- Medina, A., Gamero, P., Querol, X., Moreno, N., Leon, B. D., Almanza, M., Vargas, G., Izquierdo, M., & Font, O. (2010). Fly ash from a Mexican mineral coal I: Mineralogical and chemical characterization. *Journal of Hazardous Materials*, 181(2010), 82-90.
- Mehra, R., Kumar, S., Sonkawade, R., Singh, N., & Badhan, K. (2010). Analysis of terrestrial naturally occurring radionuclides in soil samples from some areas of Sirsa district of Haryana, India using gamma ray spectrometry. *Environmental Earth Sciences*, 59(5), 1159-1164.
- Michalik, B. (2008). NORM impacts on the environment: An approach to complete environmental risk assessment using the example of areas contaminated due to mining activity. *Applied Radiation and Isotopes*, 66(2008), 1661-1665.
- Mondal, T., Sengupta, D., & Mandal, A. (2006). Natural radioactivity of ash and coal in major thermal power plants of West Bengal, India. *Current Science*, 91(10), 1387-1393.
- Mora, J. C., Baeza, A., Robles, B., Corbacho, J. A., & Cancio, D. (2009). Behaviour of natural radionuclides in coal combustion. *Radioprotection*, 44(05), 577-580.

- Morsy, Z., El-Wahab, M. A., & El-Faramawy, N. (2012). Determination of natural radioactive elements in Abo Zaabal, Egypt by means of gamma spectroscopy. *Annals of Nuclear Energy*, 44, 8-11.
- Mustapha, A., Mbuzukongira, P., & Mangala, M. (2007). Occupational radiation exposures of artisans mining columbite–tantalite in the eastern Democratic Republic of Congo. *Journal of Radiological Protection*, 27(2), 187.
- NEA-OECD. (1979). Exposure to Radiation from Natural Radioactivity in Building Materials. Report by NEA Group of Experts. OECD, Paris
- Obaje, N. G., Funtua, I. I., Ligouis, B., & Abaa, S. I. (1996). Maceral associations, organic maturation and coal-derived hydrocarbon potential in the cretaceous Awgu Formation, Middle Benue Trough, Nigeria. *Journal of African Earth Sciences*, 23(1), 89-94.
- Obaje, N. G., & Ligouis, B. (1996). Petrographic evaluation of the depositional environments of the cretaceous Obi/Lafia coal deposits in the Benue trough of Nigeria. *Journal of African Earth Sciences*, 22(2), 159-171.
- Ogala, J., Silvanus, G., & Christanis, K. (2012). Coal petrography, mineralogy and geochemistry of lignite samples from Ogwashi-Asaba Formation, Nigeria. *Journal of African Earth Sciences*, 66-67(2012), 35-45.
- Onoduku, U., Okosun, E., & Akande, W. (2013). An Assessment of the Hydrocarbon Potential of the Gombe Formation, Upper Benue Trough, Northeastern Nigeria: Organic Geochemical Point of View. *Earth Science Research*, 2(2).
- Pandit, G., Sahu, S., Puranik, V., Pandit, G., Sahu, S., & Puranik, V. (2011). Natural radionuclides from coal fired thermal power plants—estimation of atmospheric release and inhalation risk. *Radioprotection*, 46(06), S173-S179.
- Pandit, G. G., Sahu, S. K., & Puranik, V. D. (2011). Natural radionuclides from coal fired thermal power plants-estimation of atmospheric release and inhalation risk. *Radioprotection*, 46(6), S173-S179.
- Papastefanou, C. (2010). Escaping Radioactivity from coal-fired power plants (CPPs) due to coal burning and the associated hazards: a review. *Journal of Environmental Radioactivity*, 101(2010), 191-200.
- Papp, Z., Dezső, Z., & Daroczy, S. (2002). Significant radioactive contamination of soil around a coal-fired thermal power plant. *Journal of Environmental Radioactivity*, 59(2), 191-205.
- Patra, K. C., Rautray, T. R., Tripathy, B. B., & Nayak, P. (2012). Elemental analysis of coal and coal ASH by PIXE technique. *Applied Radiation and Isotopes*, 70(2012), 612-616.
- PECH(Panel on the Trace Element Geochemistry of Coal Resource Development Related to Health). (1980). *Trace Element Geochemistry of Coal Resource Development Related to Environmental Quality and Health*: National Academy Press.

- Pfister, H., & Pauly, H. (1980). *External radiation exposure due to natural radionuclides in phosphate fertilizers in the Federal Republic of Germany*. Paper presented at the Seminar on The Radiological Burden of Man from Natural Radioactivity in the Countries of the European Communities, CEC.
- Polic, P. S., Ilic, M. R., & Popovic, A. R. (2005). Environmental impact assessment of lignite fly ash and its utilization products as recycled hazardous wastes on surface and ground water quality *Water Pollution* (pp. 61-110): Springer.
- Querol, X., Alastuey, A., Lopez-Soler, A., Plana, F., Fernandez-Turiel, J., Zeng, R., Xu, W., Zhuang, X., & Spiro, B. (1997b). Geological controls on the mineral matter and trace elements of coals from the Fuxin basin, Liaoning Province, northeast China. *International Journal of Coal Geology*, *34*, 89-109.
- Querol, X., Fernández-Turiel, J., & Lopez-Soler, A. (1995). Trace elements in coal and their behaviour during combustion in a large power station. *Fuel*, *74*(3), 331-343.
- Querol, X., Izquierdo, M., Monfort, E., Alvarez, E., Font, O., Moreno, T., Alastuey, A., Zhuang, X., Lu, W., & Wang, Y. (2008). Environmental characterization of burnt coal gangue banks at Yangquan, Shanxi Province, China. *International Journal of Coal Geology*, *75*(2), 93-104.
- Querol, X., Whateley, M., Fernandez-Turiel, J., & Tuncali, E. (1997a). Geological controls on the mineralogy and geochemistry of the Beypazari lignite, central Anatolia, Turkey. *International Journal of Coal Geology*, *33*, 255-271.
- Querol, X., Zhuang, X., Font, O., Izquierdo, M., Alastuey, A., Castro, I., van Drooge, B. L., Moreno, T., Grimalt, J. O., Elvira, J., Cabañas, M., Bartroli, R., Hower, J. C., Ayora, C., Plana, F., & López-Soler, A. (2011). Influence of soil cover on reducing the environmental impact of spontaneous coal combustion in coal waste gobs: a review and new experimental data. *International Journal of Coal Geology*, *85*(1), 2-22.
- Quindos, L., Fernandez, P., Soto, J., Rodenas, C., & Gomez, J. (1994). Natural radioactivity in Spanish soils. *Health physics*, *66*(2), 194-200.
- Radenović, A. (2006). Inorganic constituents in coal. *Kemija u industriji*, *55*(2), 65-72.
- Ramasamy, V., Suresh, G., Meenakshisundaram, V., & Ponnusamy, V. (2011). Horizontal and vertical characterization of radionuclides and minerals in river sediments. *Applied Radiation and Isotopes*, *69*(1), 184-195.
- Ravisankar, R., Vanasundari, K., Suganya, M., Raghu, Y., Rajalakshmi, A., Chandrasekaran, A., Sivakumar, S., Chandramohan, J., Vijayagopal, P., & Venkatraman, B. (2014). Multivariate statistical analysis of radiological data of building materials used in Tiruvannamalai, Tamilnadu, India. *Applied Radiation and Isotopes*, *85*(0), 114-127.
- Ribeiro, J., Silva, T., & Flores, D. (2012). Polycyclic aromatic hydrocarbons (PAHs) in burning and non-burning coal waste piles. *Journal of Hazardous Materials*, *199*, 105-110.

- Ribeiro, J., Taffarel, S. R., Sampaio, C. H., Flores, D., & Siva, L. F. O. (2013). Mineral speciation and fate of some hazardous contaminants in coal waste pile from anthracite mining in Portugal. *International Journal of Coal Geology*, 109-110(2013), 15-23.
- Riepe, W. (1993). Coal and environment: Analytical aspects. *Pure and Applied Chemistry*, 65(12), 2473-2479.
- Rodushkin, I., Axelsson, M. D., & Burman, E. (2000). Multielement analysis of coal by ICP techniques using solution nebulization and laser ablation. *Talanta*, 51(4), 743-759.
- Roy, W. R., Griffin, R. A., Dickerson, D. R., & Schuller, R. M. (1984). Illinois Basin coal fly ashes. 1. Chemical characterization and solubility. *Environmental Science & Technology*, 18(10), 734-739.
- Sarate, O. S. (2010). Petrographic characteristics of coal from Mailaram coalfield, Godavari Valley, Andhra Pradesh. *Journal Geological Society of India*, 76, 557-564.
- Scott, A. C. (2002). Coal petrology and the origin of coal macerals: A way ahead. *International Journal of Coal Geology*, 50(2002), 119-134.
- Shibaoka, M., & Smyth, M. (1975). Coal petrology and the formation of coal seams in some Australian Sedimentary Basins. *Economic Geology*, 70, 1463-1473.
- Sia, S.-G., & Abdullah, W. H. (2011). Concentration and association of minor and trace elements in Mukah coal from Sarawak, Malaysia, with emphasis on the potentially hazardous trace elements. *International Journal of Coal Geology*, 88(2011), 179-193.
- Sia, S.-G., & Abdullah, W. H. (2012a). Enrichment of arsenic, lead, and antimony in Balingian coal from Sarawak, Malaysia: Modes of occurrence, origin, and partitioning behaviour during coal combustion. *International Journal of Coal Geology*, 101, 1-15.
- Sia, S.-G., & Abdullah, W. H. (2012b). Geochemical and petrographical characteristics of low-rank Balingian coal from Sarawak, Malaysia: Its implications on depositional conditions and thermal maturity. *International Journal of Coal Geology*, 96-97(2012), 22-38.
- Singh, P. K., Singh, M. P., Singh, A. K., & Arora, M. (2010). Petrographic characteristics of coal from the Lati Formation, Tarakan basin, East Kalimantan, Indonesia. *International Journal of Coal Geology*, 81(2010), 109-116.
- Singh, S., Ram, L. C., Masto, R. E., & Verma, S. K. (2011). A comparative evaluation of minerals and trace elements in the ashes from lignite, coal refuse, and biomass fired power plants. *International Journal of Coal Geology*, 87(2), 112-120.
- Singh, S., Rani, A., & Kumar Mahajan, R. (2005). ^{226}Ra , ^{232}Th and ^{40}K analysis in soil samples from some areas of Punjab and Himachal Pradesh, India using gamma ray spectrometry. *Radiation Measurements*, 39(4), 431-439.

- Smith, R. D. (1980). The trace element chemistry of coal during combustion and the emissions from coal-fired plants. *Progress in Energy and Combustion Science*, 6.1 (1), 53-119.
- Spaits, T., Divós, F., & Simon, T. (2007). Dose contribution from buildings containing bottom ash insulation with elevated concentrations of natural radionuclides. *Radiation Measurements*, 42(10), 1727-1730.
- Spears, D., & Zheng, Y. (1999). Geochemistry and origin of elements in some UK coals. *International Journal of Coal Geology*, 38(3), 161-179.
- Speight, J. (2005). *Handbook of coal analysis.*: New Jersey: John Wiley & Sons, Inc.
- Sroor, A., El-Bahi, S., Ahmed, F., & Abdel-Haleem, A. (2001). Natural radioactivity and radon exhalation rate of soil in southern Egypt. *Applied Radiation and Isotopes*, 55(6), 873-879.
- Swaine, D. J. (1990). Trace elements in coal (pp. 290): Butterworth London.
- Swaine, D. J. (2000). Why trace elements are important. *Fuel Processing Technology*, 65, 21-33.
- Swaine, D. J., & Goodarzi, F. (1995). *Environmental aspects of trace elements in coal* (Vol. 2): Springer.
- Tabaksblat, L. S. (2002). Specific features in the formation of the mine water microelement composition during ore mining. *Water Resources*, 29(3), 333-345.
- Tadmor, J. (1986). Radioactivity from coal-fired power plants: A review. *Journal of Environmental Radioactivity*, 4(1986), 177-204.
- Taskin, H., Karavus, M., Ay, P., Topuzoglu, A., Hidiroglu, S., & Karahan, G. (2009). Radionuclide concentrations in soil and lifetime cancer risk due to gamma radioactivity in Kirklareli, Turkey. *Journal of Environmental Radioactivity*, 100(1), 49-53.
- Teichmüller, M. (1989). The genesis of coal from the viewpoint of coal petrology. *International Journal of Coal Geology*, 12(1), 1-87.
- Theis, T. L., & Wirth, J. L. (1977). Sorptive behavior of trace metals on fly ash in aqueous systems. *Environmental Science & Technology*, 11(12), 1096-1100.
- Tipler, P. A., & Llewellyn, R. (2007). *Modern physics*: Macmillan.
- Tsai, L.-Y., Chen, C.-F., & Finkelman, R. B. (2005). Composition and trace element content of coal in Taiwan. *TAO*, 16(3), 641-651.
- Tsikritzis, L., Fotakis, M., Tzimkas, N., Kolovos, N., & Tsikritzi, R. (2008). Distribution and correlation of the natural radionuclides in a coal mine of the West Macedonia Lignite Center (Greece). *Journal of Environmental Radioactivity*, 99(2), 230-237.

- Tso, M.-y. W., & Leung, J. K. C. (1996). Radiological impact of coal ash from the power plants in Hong Kong. *Journal of Environmental Radioactivity*, 30(1), 1-14.
- Tsoufanidis, N. (1995). *Measurement and detection of radiation*. Washington DC, USA: Taylor & Francis.
- Turhan, Ş., Arıkan, I., Demirel, H., & Güngör, N. (2011). Radiometric analysis of raw materials and end products in the Turkish ceramics industry. *Radiation Physics and Chemistry*, 80(5), 620-625.
- Turhan, S., Parmaksız, A., Kose, A., Yuksel, A., Arıkan, I. H., & Yucel, B. (2010). Radiological characteristics of pulverized fly ashes produced in Turkish coal-burning thermal power plants. *Fuel*, 89(2010), 3892-3900.
- Tykva, R., & Berg, D. (2004). *Man-made and natural radioactivity in environmental pollution and radiochronology*: Springer.
- Tzortzis, M., Svoukis, E., & Tsertos, H. (2004). A comprehensive study of natural gamma radioactivity levels and associated dose rates from surface soils in Cyprus. *Radiation Protection Dosimetry*, 109(3), 217-224.
- UNSCEAR. (1982). Ionizing radiation: sources and biological effects.
- UNSCEAR. (1988). Effects and Risks of Ionizing Radiation. *United Nations, New York*, 565-571.
- UNSCEAR. (2000). Sources and Effects of Ionizing Radiation. Report to General Assembly, with Scientific Annexes. United Nations, New York.
- UNSCEAR. (2008). *Effects of ionizing radiation: report to the General Assembly, with scientific annexes* (Vol. 1): United Nations Publications.
- Uosif, M., & El-Taher, A. (2008). Radiological assessment of ABU-TARTUR phosphate, western desert Egypt. *Radiation Protection Dosimetry*, 130(2), 228-235.
- U. S. Public Law (1990). Clean Air Act Amendments of 1990. *Public Law*, 101-549 (441 pp).
- Valkovic, V. (1985). Trace elements in coal.
- Varley, N., & Flowers, A. (1998). The influence of geology on radon levels in SW England. *Radiation Protection Dosimetry*, 77(3), 171-176.
- Vijayan, V., Behera, S. N., Ramamurthy, V. S., Puri, S., Shashi, J. S., & Singh, N. (1997). Elemental Composition of Fly Ash from a Coal-Fired Thermal Power Plant: a Study Using PIXE and EDXRF. *X-Ray Spectrometry*, 26, 65-68.
- Voellkopf, U., Paul, M., & Denoyer, E. (1992). Analysis of solid samples by ICP-mass spectrometry. *Fresenius' journal of analytical chemistry*, 342(12), 917-923.

- Wagner, N. J., & Hlatshwayo, B. (2005). The occurrence of potentially hazardous trace elements in five Highveld coals, South Africa. *International Journal of Coal Geology*, 63(2005), 228-246.
- Ward, C. R. (1984). Coal geology and coal technology. *Blackwell Scientific Publications, Melbourne*, 345.
- Ward, C. R. (2002). Analysis and significance of mineral matter in coal seams. *International Journal of Coal Geology*, 50(1), 135-168.
- Ward, C. R., Corcoran, J., Saxby, J., & Read, H. (1996). Occurrence of phosphorus minerals in Australian coal seams. *International Journal of Coal Geology*, 30(3), 185-210.
- Wong, M. H. (2003). Ecological restoration of mine degraded soils, with emphasis on metal contaminated soils. *Chemosphere*, 50(2003), 775-780.
- Wuyep, E. O., & Obaje, N. G. (2012). Petrographic evaluation of the ranks and technological applications of some coal deposits in the Anambra Basin and Middle Benue trough of Nigeria. *Journal of Earth Science and Engineering*, 2(2012), 220-234.
- www.uky.edu/KGS/coal/coalkinds.htm
- Yaprak, G. (1999). Indoor ²²²Rn concentrations in the vicinity of a Turkish coal-fired power plant. *Journal of Environmental Radioactivity*, 46(1), 131-135.
- Yenilmez, F., Kuter, N., Emil, M. K., & Aksoy, A. (2011). Evaluation of pollution levels at an abandoned coal mine site in Turkey with the aid of GIS. *International Journal of Coal Geology*, 86(2011), 12-19.
- Zarate-Morales, A., & Buenfil, A. (1996). Environmental gamma dose measurements in Mexico City using TLD. *Health physics*, 71(3), 358-361.
- Zhang, J. Y., Ren, D., Zhu, Y., Chou, C.-L., Zeng, R., & Zheng, B. (2004). Mineral matter and potentially hazardous trace elements in coals from Qianxi Fault Depression Area in southwestern Guizhou, China. *International Journal of Coal Geology*, 57(2004), 49-61.
- Zhang, J. Y., Zheng, C. G., Ren, D. Y., Chou, C.-L., Liu, J., Zeng, R. S., Wang, Z. P., Zhao, F. H., & Ge, Y. T. (2004). Distribution of potentially hazardous elements in coals from Shanxi province, China. *Fuel*, 83(2004), 129-135.
- Zhao, F., Cong, Z., Sun, H., & Ren, D. (2007). The geochemistry of rare earth elements (REE) in acid mine drainage from the Sitai coal mine, Shanxi Province, North China. *International Journal of Coal Geology*, 70(2007), 184-192.
- Zielinski, R. A., & Finkelman, R. B. (1997). *Radioactive elements in coal and fly ash: abundance, forms, and environmental significance*: US Geological Survey.
- Životić, D., Stojanović, K., Gržetić, I., Jovančićević, B., Cvetković, O., Šajnović, A., Simić, V., Stojaković, R., & Scheeder, G. (2013). Petrological and geochemical

composition of lignite from the D field, Kolubara basin (Serbia). *International Journal of Coal Geology*, 111, 5-22.

University of Malaya

LIST OF PUBLICATIONS AND PAPERS PRESENTED



International Journal of
Radiation Research

Date: 28.02.2016
Ref: IJRR-02-166

EDITORIAL OFFICE

Editor - in - chief
Hossein Mozdarani, Ph.D

Editorial Staff
Shahram Akhlaghpour, Senior Editor
Eshraq Darsi, Language Text Editor
Miranda Firoozbakht, Editorial Assistant
Sohail Mozdarani, Editorial Assistant

P.O.Box: 14886/699
Tehran, Iran
Tel: +98-21-88831199
Fax: +98-21-88831199
http://www.ijrr.com
E-mail: info@ijrr.com

EDITORIAL BOARD

Aghamiri SMR, Ph.D (Iran)
Akhlaghpour Sh, MD (Iran)
Amoui M, MD (Iran)
Bakac M., Ph.D (Turkey)
Behrooz M. A., Ph.D (Iran)
Eftekhari M., M.D (Iran)
Foroughizadeh M, Ph.D (Iran)
Ghannati H, MD (Iran)
Kant K, Ph.D (India)
Kim JK, Ph.D (Korea)
Mahdavi SR, Ph.D (Iran)
Meigooni AS, Ph.D (USA)
Mebahi A., Ph.D (Iran)
Mohammadi M, Ph.D (Iran)
Moufared AS, Ph.D (Iran)
Mousleh Shariati MA, Ph.D (Iran)
Mozdarani H, Ph.D (Iran)
Nair, CCK, Ph.D (India)
Samsi F, MD (Iran)
Sarkar S, Ph.D (Iran)
Sohrabi M, Ph.D (Iran)

K.M. Tilpangi, Y.M. Amin, M.U. Khandaker, W.H.
Binti Abdullah

Dear Dr. Khandaker

I am pleased to inform you that your revised manuscript entitled"

Radionuclide concentrations and excess life cancer risk due to gamma radioactivity in tailing enriched soil around Maiganga coal mine, Northeast Nigeria

is accepted for publication in the *International Journal of Radiation Research (IJRR)*.

You will hear from us when the galley proof of the manuscript is ready for final check. Please let us know if there is any question in the meantime. Thank you for being patient to receive the evaluation result of your manuscript and your interest for publishing in IJRR. *In order to proceed processing of your manuscript, please confirm that the content of this manuscript is neither published nor under publication elsewhere. Also please declare the authors have no conflicts of interests.*

Best Regards

Prof. Hossein Mozdarani
Editor-in-Chief, IJRR

RESEARCH ARTICLE

Quantification and Radiological Risk Estimation Due to the Presence of Natural Radionuclides in Maiganga Coal, Nigeria

Matthew Tikpangi Kolo^{1,3}, Mayeen Uddin Khandaker^{1*}, Yusoff Mohd Amin¹, Wan Hasiah Binti Abdullah²

1 Department of Physics, University of Malaya, 50603, Kuala Lumpur, Malaysia, **2** Department of Geology, University of Malaya, 50603, Kuala Lumpur, Malaysia, **3** Department of Physics, Federal University of Technology, Minna, Niger state, Nigeria

* mu_khandaker@um.edu.my; mu_khandaker@yahoo.com



OPEN ACCESS

Citation: Kolo MT, Khandaker MU, Amin YM, Abdullah WHB (2016) Quantification and Radiological Risk Estimation Due to the Presence of Natural Radionuclides in Maiganga Coal, Nigeria. PLoS ONE 11(6): e0158100. doi:10.1371/journal.pone.0158100

Editor: Roberto Amendola, ENEA, ITALY

Received: November 10, 2015

Accepted: June 11, 2016

Published: June 27, 2016

Copyright: © 2016 Kolo et al. This is an open access article distributed under the terms of the [Creative Commons Attribution License](#), which permits unrestricted use, distribution, and reproduction in any medium, provided the original author and source are credited.

Data Availability Statement: All relevant data are within the paper.

Funding: This study was fully funded by the Federal Government of Nigeria through the Tertiary Education Trust Fund (TetFund). Financial support from University of Malaya Research Grants: FP042-2013A, and RP006D-13AFR, are highly acknowledged. The funders had no role in study design, data collection and analysis, decision to publish, or preparation of the manuscript.

Competing Interests: The authors have declared that no competing interests exist.

Abstract

Following the increasing demand of coal for power generation, activity concentrations of primordial radionuclides were determined in Nigerian coal using the gamma spectrometric technique with the aim of evaluating the radiological implications of coal utilization and exploitation in the country. Mean activity concentrations of ²²⁶Ra, ²³²Th, and ⁴⁰K were 8.18±0.3, 6.97±0.3, and 27.38±0.8 Bq kg⁻¹, respectively. These values were compared with those of similar studies reported in literature. The mean estimated radium equivalent activity was 20.26 Bq kg⁻¹ with corresponding average external hazard index of 0.05. Internal hazard index and representative gamma index recorded mean values of 0.08 and 0.14, respectively. These values were lower than their respective precautionary limits set by UNSCEAR. Average excess lifetime cancer risk was calculated to be 0.04×10⁻³, which was insignificant compared with 0.05 prescribed by ICRP for low level radiation. Pearson correlation matrix showed significant positive relationship between ²²⁶Ra and ²³²Th, and with other estimated hazard parameters. Cumulative mean occupational dose received by coal workers via the three exposure routes was 7.69 ×10⁻³ mSv y⁻¹, with inhalation pathway accounting for about 98%. All radiological hazard indices evaluated showed values within limits of safety. There is, therefore, no likelihood of any immediate radiological health hazards to coal workers, final users, and the environment from the exploitation and utilization of Maiganga coal.

Introduction

The ever growing challenge of population explosion, human civilization, rapid urbanization, and high level industrialization has led to increasing demand for energy and power generation all over the world [1–3]. Whereas many nations are developing their nuclear energy base and others expanding their biomass and wind energy capacities, coal has proven to be the most abundant, most versatile, readily available, and easily assessable source of fossil fuel [4, 5]. Previous studies have highlighted significant contributions of coal to the sustenance of rapidly

Evaluation of radiological risks due to natural radioactivity around Lynas Advanced Material Plant environment, Kuantan, Pahang, Malaysia

Matthew Tikpangi Kolo¹ · Siti Aishah Binti Abdul Aziz¹ · Mayeen Uddin Khandaker¹ · Khandoker Asaduzzaman¹ · Yusoff Mohd Amin¹

Received: 19 December 2014 / Accepted: 21 April 2015 / Published online: 1 May 2015
© Springer-Verlag Berlin Heidelberg 2015

Abstract Understanding the public awareness concerning the Lynas Advanced Material Plant (LAMP), an Australian rare earths processing plant located in Malaysia, a radiological study in soil and water samples collected at random surrounding the LAMP environment was undertaken using HPGe gamma-ray spectrometry. The mean soil activities for ²²⁶Ra, ²³²Th, and ⁴⁰K were found to be 6.56±0.20, 10.62±0.42, and 41.02±0.67 Bq/kg, respectively, while for water samples were 0.33±0.05, 0.18±0.04, and 4.72±0.29 Bq/l, respectively. The studied areas show typical local level of radioactivity from natural background radiation. The mean gamma absorbed dose rate in soils at 1 m above the ground was found to be 11.16 nGy/h. Assuming a 20 % outdoor occupancy factor, the corresponding annual effective dose showed a mean value of 0.014 mSv year⁻¹, significantly lower than the worldwide average value of 0.07 mSv year⁻¹ for the annual outdoor effective dose as reported by UNSCEAR (2000). Some other representative radiation indices such as activity utilization index (AUI), *H_{ex}*, *H_{in}*, excess lifetime cancer risk (ELCR), and annual gonadal dose equivalent (AGDE) were derived and also compared with the world average values. Statistical analysis performed on the obtained data showed a strong positive correlation between the radiological variables and ²²⁶Ra and ²³²Th.

Keywords LAMP · HPGe detector · Statistical analysis · External absorbed dose rate · Radiological hazard and excess lifetime cancer risk

Responsible editor: Stuart Simpson

✉ Mayeen Uddin Khandaker
mu_khandaker@yahoo.com

¹ Department of Physics, University of Malaya, Kuala Lumpur 50603, Malaysia

Introduction

Lynas Advanced Material Plant (LAMP) is acclaimed as the largest rare earth refinery project in the world. It is an Australian rare earth refining industry located in Malaysia, with the sole responsibility of production and recovery of rare earth elements (REEs) from the concentrated raw materials supplied from Australia. REEs are metals, which by virtue of their unique physical and chemical properties, find great demands in the ever-expanding technological market all around the world (Rim et al. 2013). The citing of this processing plant in Malaysia has become a boost to the efforts of Malaysian government in turning the country into a manufacturing nerve centre and a more attractive environment for further domestic businesses.

Whereas the REEs have become an indispensable integral of green technology, their extraction and processing can pose serious environmental challenge and health risk to plant workers and the entire public in terms of radiation exposure. Although REEs are not, in themselves, radioactive, they exist in the earth crusts in mixture with naturally occurring radioactive materials (NORM). Schmidt (2013) reported that the raw materials and the rare earth ore imported from Australia for processing at LAMP are a concentrated mixture of REEs and radioactive thorium, uranium, and their decay products. The processing of the ore can therefore concentrate these NORMs in the wastes (TENORM), which, if not handled effectively, can become a channel of public exposure. Thorium dust, which is a known cancer-inducing agent, is easily blown by wind and carried by water over long distances, thereby create radiation hazards over large span of areas. Thus, all the steps of REE production, from mining through transportation, processing and waste disposal stages, are potential pathways for contamination of soil and water by radioactive and hazardous chemicals.